Fluoreszierendes gelöstes organisches Material (FDOM) in Küstenmeeren: Charakterisierung, biogeochemische Prozesse, und die Möglichkeit der in situ Überwachung

Fluorescent dissolved organic matter (FDOM) in the coastal ocean: characterization, biogeochemical processes, and the possibility of in situ monitoring

Von der Fakultät für Mathematik und Naturwissenschaften

der Carl von Ossietzky Universität Oldenburg

zur Erlangung des Grades und Titels eines Doktors der

Naturwissenschaften

– Dr. rer. nat. –

angenommene Dissertation von

I Gusti Ngurah Agung Suryaputra

geboren am 17.12.1977 in Bali, Indonesien

Gutachter: Dr. Thorsten Dittmar

Zweitgutachter: Prof. Dr. Oliver Zielinski

Tag der Disputation: 18. Oktober 2012

Abstract

The main goal of this study was to characterize fluorescent dissolved organic matter (FDOM) and examine its variability in the coastal ocean. FDOM is an important fraction of DOM which strongly impacts the penetration depth of sunlight in water columns. Moreover, as FDOM can be easily measured in situ, it has great potential for monitoring selected parameters of interest. The study was organized into three parts: (1) FDOM production in a subterranean estuary studied during three weeks of in situ measurement; (2) FDOM biogeochemical variability in a subterranean estuary using novel multivariate statistical analyses approaches; and (3) linking fluorescence properties and molecular data of estuarine dissolved organic matter.

The purpose of the first part in this study was to examine if FDOM was produced in the coastal sediments and released via submarine groundwater discharge (SGD). Additionally, the possibility of using FDOM to calculate dissolved organic carbon (DOC) fluxes to the adjacent coastal ocean was also the scope of this part. The questions were addressed by three weeks of continuous FDOM measurements conducted in the sediment and in the bay at Turkey Point, FL, USA, using two in situ sensors. Hourly DOC and total dissolved nitrogen (TDN) concentrations were also determined from both stations on 15 hours sampling. It was discovered that FDOM was produced in the top of sediment and affected by SGD and further uncharacterized processes. Although FDOM was dominantly terrigenous, intrusion of marine algae in the sediment was also evident. Meanwhile, based on a tidal cycle sampling, FDOM could be used to calculate DOC concentrations and the SGD load of DOC, emphasizing the significance of terrestrial DOC delivered via SGD.

As the first part concluded that coastal sediment was an important source of FDOM to the coastal ocean, the second part aimed to characterize FDOM and to inspect its variability in the processes occurring in the coastal sediment. Therefore, sampling was conducted in the same coastal sediment at Turkey Point, Florida, USA. Water samples for FDOM, DOC, and TDN were collected every 90 minutes for a tidal cycle. Parallel factor (PARAFAC) analysis was used to statistically decompose FDOM into its components; and partial least square (PLS) regression analysis was applied to reduce the complexity of the data, and to obtain linear correlation of all measured data. Three "humic-like" components and one "protein-like" component were modeled using PARAFAC analysis. Apparently, instead of salinity (as expected in estuarine systems), DOC, NH_4, and NO_3 concentrations correlated with one "humic-like" component. This component was probably derived from the soil and sediment of the adjacent pine forest, and influenced by nitrification in the sediment. On the other hand, none of the auxiliary data could explain the variability of the other PARAFAC components. However, those components were not introduced by fresh or seawater, but were likely the result from microbial decomposition of sedimentary organic matter. Nevertheless, regression matrix analyses that were for the first time introduced in this section confirmed the results from PLS regression analysis. Supplementary information regarding the appropriate fluorescence wavelengths, where specific processes (e.g. mixing and nitrification) affect FDOM intensities most significantly, could be identified from the regression matrices.

FDOM intensities alteration was coupled to changes in environmental condition, physically, biologically, and chemically. A more in-depth study was performed to identify the molecular reasons behind FDOM alterations, as the third part of this thesis. A complete salinity gradient was sampled for DOC, TDN, FDOM, and molecular DOM analyses from the Suwannee

River Estuary System (Florida, USA). The molecular information consisted of 1000's of molecular formulae of DOM compounds obtained from ultrahigh-resolution mass spectrometry. PARAFAC analysis was used to statistically determine the number of FDOM components. PLS regression analysis was performed to explore linear correlations of FDOM components, DOM data, DOM molecular information, and environmental data altogether. Four terrestrial "humic-like" components were found using PARAFAC analysis. As shown by PLS plots, three of the PARAFAC components were discharged to the ocean via river flow, while one of the components was probably leached from the sediment into the estuary by groundwater discharge. Distinct thousands wavelengths could be linked to molecular DOM properties and processes with help of regression matrices, confirming that these tools are suited to gain further insights into DOM dynamics in coastal zone.

The statistical approaches that were developed in this thesis are currently being applied to groundwaters in the Wadden Sea. In a final chapter of this thesis, an outlook is given on the progress of this study which will be subject of my postdoctoral research.

Kurzfassung

Das Ziel dieser Studie war es, fluoreszierendes organisches Material (fluorescent dissolved organic matter, FDOM) zu charakterisieren und seine Variabilität im Ozean zu untersuchen. FDOM ist die fluoreszierende Komponente des gelösten organischen Materials (DOM), und beeinflusst wesentlich die optischen Eigenschaften natürlicher Gewässer. FDOM kann verhältnismäßig einfach *in situ* gemessen werden und die Bestimmung dieser DOM-Komponente hat großes Potential zur automatischen Überwachung verschiedener Parameter. Die vorliegende Arbeit gliedert sich in drei Abschnitte: (1) die Produktion von FDOM wurde im Laufe von drei Wochen in einem unterirdischen Ästuar u.a. mit Hilfe von *in situ* Messverfahren verfolgt. (2) Die biogeochemische Umsetzung von FDOM in einem unterirdischen Ästuar war das Ziel der zweiten Studie, hierzu wurden moderne multivariate statistische Methoden erstmalig angewandt. (3) Das Ziel der dritten Studie war, optische Eigenschaften von DOM eines Ästuars auf molekularer Ebene zu erklären.

Im ersten Teil der Studie sollte untersucht werden, ob FDOM in küstennahen Sedimenten produziert und über unterseeischen Grundwasserausfluss (submarine groundwater discharge, SGD) in den Ozean gelangt. Zusätzlich wurde die Möglichkeit, anhand von FDOM die Einträge von gelöstem organischem Kohlenstoff (dissolved organic carbon, DOC) in Küstengewässer zu bestimmen, untersucht. Zur Beantwortung dieser Fragen wurden mit zwei *in-situ* Sensoren über einen Zeitraum von drei Wochen kontinuierlich FDOM-Bestimmungen im Sediment und der Wassersäule in der Bucht von Turkey Point (Florida, USA) durchgeführt. Eine stündliche Konzentrationsbestimmung von DOC- und Gesamtstickstoff (TDN, total dissolved nitrogen) über 15 Stunden vervollständigte diese Probennahme. Die Untersuchungen zeigten, dass FDOM

im Oberflächenseediment produziert und dort vom SGD und auch weiteren nicht charakterisierten Prozessen beeinflusst wird. Obwohl terrigene Huminstoffe die Zusammensetzung des FDOMs dominieren, trugen auch Algen zum FDOM bei. Die Beprobung des Tidenzyklusses machte es möglich, die Langzeitmessung von FDOM für eine Abschätzung der DOC-Konzentrationen zu nutzen und den DOC-Eintrag über das Grundwasser abzuschätzen.

Der erste Teil der Arbeit zeigte, dass Küstensedimente eine Quelle von FDOM darstellen. Im Folgenden wurde die Zusammensetzung des FDOMs und seine biogeochemische Umsetzung genauer untersucht. Für diesen zweiten Teil der Arbeit wurden über einen Tidenzyklus alle 90 Minuten Wasserproben in der Bucht und entlang des Salinitätsgradienten im Grundwasser von Turkey Point (Florida, USA) entnommen und auf FDOM, DOC, und TDN untersucht. Eine Parallel Factor Analysis (PARAFAC) wurde verwendet, um FDOM statistisch in seine Komponenten zu zerlegen. Anschließend wurde mit einer Partial Least Square (PLS) Regression die Komplexität der Daten reduziert und lineare Korrelationen zwischen den gemessenen Parametern bestimmt. Drei sogenannte Huminstoff- und eine Protein-Komponente konnten mit der PARAFAC-Analyse modeliert werden. Allerdings erklärte nicht der Salzgehalt - wie in einem Ästuar eigentlich erwartet - sondern die DOC-, NH_4- und NO_3-Konzentrationen eine der Huminstoff-Komponenten. Diese Komponente stammte wahrscheinlich ursprünglich aus dem Boden und Sediment des angrenzenden Kiefernwaldes, wurde aber anschließend im Sediment in einer Nitrifikationszone mikrobiell umgesetzt. Die Variabilität der anderen PARAFAC Komponenten konnte durch keinen der gemessenen Umweltparameter erklärt werden. Die verbleibenden Komponenten stammten weder direkt aus dem Süßwasser noch wurden sie direkt von Meerwasser in das Sediment eingetragen. Es wurden allerdings Hinweise darauf gefunden, dass der Großteil des FDOM und DOC direkt im Sediment mikrobiell aus marinen und

terrestrischen Ablagerungen gebildet wird. Diese mit Hilfe der PLS identifizierten Prozesse wurden von den Ergebnissen der Regressionsmatrizen, die hier in diesem Zusammenhang erstmals Verwendung fanden, unterstützt. Diese Regressionsmatrizen waren zudem zur Identifikation geeigneter Wellenlängen hilfreich, um bestimmte Umweltparameter und DOM-Komponenten gezielt mit Hilfe von Fluoreszenz *in situ* zu überwachen.

Der Einfluss physikalischer, biologischer und chemischer Umweltparameter auf FDOM in einem unterirdischen Ästuar war Gegenstand der zweiten Studie. Im dritten Teil der vorliegenden Arbeit wurde eine tiefergehende Untersuchung durchgeführt, um die Variabilität von FDOM auf molekularer Ebene zu verstehen. Dazu wurden entlang eines Salzgradienten im Suwannee Ästuar (Florida, USA) Wasserproben für die Analyse von DOC, TDN, FDOM und der molekularen Zusammensetzung des DOM entnommen. Anhand von ultrahochauflösender Massenspektrometrie wurden tausende von Summenformeln individueller Moleküle im DOM bestimmt. Zunächst wurden auch in dieser Studie die FDOM-Komponenten statistisch mit einer PARAFAC-Analyse ermittelt. PLS-Regression wurde verwendet, um lineare Korrelationen zwischen den FDOM-Komponenten, der molekularen DOM Zusammensetzung und den Umweltparametern zu identifizieren. Vier terrigene Huminstoff-Komponenten konnten anhand der PARAFAC-Analyse identifiziert werden. Die PLS-Regressionsanalyse zeigte, dass drei der PARAFAC-Komponenten durch den Fluss in den Ozean gelangten, während eine Komponente durch Grundwasser in das Ästuar eingetragen wurde. Zusammenhänge zwischen tausenden, individuellen Wellenlängen und molekularen Eigenschaften des DOMs und auch bestimmten Prozessen wurden mit Hilfe der Regressionsmatrizen gefunden. So konnte vor allem auch gezeigt werden, dass diese statistischen Werkzeuge eine wichtige Rolle bei weiteren Untersuchungen der DOM-Dynamik in Küstengebieten spielen können.

Die statischen Ansätze, die in dieser Arbeit entwickelt wurden, finden zur Zeit Anwendung in einer Untersuchung zur Biogeochemie des DOM in Grundwässern des Wattenmeers. Diese Untersuchungen werden in einem letzten Kapitel dieser Arbeit vorgestellt und werden Gegenstand meiner Forschung als Postdoc sein.

Table of contents

Chapter 1

General Introduction

General Introduction

1. Introduction

This introduction chapter provides background information about dissolved organic matter (DOM) in the coastal ocean region. Analyses of DOM applied in this thesis, are also presented.

A. The dynamics of DOM

DOM is usually defined all organic molecules in natural waters, which pass through a filter less than 0.7 μm pore size, although DOM size can be variable (Kalbitz et al., 2000). DOM is produced from decomposition of bacterial, algal, and higher plant organic material (Cory and McKnight, 2005; Klapper et al., 2002) which consists of a refractory fraction like humic substances, and labile fraction like carbohydrates, amino acids, low molecular weight organic acids and fatty acids (Kronberg, 1999; Thurman, 1985). Based on its solubility on different pH, humic substances can be operationally grouped into two classes: humic acids are soluble at pH>2 and insoluble at pH<2; and fulvic acids are soluble at any pH (Thurman and Malcolm, 1981).

The occurrence of DOM has many implications for aquatic ecosystem, either directly or indirectly. Most biogeochemical cycles of elements, including carbon, nitrogen, and trace metals, are affected by the existence of DOM (Baines and Pace, 1991; Jumars et al., 1989). In the aquatic food web, DOM provides carbon and nutrients (Maranger and Pullin, 2003; Mulholland, 2003) which are essential for primary production. In the freshwater, DOM also contributes to acidification processes (Muniz, 1990).

Terrestrial input is a major source of DOM to the marine environment (Blough and Del Vecchio, 2002b; Meyers-Schulte and Hedges, 1986) and rivers deliver as much as 0.25 Gt of dissolved organic carbon (DOC) per annum to the ocean (Hedges et al., 1997; Ludwig et al., 1996). In estuarine and coastal waters, DOM can be produced by phytoplankton exudation, cell autolysis, and grazing pressure (Nagata, 2000), decomposition of plant litter and organically rich soils (Keith and Yoderand Sa, 2002), seaweed decomposition (Sieburth and Jensen, 1968), by-product of primary production (Carder et al., 1989b; Del Castillo et al., 2000b), and anthropogenic input (Bricaud et al., 1981). Although terrestrial-derived DOM is released mainly via surface estuaries, subterranean estuaries contribution is also of importance.

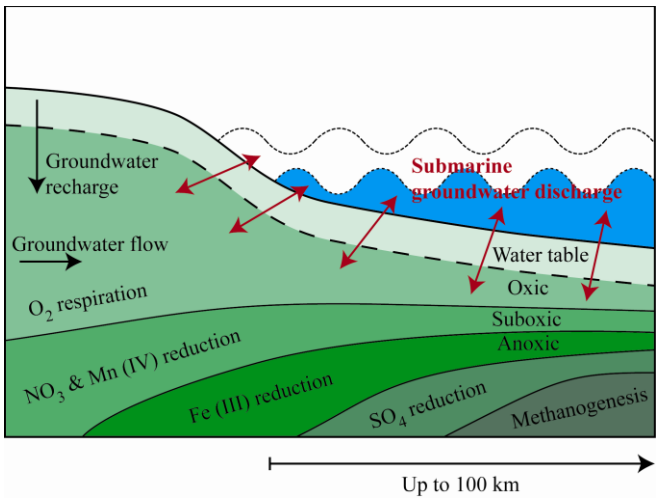

Fig. 1.1. Submarine groundwater discharge and nutrients changes in the coastal aquifer, modified after Moore (2010) and Slomp and Van Capellen (2004b).

The concept of the subterranean estuary (STE) was introduced by Moore (1999a) to emphasize the similarity of coastal aquifers where mixing between freshwater and saline water occurs, with surface estuaries. Mixed brackish water can be delivered to the ocean via submarine groundwater discharge (SGD). Contrasting to hydrologists who usually refer the term

"groundwater" to fresh groundwater, oceanographers define SGD as any discharge water flow, regardless of composition or driving force, on continental margins from the seabed to the adjacent coastal ocean, near the shoreline or up to kilometers offshore (Fig.1.1) (Burnett and Dulaiova, 2003; Moore, 2010). Several studies have been focused on the importance of STE, and it became evident that even though the flux of fresh groundwater was not comparable to that of rivers, significant amount of nutrients are discharged to the adjacent coastal ocean via the SGD pathway (Santos et al., 2008; Slomp and Van Cappellen, 2004b; Valiela et al., 1999). SGD can also be important for chemical and biological processes taken place in the coastal zone (Riedl et al., 1972), with respect to, e.g. trace elements source to the coastal ocean (Shaw et al., 1998b), and nutrients, metals, and carbon concentration alteration (Moore, 1999b; Rutkowski et al., 1999; Slomp and Van Cappellen, 2004b).

B. Analyses of DOM

1. Bulk DOM

DOM has been measured as DOC and dissolved organic nitrogen (DON) for several decades. Wet combustion oxidation (WCO) had been a common method in quantifying DOM, but after high temperature catalytic oxidation (HTCO) was introduced by Suzuki et al. (1985) and Sugimura and Suzuki (1988), the latter method with platinum catalyst became the standard. With this method, laboratory data comparison is possible, assuming careful sample handling and precise blank measurement. Moreover, the availability of external deep sea reference (DSR) waters collected from the Sargasso Sea or Florida Strait and distributed by the Hansell group from the University of Miami, led to DOM quantification in high precision.

Bulk DOM can also be quantified based on its optical fractions, either by absorbance or fluorescence spectroscopy. When light with enough energy hits DOM molecules in natural waters, the typically aromatic molecules will absorb this energy and be excited from their ground state to an excited state. After a short internal relaxation conversion to the lowest vibrational level in the excited state, the molecules will return to their ground state by emitting light at lower energy or longer wavelength than that of absorption. The complete fluorescence cycle of absorption, internal conversion, and emission, can be visualized in a Jablonski diagram (Fig. 1.2).

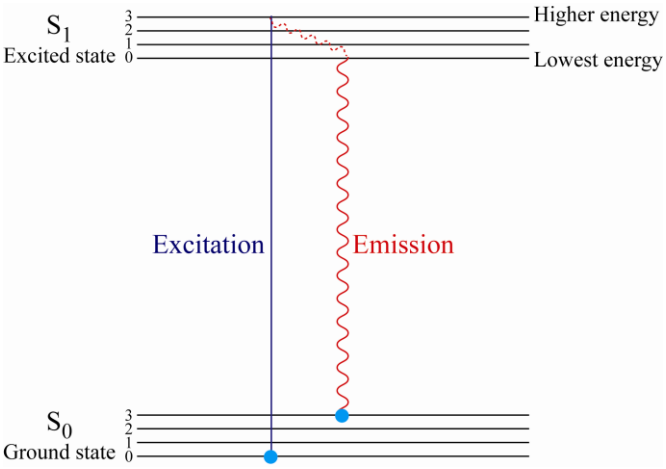

Fig. 1.2. Jablonski diagram of a fluorescence process (Lakowicz and Masters, 2008). Blue dots symbolize electrons; the horizontal lines are different energy states in molecular electron orbitals.

Fluorescent dissolved organic matter (FDOM) is measured by repeating a range of emission scans at a range of excitation wavelengths and building a so-called excitation emission matrix (Coble, 1996). Some corrections have to be applied prior to EEM data analysis. Instruments, for example, have to be corrected based on their configuration. Furthermore, removing Raman and Rayleigh scattering is also important to avoid interference in data interpretation caused by the intense noises. Corrected EEM can be analyzed using three common

methods. The easiest and simplest way is by choosing certain peaks or taking the ratio between peaks (e.g. Coble, 1996). Regional integration is a method introduced by Chen et al. (2003), which calculated the area below certain peaks. The third method, which applies the multivariate statistical method of parallel factor (PARAFAC) analysis, was presented by Stedmon et al. (2003) and increased the number of publications in FDOM analysis significantly.

The succession of FDOM characterization using PARAFAC in natural waters (Bro and Ohno, 2006; Kowalczuk et al., 2009; Murphy et al., 2008) provided the basic step for major advances. Further studies showed that a "humic-like" FDOM intensity was negatively correlated with salinity, indicating a terrestrial origin of this FDOM component (Blough and Del Vecchio, 2002b; Murphy et al., 2008; Yamashita et al., 2008). Meanwhile, three characterized protein-like components, similar to the spectra of amino acids tryptophan, tyrosine, and phenylalanine (Murphy et al., 2006; Murphy et al., 2008; Yamashita and Tanoue, 2003), are indicative of microbial activity (Urban-Rich et al., 2006). Although microbial activity also degrades FDOM, photodegradation is known as the most significant sink in water columns (Stedmon et al., 2007b).

2. Solid phase extraction (SPE)-DOM

Despite its simple and straightforward application, optical analyses of bulk DOM do not reveal the DOM composition on a molecular level. Molecular analyses of marine DOM, however, are challenged by low DOM concentrations and high concentrations of inorganic salts. Additional steps are required not only to isolate but also to concentrate DOM. For instance, SPE using PPL (styrene divinyl benzene polymer sorbents) cartridges is a simple DOM isolation

method which is suitable for open ocean and coastal waters (Dittmar et al., 2008). The DOM extract, which is called SPE-DOM, is then ready for a molecular study in any detail.

The complexity of DOM cannot be completely resolved using conventional mass spectrometers. An ultra-high resolution spectrometry so-called Fourier transform ion cyclotron resonance mass spectrometry (FT-ICR-MS), is a relatively new method which is able to resolve thousands of DOM molecular formulae (Koch et al., 2005; Stenson et al., 2002). The DOM formulae of natural waters typically range from 200 Da to 800 Da (Fig. 1.3). Studies have been performed accordingly, focusing on the determination of formulae, calibration, and the reproducibility of results at first (Sleighter et al., 2008; Stenson et al., 2003; Stenson et al., 2002), and later on to the characterization of DOM on the molecular level. For instance, decreasing of DOM aromaticity, from fresh to saline samples, was confirmed using FT-ICR-MS (Liu et al., 2011). The loss of DOM due to photochemistry was also studied in laboratory scales and found that the aromatic compounds of DOM were significantly degraded into more aliphatic compounds (Gonsior et al., 2008; Stubbins et al., 2010).

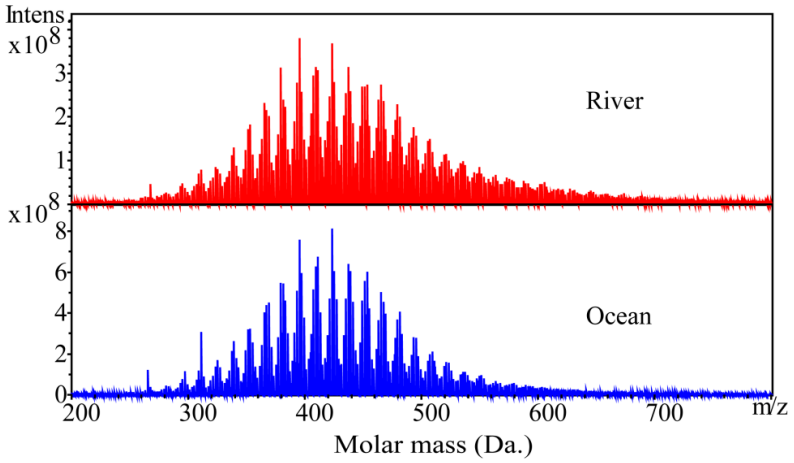

Fig. 1.3. FT-ICR-MS spectra of a riverine and oceanic sample (SPE-DOM). Because of the soft electrospray ionization (Chen et al.), molecules are not fragmented during analysis. The signals are from intact, singly charged molecules.

2. Thesis outline

The general objectives of this thesis were to characterize and identify FDOM in different coastal ocean environments. Furthermore, the sources, sinks and driving forces of FDOM variability and molecular distribution were also explored.

Chapter 2 describes FDOM variability measured in situ in a STE and adjacent coastal ocean. The aim was to determine if FDOM was produced or consumed in a STE. Correlation statistics with DOC concentrations were performed for a prediction purpose. Results on Chapter 2 provided basic knowledge for the study in Chapter 3.

Chapter 3 focuses on the characterization and identification of FDOM in a STE with help of PARAFAC analysis. The physical and chemical processes, which affected FDOM intensities in the system, were also determined.

Chapter 4 addresses specific questions regarding molecular variability of FDOM. A surface estuary system dominated by a mixing process was chosen to simplify data interpretation.

Chapter 5, 6, and 7 are publications accepted and published in international journal to which I contributed. Chapter 5 provides information on FDOM variability in a STE of a tidal flat in South Korea. Chapter 6 focuses on a DOM study in a salt marsh where a single wavelength FDOM was applied. Chapter 7 addresses a different topic in which DOM data was used to explain dissolved metal dynamics in a STE.

Chapter 8 is an outlook of FDOM studies in submarine groundwaters of the North Sea. Novel approaches in data analyses from previous chapters will be applied as part of my

postdoctoral study. All sampling and data measurements have been completed, although more in-depth data analyses are still necessary for completion.

3. Contributions to publications

This thesis consists of the manuscripts of three papers that have been submitted to international research journals and an outlook for future publications. My contributions to each of the manuscripts was the following:

Chapter 2 – full manuscript

I Gusti Ngurah Agung Suryaputra, Isaac R. Santos, Markus Huettel, William C. Burnett, Thorsten Dittmar

Fluorescent dissolved organic matter (FDOM) production in a subterranean estuary

Sampling was conducted by I Gusti Ngurah Agung Suryaputra and Isaac R. Santos. FDOM, dissolved organic carbon (DOC), and total dissolved nitrogen (TDN) measurements and data analysis were performed by I Gusti Ngurah Agung Suryaputra. Other data were provided by Isaac R. Santos. The manuscript was written by I Gusti Ngurah Agung Suryaputra with inputs from all co-authors and has been submitted to *Estuarine, Coastal, and Shelf Science*.

Chapter 3 – full manuscript

I Gusti Ngurah Agung Suryaputra, Isaac R. Santos, Thorsten Dittmar

Fluorescent dissolved organic matter (FDOM) variability in a subterranean estuary, from multiple wavelengths to a single wavelength approach

I Gusti Ngurah Agung Suryaputra carried out sampling and data handling of FDOM, DOC, and TDN. Isaac R. Santos contributed in sampling and other data. All co-authors provided input for

the manuscript written by I Gusti Ngurah Agung Suryaputra. This manuscript has been submitted to *Marine Chemistry*.

Chapter 4 – full manuscript

I Gusti Ngurah Agung Suryaputra, Pamela Rossel,Thorsten Dittmar

Linking fluorescence and molecular properties of estuarine dissolved organic matter

I Gusti Ngurah Agung Suryaputra performed all sampling and data analyses, except molecular DOM measurement using FT-ICR-MS which was provided by Pamela Rossel. All co-authors contributed with editorial inputs for the manuscript written by I Gusti Ngurah Agung Suryaputra. This manuscript has been submitted to *Marine Chemistry*.

Chapter 5 – abstract only

Tae-Hoon Kim, Hannelore Waska, Eunhwa Kwon, Guebuem Kim, I Gusti Ngurah Agung Suryaputra

Production, degradation, and fluxes of dissolved organic matter in the subterranean estuary of a large tidal flat

I Gusti Ngurah Agung Suryaputra performed PARAFAC analysis for FDOM data in this study. The manuscript has been published in *Marine Chemistry*.

Chapter 6 – abstract only

Thorsten Dittmar, Jiyoung Paeng, Thomas M. Gihring, I Gusti Ngurah Agung Suryaputra, Markus Huettel

Discharge of dissolved black carbon from a fire-affected intertidal system

I Gusti Ngurah Agung Suryaputra contributed in sampling, FDOM data handling, DOC and TDN measurements, and writing the manuscript. The article has been published in *Limnology and Oceanography*.

Chapter 7 – abstract only

Isaac R. Santos, William C. Burnett, Sambuddha Misra, I Gusti Ngurah Agung Suryaputra, Jeffrey P. Chanton, Thorsten Dittmar, Richard N. Peterson, Peter W. Swarzenski

Uranium and barium cycling in a salt wedge subterranean estuary: The influence of tidal pumping

I Gusti Ngurah Agung Suryaputra contributed in sampling, DOC measurements, and writing the manuscript. The article has been published in *Chemical Geology*.

Chapter 8 – outlook only

I Gusti Ngurah Agung Suryaputra, Michael Seidel, Thorsten Dittmar

Fluorescent dissolved organic matter in submarine groundwaters of the Southern North Sea

Sampling was carried out by I Gusti Ngurah Agung Suryaputra and Michael Seidel. The measurements of DOC, TDN, and FDOM, as well as PARAFAC analysis were performed by I Gusti Ngurah Agung Suryaputra.

Chapter 2

Fluorescent dissolved organic matter (FDOM) production in a subterranean estuary

Fluorescent dissolved organic matter (FDOM) production in a subterranean estuary

I Gusti Ngurah A. Suryaputra[1], Isaac R. Santos[2], Markus Huettel[3],

William C. Burnett[3], Thorsten Dittmar[1]

Submitted to Estuarine, Coastal and Shelf Science

[1] Max Planck Research Group for Marine Geochemistry, Carl von Ossietzky University, ICBM, Carl-von-Ossietzky-Str. 9-11, D-26129 Oldenburg, Germany

[2] Centre for Coastal Biogeochemistry, Southern Cross University, Lismore, NSW, 2480, Australia

[3] Department of Earth, Ocean, and Atmospheric Science, Florida State University, Tallahassee, Florida 32306, USA

Abstract

The importance of submarine groundwater discharge (SGD) in releasing fluorescent dissolved matter (FDOM) to the coastal ocean and the possibility of using FDOM as a proxy of dissolved organic carbon (DOC) was studied in a subterranean estuary in the northeastern Gulf of Mexico. FDOM was continuously monitored in situ for three weeks in beach groundwater and in the adjacent coastal waters. Radon (^{222}Rn) was used as a natural groundwater tracer. Discrete samples for DOC analysis and associated variables were collected over one complete tidal cycle. Correlations between detrended ^{222}Rn-derived SGD and detrended FDOM concentrations in the coastal waters showed that FDOM in the near shore waters was mainly driven by tidally-modulated SGD and by mixing between offshore and onshore waters. Independent statistical tests, including chlorophyll-a, salinity and water level data, confirmed that FDOM in the coastal waters was mainly driven by SGD of freshwater. FDOM and DOC were significantly correlated for the groundwater end-member, and FDOM could thus be transformed into DOC concentrations. A salinity scatter plot revealed FDOM production in the high salinity region of the subterranean estuary probably as a result of infiltration of labile marine particulate organic matter into the beach face. The non-conservative FDOM behavior in this subterranean estuary contrasts to most surface estuaries where FDOM often behaves conservatively. We estimated that at least 0.6 mega-moles of DOC, about 10% of the load of the largest regional river (Apalachicola River), could be delivered every day to the entire Gulf Coast of Florida via SGD.

2.1. Introduction

Submarine groundwater discharge (SGD) is considered a significant source of nutrients to the coastal ocean. A large fraction of these nutrients reach the sea associated with dissolved

organic matter (Santos et al., 2009b). SGD-derived nutrient fluxes may influence coastal ecosystem functioning by enhancing the productivity of coastal waters (Moore, 1999; Nixon et al., 1996). Closing of coastal nutrient budgets thus requires the quantitative determination of the nutrient and dissolved organic matter (DOM) release through SGD.

SGD, both fresh and saline, was calculated to account for as much as 40% of the total river flow in specific regions (Moore, 1996), but other studies found that the discharge may be less than that (Bokuniewicz, 1980; Hussain et al., 1999; Sekulic and Vertacnik, 1996). Nevertheless, this water pathway has been considered important to coastal biogeochemical budgets. Valiela et al. (1990) emphasized that nutrient concentrations in coastal groundwater can be several orders of magnitude higher than in surface waters, highlighting the potential role of SGD as significant source of nutrients to coastal oceans, possibly affecting element cycles on the global scale.

The coastal aquifer functions as a biogeochemical reactor, mobilizing nutrients and releasing DOM from sediments. Where freshwater and seawater mix in the aquifer, biogeochemical processing of organic matter and inorganic constituents is apparently accelerated. The release of trace elements (Shaw et al., 1998), and the processing of nutrients, metals, and carbon (Cai and Wang, 1998; Moore, 1999; Slomp and Van Cappellen, 2004) have been described in the literature. The long residence time of water in subterranean estuaries compared to surface estuaries increases the importance of biogeochemical reactions modifying the chemical signature of the groundwater prior to discharge into the coastal ocean (Santos et al., 2008).

Compared to information regarding inorganic nutrients in subterranean estuaries (STEs), our knowledge on the role of organic constituents in SGD is scarce. DOM from continental

runoff can reach groundwater and high concentrations of DOM have been observed in shallow subterranean estuaries (Santos et al., 2008). It is likely that this DOM contains degradable substrates that support growth of heterotrophic microbes in the sediment (Williams and Yentsch, 1976). DOM is often quantified as dissolved organic carbon (DOC). However, the analysis of DOC requires discrete samples and high-resolution observations are thus difficult to obtain. This is problematic, because STEs are highly dynamic and strongly affected by tidal fluctuations (Santos et al., 2008). Fluorescent dissolved organic matter (FDOM) is a major component of DOC and can be determined automatically in situ via fluorescence detection, allowing one to obtain detailed time series observations. In a coastal aquifer, freshwater FDOM mixes with seawater FDOM and is then discharged to the coastal ocean. Possible sources of FDOM in the coastal aquifer are the decomposition of terrestrial plant materials (Nakane et al., 1997; Uchida et al., 2000; Volk et al., 1997), anthropogenic input (de Almeida Azevedo et al., 2000; Derbalah et al., 2003; Mostofa et al., 2005), and by-products of primary or bacterial production (Carder et al., 1989; Del Castillo et al., 2000). The measurements of FDOM with fluorescence sensors and relating these readings to SGD thus could be a method to determine the impact of SGD on FDOM release to the coastal zone.

To quantify SGD, a common tracer is the radon isotope ^{222}Rn (Burnett et al., 2006) because it is continuously released from aquifer minerals through the radioactive decay of ^{226}Ra, which in turn is a product of the longer-lived parent ^{238}U. The short half-life of 3.8 days makes ^{222}Rn a good tracer for short-term mixing processes in coastal waters. The radon technique has been successfully applied to calculate nutrient (Crusius et al., 2005; Santos et al., 2008; Smith and Swarzenski, 2012) and mercury fluxes (Black et al., 2009; Ganguli et al., 2012) caused by SGD.

The objective of this study was to investigate the possibility of using the FDOM flux of a subterranean estuary (STE) to the coastal ocean as a proxy for the DOM release, and to determine the role of the SGD as a source of FDOM and DOM to the coastal ocean. FDOM was monitored in a STE and in the adjacent near shore waters for three weeks, along with a groundwater tracer (radon). In order to assess whether FDOM monitoring can be a proxy for DOC, discrete water samples were taken for chemical analysis. Our results revealed an unexpected production of FDOM within the subterranean estuary that FDOM is a valuable proxy for DOM discharge, and that SGD contributes significantly to the coastal DOM flux in the northeastern Gulf of Mexico (GOM).

2.2. Materials and Methods

2.2.1. The study area

The study site was located on the northeastern coast of the GOM (Turkey Point, Florida, USA). Several studies on SGD have been conducted in this area (Burnett and Dulaiova, 2003; Cable et al., 1996; Lambert and Burnett, 2003; Moore, 2010) including studies of the biogeochemistry of the subterranean estuary (Santos et al., 2008; Santos et al., 2009a). Even though fresh water here accounts for only ~5% of the total SGD volume, SGD is an important pathway of nutrients as a result of the biogeochemical processes in the subterranean mixing zone (Santos et al., 2008; Santos et al., 2009a). The concentrations of dissolved organic nitrogen (DON) and DOC are high in the shallow aquifer (Santos et al., 2008).

Detailed information about the study site is available in the several previous studies performed at Turkey Point. Briefly, the subterranean estuary in this area combines diffuse fresh and saline water seepage near shore from an unconfined shallow aquifer and submarine springs

from the deeper, confined Floridan Aquifer. The annual precipitation is ~1500 mm on average with maximum rainfall occurring between June and October (Lambert and Burnett, 2003). The water depth is only ~2 m as far as 1,000 m off shore (Lambert and Burnett, 2003) and the average tidal range is 1.0 m (Santos et al., 2009a). The upper meter of the sediment consists of sand and muddy-sand beneath it until carbonate rock substrate is reached at around 5 m below the surface. Groundwater temperature in the shallow subterranean estuary slightly fluctuates between seasons with a minimum of 21^{o}C in winter, and 25^{o}C in fall (Santos et al., 2008). The seawater temperature is around 30^{o}C in the summer and 14^{o}C in the winter. With averages of 786 μM (maximum of 952 μM), the concentrations of DOC in shallow beach groundwater are high (Santos et al., 2008).

2.2. Sampling

Groundwater in the subterranean estuary and the adjacent coastal waters were continuously monitored for FDOM, radon (^{222}Rn) and accessory parameters (salinity, pH, and temperature) from 22 Sep. to 13 Oct. 2007. In addition, discrete water samples were taken hourly over one complete tidal cycle on 28 September 2007 for analysis of DOC and total dissolved nitrogen (TDN). Groundwater samples were drawn from a 0.5 m deep well which was located 2.3 m onshore of the high tide mark. Previous studies indicated that this is the most dynamic location of the subterranean estuary in terms of salinity fluctuations (Santos et al., 2008; Santos et al., 2009b). Seawater samples were collected from the coastal GOM through a pipe through which water was continuously pumped from 300 m offshore and 1.6 m depth.

2.3. FDOM Measurements

Two FDOM sensors were deployed over the three-week period. One was installed in the well (hereafter referred to as FDOM groundwater) and one connected to the end of the seawater line in the marine laboratory (hereafter referred to as FDOM seawater). FDOM groundwater was measured with a WET Labs ECO 3 sensor that simultaneously determines FDOM and chlorophyll-a fluorescence. FDOM in seawater was measured by a WET Labs ECO Fluorometer, equipped with a copper brush wiper to avoid biofouling. The sensors were calibrated by the manufacturer using quinine dihydrate and the FDOM concentration is expressed in ppb ($\mu g\ L^{-1}$) quinine. The excitation/emission wavelengths used in these devices are 370/460 nm for FDOM and 470/695 nm for chlorophyll-a. Both sensors were configured to measure FDOM (and chlorophyll-a in the well) in 5 minute time steps.

Mixing between freshwater with high DOM and seawater with low DOM concentrations may occur conservatively, or occur in conjunction with production or consumption of DOM. This non-conservative behavior can be identified as deviations from the conservative mixing line obtained from plotting salinity versus the concentration of the parameter of interest. To calculate DOM production or consumption in the groundwater, we calculated the area between the linear conservative mixing line (in the salinity versus concentration plot) and the actual data by using the 'trapezoidal rule' approach (e.g. Bourget and Delouis, 1993). It was done by dividing the area under the production curve into several trapezoids, calculating the area of each trapezoid, summing all the areas, and this total area was then subtracted by the area below conservative mixing line curve.

2.4. Physicochemical parameters

A CTD (conductivity, temperature and depths) probe was deployed in the well and in the seawater outlet to continuously measure salinity and temperature, and water level in the well. Precipitation data were obtained online (www.wunderground.com) from a weather station located at Alligator Point, about 10 km away from our study site. In addition to continuous in situ monitoring, salinity, temperature, and pH were measured with a YSI-85 probes immediately after collection of the discrete samples. The concentration of ^{222}Rn was measured at a sampling rate of 1 hour in the seawater outlet of the marine laboratory using a RAD-7 device (Santos et al., 2009b). Groundwater flux was estimated based on the assumptions and equations explained elsewhere (Burnett and Dulaiova, 2003).

2.5. Discrete DOC and TDN Measurements

Samples for DOC and TDN (total dissolved nitrogen) were collected hourly from the well and GOM over a 15-hour period on September 28, 2007. Water was drawn from the well through acid-cleaned Teflon tubing using a polyethylene syringe. The tubing was thoroughly flushed with groundwater before sampling. Samples from the GOM were directly taken from the seawater outlet in the laboratory through which seawater was continuously flowing. Immediately after sampling the water was filtered through disposable 0.7 μm Whatman GF/F syringe filters, acidified with HCl (analytical grade) to pH 2 to remove inorganic carbon, and fire-sealed into pre-muffled (500°C) glass ampoules. DOC and TDN were analyzed using a Shimadzu TOC-V_{CPH} total organic carbon analyzer equipped with a TNM-1 total nitrogen measuring unit. Analytical errors for DOC and TN were <5% with a detection limit of 5 μM. We included deep

sea reference samples distributed by Dennis Hansell of the University of Miami as external standards in the measurements.

Table 2.1. Average (Avg) ± standard deviation (St. Dev.) of FDOM, DOC, and TDN concentration, temperature, salinity, chlorophyll-a concentration, water level, and Radon-222 concentration in groundwater and seawater during the long-term time series.

		Groundwater	Seawater
FDOM, ppb	Avg. ± St. Dev	156 ± 19	28 ± 2
	Min. - Max.	98 - 234	22 - 34
DOC, μM	Avg. ± St. Dev	72 ± 42	294 ± 42
	Min. - Max.	634 - 777	272 - 340
TDN, μM	Avg. ± St. Dev	93 ± 15	26 ± 2
	Min. - Max.	66 - 115	24 - 29
Temp, ^{o}C	Avg. ± St. Dev	26 ± 1	29 ± 2
	Min. - Max.	24 - 27	25 - 33
Salinity	Avg. ± St. Dev	28 ± 6	35 ± 1
	Min. - Max.	3 - 336	34 - 36
Chl-a, mg L^{-1}	Avg. ± St. Dev	7 ± 2	na
	Min. - Max.	3 - 12	na
Water Level, cm	Avg. ± St. Dev	28 ± 12	17 ± 28
	Min. - Max.	11 - 65	-71 - 73
Rn, dpm m^{-3}	Avg. ± St. Dev	na	4843 ± 1005
	Min. - Max.	na	2013 - 6935

2.3. Results and discussion

2.3.1. Temporal distribution of FDOM and DOC in seawater and groundwater

FDOM concentrations in the groundwater were much higher than those in seawater (Table 2.1). The mean FDOM concentrations for groundwater and seawater were 156 ppb and 28.1 ppb, respectively. In the well, salinity ranged from 2.5 to 35.4 while salinity in seawater ranged from 33.8 to 36.4. The average temperature in groundwater was only slightly different than that in seawater. Freshening of groundwater driven by a 26 mm rain event at the beginning of the experiment was associated with a maximum in FDOM concentration in the groundwater (Fig. 2.1). During the rain event, water level, FDOM concentration, and chlorophyll-a concentration were comparably higher than the respective averages, while temperature did not show any changes during this period. No additional rainfall events were observed during the rest of our study. Although the freshening effect in the seawater was not as pronounced as in the groundwater, the minimum salinity coincided with a maximum water level and FDOM concentration also in the seawater (Fig. 2.2). Temperature and Rn activities did not show clear variations in seawater.

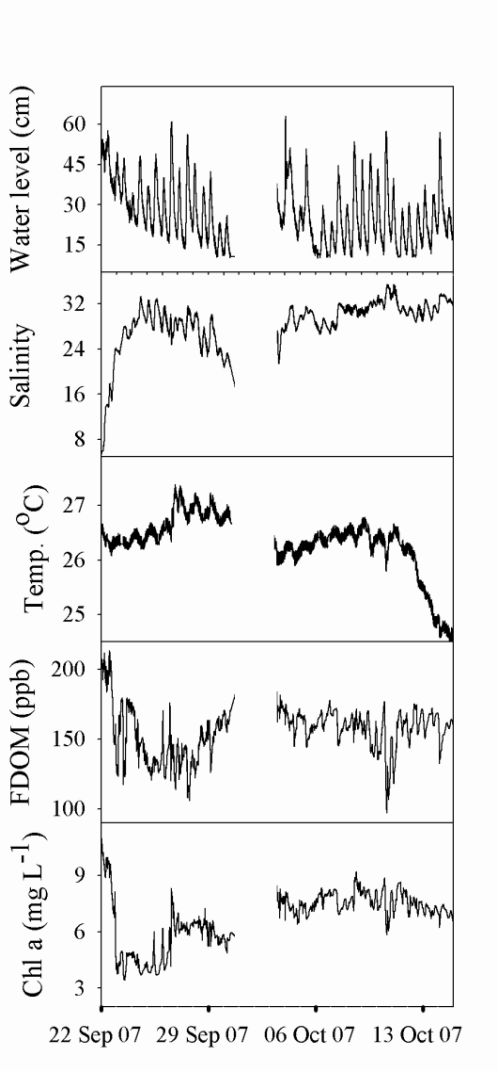

Figure 2.1. Results of the three-week time series in the 0.5-m deep beach groundwater well located at the high tide mark.

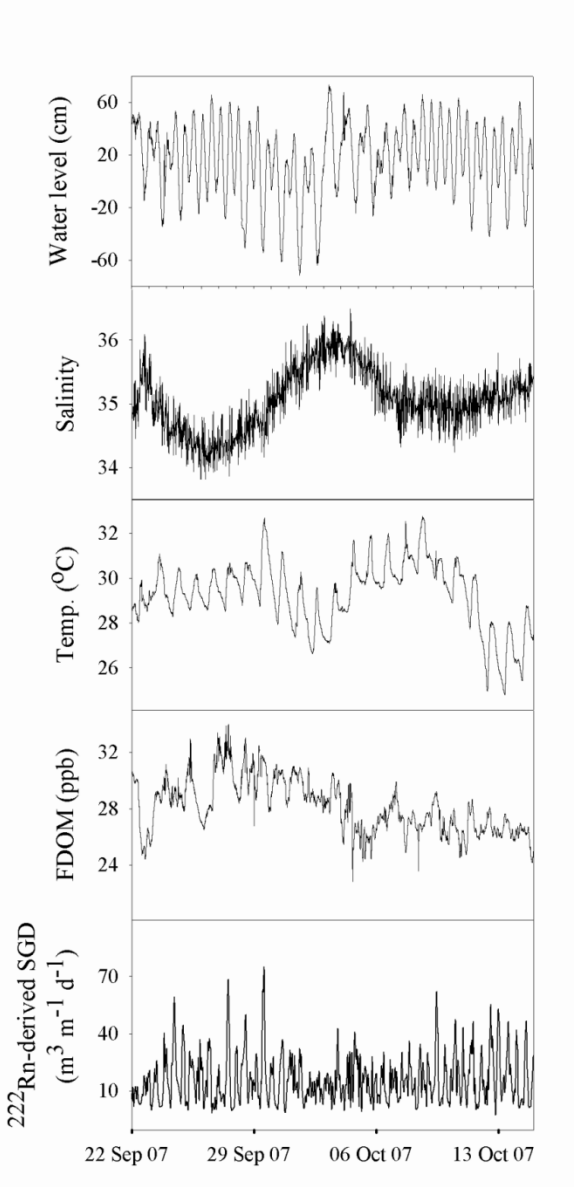

Figure 2.2. Results of the three-week time series measurements in the adjacent coastal seawater.

2.3.2. Non-conservative FDOM behavior

Processes in surface estuaries can most often be explained sufficiently by a classical mixing model of freshwater and seawater, in which salinity as a conservative tracer for seawater is plotted versus the concentration of the parameter of interest. This plot implies production of the parameter of interest if its concentration data are above the conservative mixing line, or

consumption if they are below the line. We also applied this approach to understand which process controls FDOM variability in this system on different time scales. Our results revealed that simple conservative mixing between the fresh groundwater end-member and the seawater end-member cannot explain the FDOM concentrations observed in groundwater (Fig. 2.3). The observed FDOM distribution can only be explained by biogeochemical processes within the STE releasing FDOM to solution at groundwater salinities higher than ~25. Interestingly, the FDOM concentrations in saline groundwater (~100 ppb) were about 4-fold higher than the FDOM concentrations in seawater (~25 ppb) with approximately the same salinities (~34). This implies effective FDOM production soon after seawater infiltrates the beach sediments at high tide. Based on the shape of the FDOM vs. salinity plot (i.e., steeper slopes at high salinities), we speculate that this initial increase in FDOM concentrations is a result of effective respiration of labile marine organic matter. As saline groundwater ages and mixes with fresh groundwater, the remaining organic matter likely becomes more refractory, potentially preventing significant FDOM production. As a result, a further increase in FDOM from ~150 ppb at salinity 25 to 200 ppb at salinity 0 seems to be related to conservative mixing between fresh groundwater and brackish groundwater already enriched in FDOM.

The observed FDOM and associated DOC (Santos et al., 2009b) production in the high salinity region of the Turkey point subterranean estuary contrasts to previous surface estuary investigations. For example, Yamashita et al. (2011) demonstrated that DOC and “humic-like” FDOM behave conservatively in the Liverpool Bay. Del Castillo et al. (2000) made similar conclusions for FDOM on the West Florida Shelf. This contrast between surface and subterranean estuaries is likely related to longer residence times of groundwater than surface waters (Santos et al., 2009b), higher microbial activity in beach sands than in the water column

(Wild et al., 2006), and the constant input of marine organic matter and oxygen into the beach associated with tidal pumping (Billerbeck et al., 2006). Combined, these processes make subterranean estuaries and beach sands effective bioreactors that can consume large amounts of organic matter and release dissolved products such as FDOM.

To further investigate the time scale behind these possible processes, we divided the time scale into three categories, short (a day or less), middle (a day to a week), and longer time scale (more than a week). For the short time scale analysis, we assumed that there was no accumulation of FDOM in the groundwater and groundwater flowed immediately to the coastal ocean without delay. We calculated production based on the lowest and highest daily salinities (see inset in Fig. 2.3). For the middle time scale analysis, we assumed that there was accumulation of FDOM in the groundwater, while the fresh end-member changed on a daily basis. For this category, we calculated production based on the lowest daily salinity and the highest salinity of all samples. For the longer time scale analysis, we also assumed that there was accumulation of FDOM in the groundwater but the fresh end-member did not change during the period of this study.

For each approach, we assumed that the same fresh and saline end-members mixed, and flowed back and forth depending on the residence time of water in the STE. The production was calculated based on the lowest and the highest salinity of all samples in each subset. In Figure 2.3, the highest salinity of all groundwater samples was found in marine groundwater. To avoid random errors caused by outliers, the five highest and lowest values were excluded from the calculation. The average of the next ten highest/lowest values was then calculated for area integration. The next step was to correlate production of each time scale to maximum, minimum, and average values of salinity and water level, both in groundwater and seawater. The highest

correlation (r^2=0.51, n=6188, p<0.001) was found between the maximum FDOM production for the middle time scale and average groundwater level. Interestingly, we found no significant correlation between the FDOM production and average seawater level. This suggests that FDOM production in the upper part of the sediment was controlled by the average groundwater level, and the groundwater level was driven by freshwater input, assuming that the tidal cycle was constant.

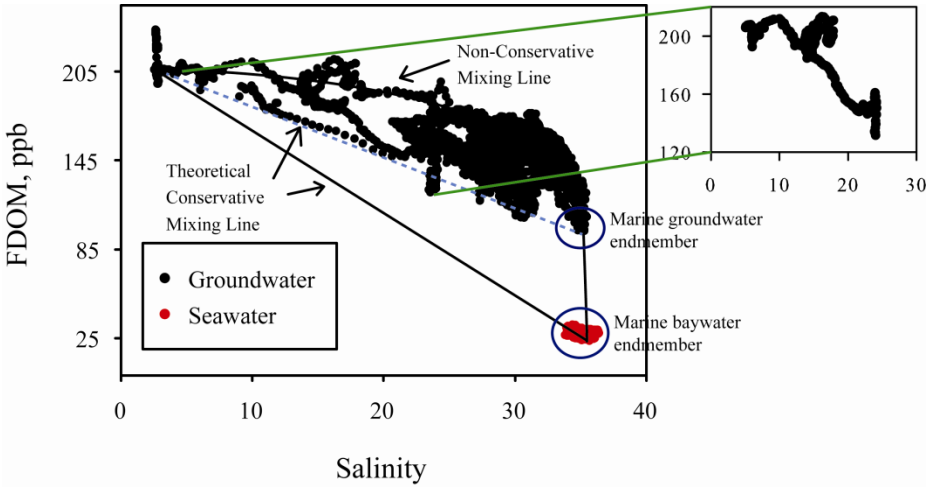

Figure 2.3. Mixing diagram for FDOM in the groundwater. The black line indicates conservative mixing of sea- and fresh groundwater. The blue dotted line indicates conservative mixing using the marine groundwater as an end-member. Inset is an example of the FDOM daily cycle in the groundwater.

2.3.3. Evidence for SGD-derived FDOM fluxes

The FDOM production curve in the groundwater suggests a flow of FDOM via SGD into the GOM. Because the coastal waters are not a closed system, alongshore and cross-shore mixing could alter FDOM concentrations. To assess this possibility we removed long-term trends and restricted our correlation analysis to tidal fluctuations of the GOM, without including the local groundwater data. For this purpose we calculated one-day moving averages for FDOM in the coastal GOM and ^{222}Rn-derived SGD and subtracted these "background" concentrations from

the respective hourly data. While a large scatter was observed, the detrended concentrations of FDOM and ^{222}Rn-derived SGD were significantly correlated (Fig. 2.4b, $p<0.001$); whereas the original raw data did not show any correlation (Fig. 2.4a). This correlation is independent evidence that FDOM in the coastal waters is at least partially driven by local tidally-driven SGD and larger-scale mixing processes.

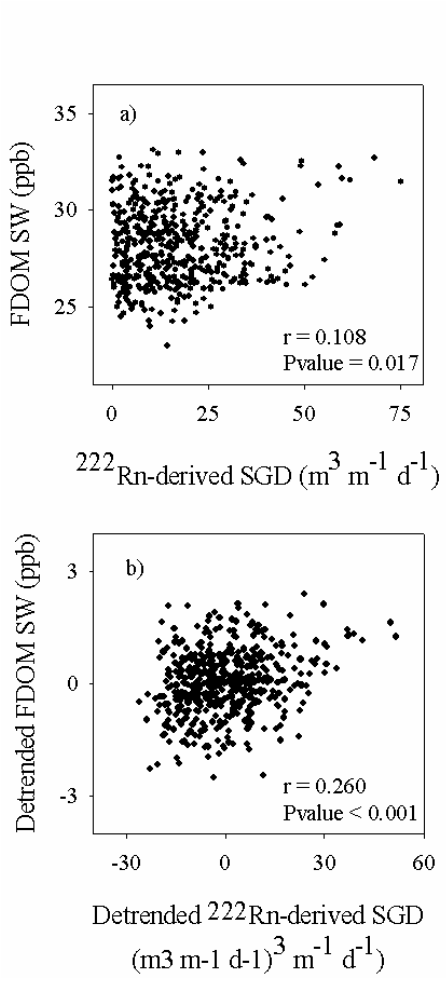

Figure 2.4. Correlation between FDOM seawater and ^{222}Rn-derived SGD a) before detrending and b) after detrending. All data passed a test for normal distribution.

The scatter in Figure 2.4b indicates the impact of processes other than those considered. For instance, it may be possible that there was a lag time of FDOM to travel from the groundwater to the adjacent coastal waters. In order to test this hypothesis, we used radon as a

groundwater tracer. The respective FDOM concentrations at a given time point in the well served as an end-member concentration for groundwater at any time point. Groundwater-related fluxes of FDOM were calculated as a function of this end-member concentration and SGD rates. Quantitative estimates of radon-derived SGD rates are reported elsewhere (Santos et al., 2009b). FDOM loads to the GOM were predicted by multiplying ^{222}Rn-derived SGD (as a measure for SGD flux) with FDOM concentrations in the well (as the groundwater end-member). To assess whether there was a lag between FDOM concentration in the coastal waters and in the well, various lag-times of groundwater were applied and Pearson correlation coefficients were calculated between the product of ^{222}Rn-derived SGD and FDOM concentration in the well versus FDOM concentration in the GOM. However, lag times did not enhance the correlation, indicating that other factors were responsible for the observed scatter.

It should be noted that the radon-derived SGD considered here includes both freshwater and seawater, which pass through the subterranean estuary. In our system, about 95% of the SGD is related to saline water recirculation into the beach face (Santos et al., 2008). During the passage through the subterranean estuary, FDOM is involved in numerous biogeochemical processes in the sediment, and when released to the surface, photobleaching will degrade FDOM (Blough and Del Vecchio, 2002). All these processes may contribute to the scatter observed for the SGD versus FDOM relationship in the coastal waters (Fig. 2.4). Nevertheless, it can be concluded that one of the many driving forces for FDOM in the near shore GOM was the discharge of groundwater high in FDOM.

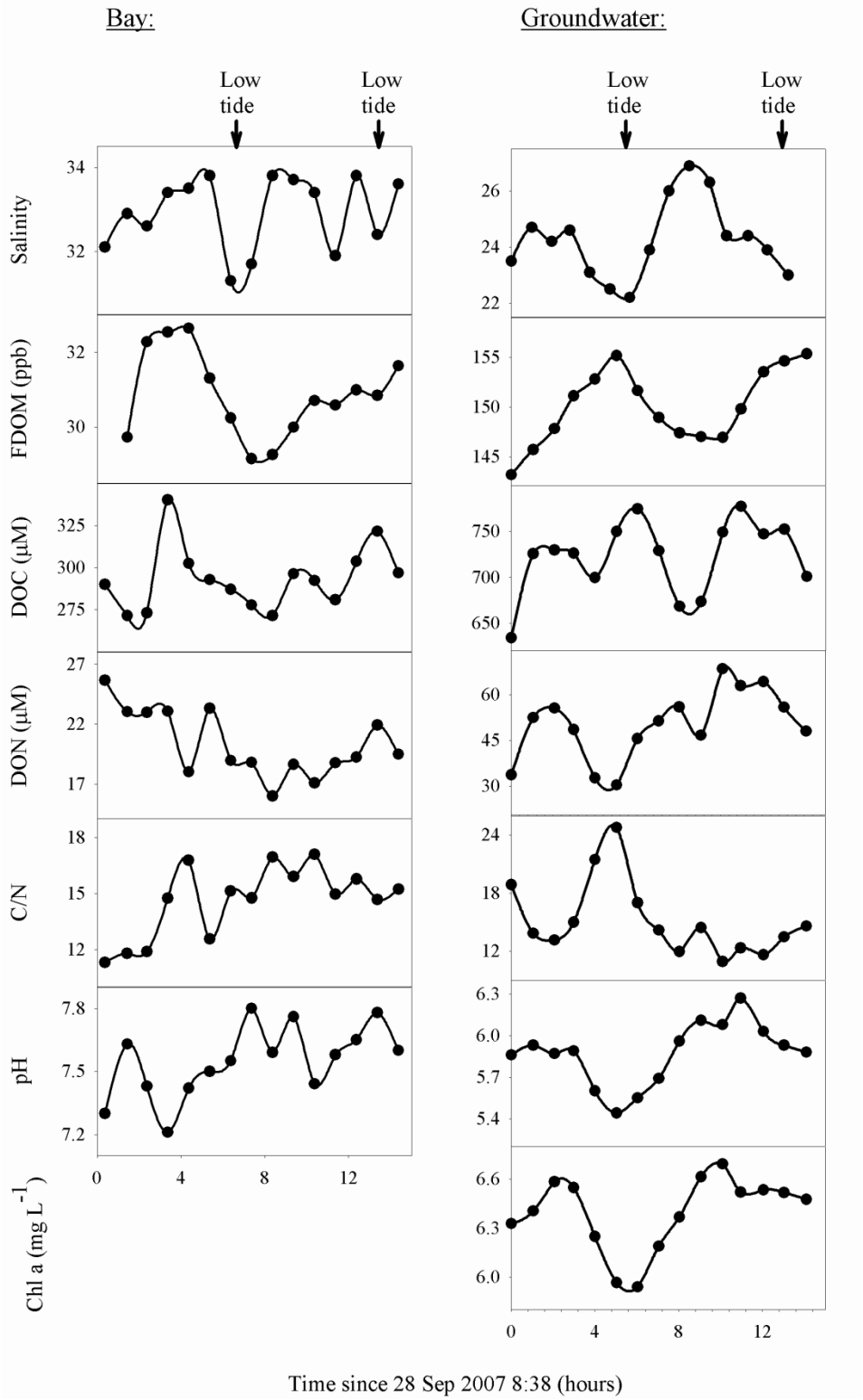

Figure 2.5. Fifteen-hour time series in the seawater (left panel) and groundwater (right panel). Note the different Y axis scales.

2.3.4. Potential sources and biogeochemical properties of FDOM

Discrete sampling (15 hours) of seawater (Fig. 2.5 left panel) showed a clear trend over the first eight hours. The salinity maximum at around five hours after the sampling started coincided with a FDOM maximum. Not only did the FDOM concentration increase but the DOC concentration increased as well at the beginning of sampling. There was a decreasing trend of DON concentration from almost 27 to approximately 17 μM during the same period. Discrete sampling in groundwater (Fig. 2.5 right panel) also showed a clear trend during the first tidal cycle. When salinity reached its minimum, FDOM and DOC concentration reached their maximum levels. In contrast, DON and chlorophyll-a reached their minimum values at the same time. An opposite trend was observed during the second tidal cycle when salinity reached its maximum. A relatively wide range in the C/N ratios suggest that there were different waters mixing in the groundwater. The two observed maxima of FDOM concentrations in the well took place at low tide and minimum salinity. The first maximum of FDOM concentration was associated with high C/N ratios, low chlorophyll, and low pH. This is consistent with a primarily freshwater source carrying terrigenous DOM. The second maximum in FDOM concentration, however, coincided with low C/N ratios, high chlorophyll, and high pH, which indicates the presence of marine DOM. It is possible that diurnal cycles of photosynthesis and respiration in the coastal waters, linked with seawater infiltration into the beach face at high tide and discharge at low tide, were responsible for these fluctuations in groundwater.

These complete tidal patterns indicate at least two major potential sources for FDOM in the groundwater: (1) terrigenous DOM of vascular plant origin, i.e. soils of the adjacent pine forest seem to contribute to the high FDOM in fresh groundwater, and (2) marine sources; i.e. phytoplankton degradation products probably contribute to the FDOM enrichment in

groundwater with high salinities. Soil-derived DOM contains more aromatic groups and therefore exhibit a stronger fluorescence than marine DOM (Esteves et al., 2009). We also noticed that there was seagrass debris accumulating on the beach at the high tide line during sampling which could be another potential source of DOM (Stabenau et al., 2004), which could support FDOM production in the STE during longer periods.

A positive correlation was also observed between FDOM and chlorophyll-a in the well ($p<0.05$; Fig. 2.6). This supports the possibility that there was a common source of chlorophyll-a and FDOM, and implies that degradation of marine DOM is likely a main factor behind the non-conservative FDOM behavior observed in groundwaters with salinities >25. Chlorophyll-a itself does not produce FDOM, but intrusion of labile, algal-derived DOM into the subterranean estuary likely increases chlorophyll-a and FDOM at the same time. Terrigenous soil-derived DOM, on the other hand, does not contain chlorophyll-a, but has strong fluorescence. The observed relationship between FDOM and chlorophyll-a therefore indicates the presence of labile algal-derived biomass in the groundwater.

The carbon-normalized FDOM (FDOM/DOC) was consistently higher in the groundwater than in the coastal waters (Fig. 2.7a). This indicates a major high fluorescence component in groundwater DOM possibly of terrestrial origin and a low fluorescence background in the associated marine waters. The low FDOM/DOC ratio in the GOM waters may be attributed to a primarily marine source of DOM (Esteves et al., 2009), or to photodegradation which can be a major sink of FDOM (Andrews et al., 2000).

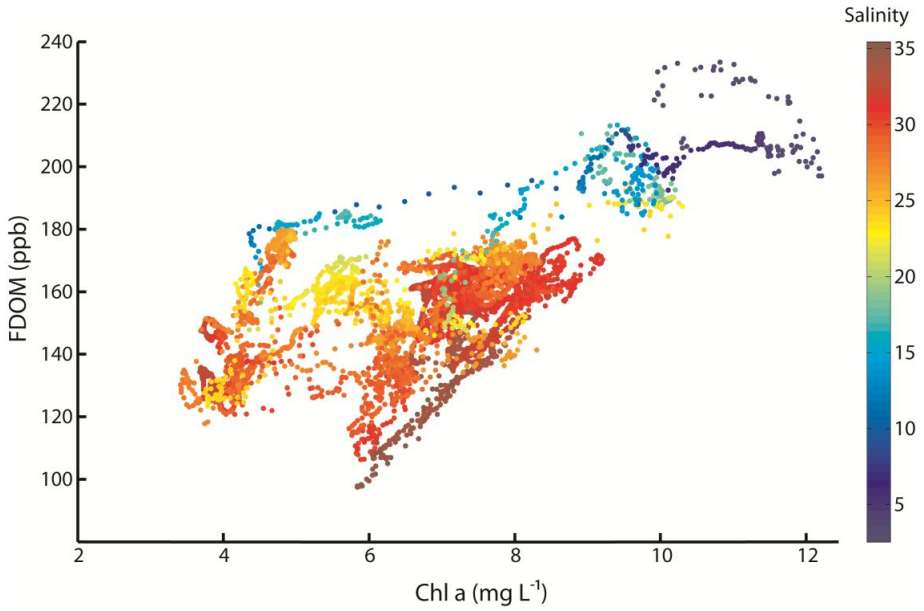

Figure 2.6. Correlation between FDOM and chlorophyll-a in the groundwater. Color gradient indicates salinity of the groundwater.

To be suitable as a source tracer, a parameter needs to be source specific. The FDOM/DOC ratio has potential as a tracer for the source of DOM in the studied system, because marine and groundwater sources of DOM could be clearly distinguished (Fig. 2.7a). Instead of the C/N ratios, Perdue and Koprivnjak (2007) pointed out that the N/C ratios should be used to estimate the source for a carbon basis. Interestingly, the N/C ratios did not show the same pattern as FDOM/DOC. A plot of salinity versus the N/C ratio (Fig. 2.7b) showed a wide range of the N/C ratio for salinities lower than 28. Moreover, a scatter plot between N/C and FDOM/DOC (Fig. 2.7c) indicated that even though the FDOM/DOC ratio clearly separated the two sources, N/C ratio could not. Thus, the N/C ratio is a weak tracer for the two sources in this system. Santos et al. (2008) suggested an intensive cycling of nitrogen in this subterranean estuary, including mineralization of organic nitrogen and denitrification, which may have contributed to the wide range of N/C values observed in this study.

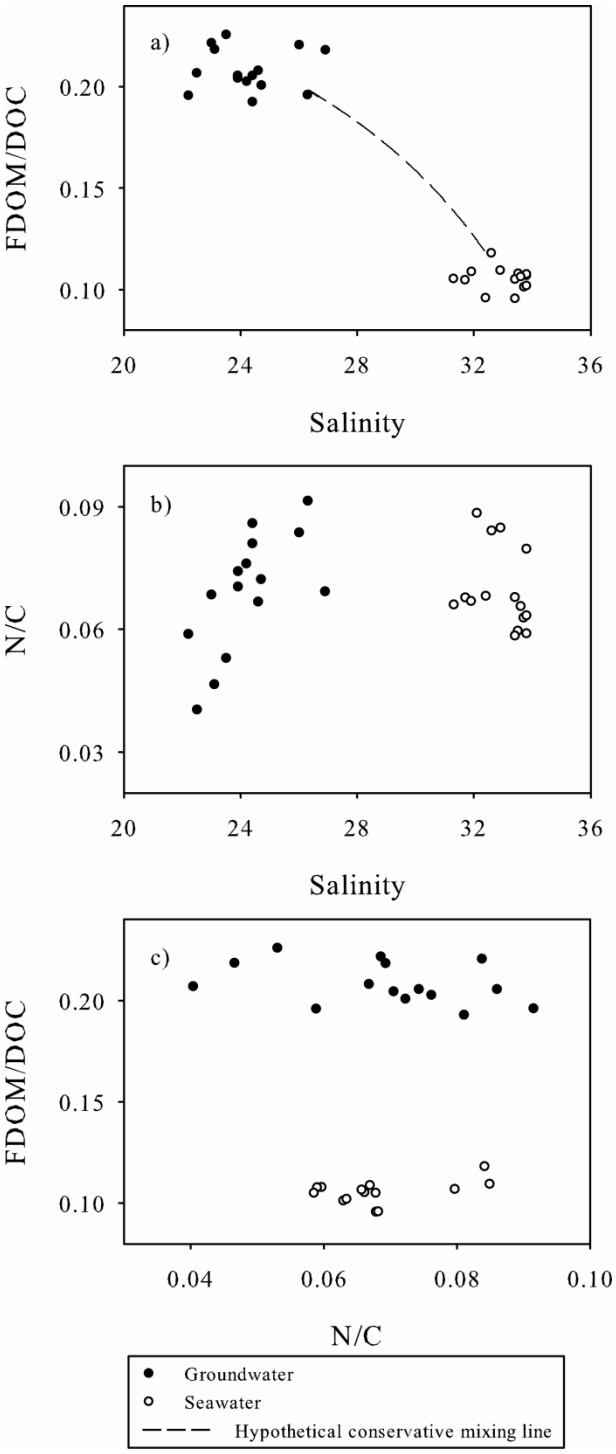

Figure 2.7. Plots of salinity versus FDOM/DOC ratio, salinity versus N/C ratio, and N/C ratio versus FDOM/DOC ratio, both in groundwater and seawater.

The use of optical properties of DOM as a proxy of DOC concentrations and sources has been explored previously with a focus on DOM absorbance (Kowalczuk et al., 2010). Significant correlations between FDOM and labile DOC concentration have been also reported (Ferrari et al., 1996). As observed in this study, FDOM/DOC ratios are source-specific, but photodegradation and seasonality may cause deviations of the source specificity on larger spatial and temporal scale.

2.3.5. FDOM as a proxy of DOC fluxes

FDOM and DOC concentrations were significantly correlated, both in the coastal GOM waters and groundwater ($p<0.01$). Therefore, there is a possibility to estimate DOC concentrations simply from the fluorescence measurements. Because the FDOM/DOC ratio was source specific, this has to be done separately for the coastal waters and groundwater.

To estimate FDOM fluxes to the coastal ocean, it is necessary to determine the effective freshwater concentration in the groundwater, which can be calculated by extrapolating the FDOM-salinity trend to obtain the intercept at zero salinity (Santos et al., 2008) or by using FDOM concentration from the lowest salinity. If the first approach is used with our groundwater data, the effective FDOM freshwater concentration would be unreasonably high or infinitive depending on the choice of the seawater end-member. The second approach can be applied for our system because the sampling included the very low (almost fresh) salinity range. Multiplying the FDOM concentration at the lowest salinity from the long-term time series (FDOM = 7 ppb) with the average DOC/FDOM ratio in the groundwater (4.8 ± 0.24 μM/ppb) results in an effective freshwater DOC concentration of 991 ± 50 μM. Using a fresh SGD flux of 0.5 $m^3 m^{-1}$ day^{-1} for this area (Santos et al., 2009b), the DOC flux would be at least 471 mmol m^{-1} day^{-1}.

Santos et al. (2009b) calculated a more than 10 times higher DOC flux in August 2007, because they estimated the freshwater end-member by extrapolating the trend of DOC production in brackish/saline water to zero salinity. This approach most likely resulted in an overestimation of the freshwater end-member. On the other hand, it must be taken into account that Santos et al. (2009b) sampled during a different time period. Even though that study as well as this study considered time series of many days to weeks, both are only snapshots in time and space. If the DOC flux via SGD in our study would be assumed to be representative for the whole Gulf Coast of Florida (shoreline length is approximately 1200 km), including the assumption that this coast has the same hydrological and biogeochemical processes as our site, the fresh SGD DOC flux would be 0.6 Mmol day^{-1}. Compared with the DOC discharge of the Apalachicola River (Santos et al., 2008), the calculated fresh SGD DOC flux is one order of magnitude lower.

In summary, we found that FDOM was introduced to the subterranean estuary from a nearby forest but also produced in the subterranean estuary itself. Subterranean estuaries may thus differ from surface estuaries where FDOM often behaves conservatively likely because of shorter residence times and lower microbial activity. On site production thus must be considered when calculating the flux of FDOM to the coastal ocean via groundwater pathways. We also demonstrated that FDOM can be used as a proxy of DOM, both as a proxy of its source and of its concentration.

Chapter 3

Fluorescent dissolved organic matter (FDOM) variability in a subterranean estuary, from multiple wavelengths to a single wavelength approach

Fluorescent dissolved organic matter (FDOM) variability in a subterranean estuary, from multiple wavelengths to a single wavelength approach

I Gusti Ngurah A. Suryaputra[1], Isaac R. Santos[2], Thorsten Dittmar[1]

Submitted to Marine Chemistry

[1] Max Planck Research Group for Marine Geochemistry, Carl von Ossietzky University, ICBM, Carl-von-Ossietzky-Str. 9-11, D-26129 Oldenburg, Germany

[2] Centre for Coastal Biogeochemistry, Southern Cross University, Lismore, NSW, 2480, Australia

Abstract

A study of fluorescent dissolved organic matter (FDOM) was performed in a subterranean estuary (STE) at Turkey Point, Florida, USA. Samples were collected over a tidal cycle from five 0.5 m deep wells installed across the beach face. The aims were to characterize FDOM fluorophores and their sources in a STE; to determine the driving forces of FDOM variability; and to explore parallel factor (PAFARAC) and other statistical tools for the interpretation of excitation/emission fluorescence matrices in a STE. Using PARAFAC analysis, one "protein-like" and three "humic-like" components were successfully modeled. With help of partial least square (PLS) regression analysis, we were able to identify major processes influencing FDOM pattern. Humic-like component C3 was probably related to microbial nitrification in the presence of vascular plant material in the STE. The other humic like components, C2 and C4, and protein like component C1, were related, but were uncoupled to C3. DOM dominated by C1, C2, and C4 was probably released in the STE during mineralization of marine-derived biomass. Regression and correlation matrices were successfully used to relate single fluorescence wavelengths to specific parameters of interest such as DOC. This novel approach is a useful statistical tool to develop in situ analytical technologies in STEs.

3.1. Introduction

Chromophoric (or colored) dissolved organic matter (CDOM) is the optical fraction of dissolved organic matter (DOM). As one of the light attenuation components, besides turbidity and chlorophyll *a*, CDOM has a great impact on the UV light penetration (Tedetti and Sempéré, 2006) and primary production in the water column (Foden et al., 2008; Zepp et al., 2008). There are two methods to analyze CDOM, i.e. by measuring its absorbance (CDOM absorbance) and

fluorescence (fluorescent DOM, FDOM). Although FDOM is a much more sensitive analysis than CDOM absorbance, only more recently has fluorescence received similar attention. Coble (1996) used the excitation emission matrix (EEM), i.e. a three dimensional matrix formed by repeated emission scans collected at certain excitation wavelengths, to investigate FDOM.

The difficulty in retrieving component information out of EEM was solved by Bro (1997) who used a statistical tool called parallel factor (PARAFAC) and applied it on fluorescence data containing tyrosine, tryptophan, and phenylalanine. Stedmon et al. (2003) then used it on FDOM data from natural waters, followed by its useful tutorial (Stedmon and Bro, 2008). PARAFAC is a method used to decompose multidimensional data into its underlying components. Compared to other multivariate data analysis, such as principal component analysis (PCA), PARAFAC analysis is more suitable for multidimensional data because the data does not need to be unfolded to make two dimension matrices. Difficulty and confusion in referring results back to its original dimension can be avoided. PARAFAC analysis has successfully been applied in seawater and freshwater, for example, to trace sources of FDOM (Murphy et al., 2008; Walker et al., 2009; Yamashita et al., 2008), to verify the importance of phytoplankton degradation as a source of FDOM (Zhang et al., 2009), and to model water quality (Murphy et al., 2011; Zhang et al., 2009; Zhuo et al., 2010).

While a number of studies have assessed FDOM dynamics in river estuaries (Murphy et al., 2008; Stedmon and Markager, 2005a; Yamashita et al., 2008), very little information is available on how FDOM behaves in subterranean estuaries. A recent study of Kim et al. (2012) observed that “protein-like” and “humic-like” fluorescence components were produced by degradation of benthic algae in a subterranean estuary (STE) in Korea; and Suryaputra et al. (submitted) emphasized the importance of a STE as a source of FDOM to the coastal ocean at

the same coastal site in the Northern Gulf of Mexico where this present study was performed. A STE is defined as the area where fresh groundwater mixes and interacts with seawater which has penetrated the aquifer (Moore, 1999). STEs can modify the chemistry of groundwater discharging into the coastal ocean and thus influence the biological communities of coastal waters (Li et al., 1999; Moore, 1996; Moore, 1999). Water circulation in a STE is driven mostly by tidal pumping and fresh groundwater discharge (Santos et al., 2008; Santos et al., 2009; Simmons, 1992).

Our study focused on FDOM in a STE which aimed at (1) characterizing FDOM fluorophores and their sources in a STE, (2) determining driving forces behind FDOM variability, and (3) testing the capability of PARAFAC and other statistical analysis to identify biogeochemical and mixing processes in a STE system.

3.2. Materials and Methods

3.2.1. The study area

This research was part of detailed beach groundwater time series study (Santos et al., 2009) in a STE in the Northern Florida, USA. Samples were collected from Turkey Point, located approximately 200 m east of the Florida State University Coastal and Marine Laboratory. Seepage water from an unconfined aquifer and submarine springs from the confined Floridan Aquifer can be found at this nearshore site. The surface sediment consists mostly of sand, followed by sandy mud until a dense grey mud layer appears at ~3 m, and carbonate rock can be found on ~5 m depth (Santos et al., 2008). More details on this site are described elsewhere (Burnett and Dulaiova, 2003; Lambert and Burnett, 2003; Santos et al., 2008).

Groundwater samples were drawn from five 0.5 m deep wells using a push-point stainless steel piezometer attached to a Teflon tubing. Each well was installed along a transect across the beach (Fig. 3.1). The tubing was thoroughly flushed with water sample prior to actual sampling. Water samples were collected using a polyethylene syringe every 90 minutes for a total of 16 hours in January 2008. A total of 60 samples for FDOM were collected and filtered with help of the syringe through 0.7 μm Whatman GF/F glass fiber syringe filters, stored in amber vials, and kept in the cold (~ 4^{o}C) and dark until further analyses. Groundwater level was measured using automated Van Essen conductivity-temperature-depth (CTD) divers.

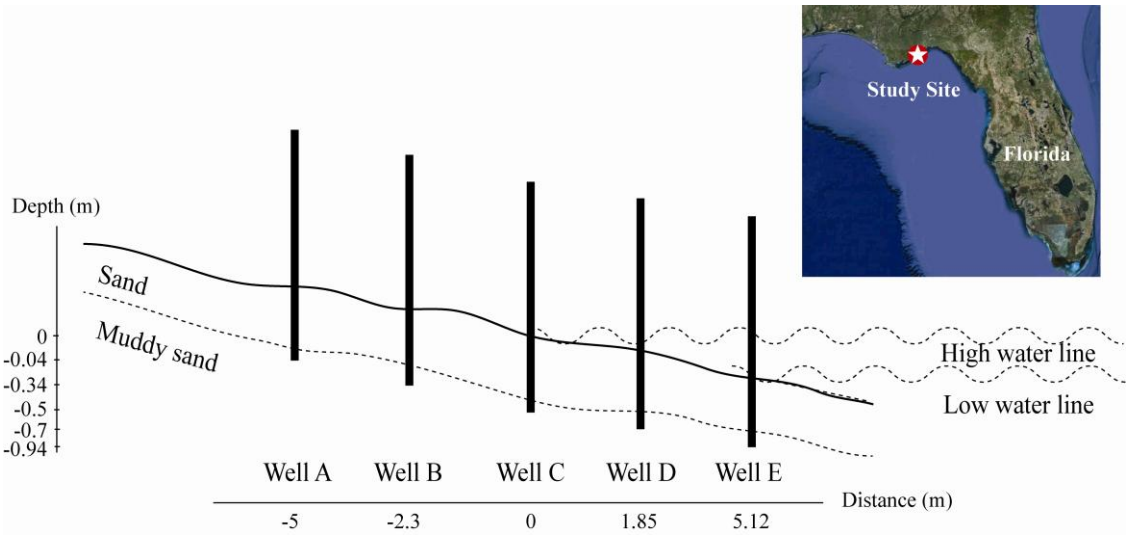

Fig. 3.1. Our study area. Five push-point piezometer wells were installed on the beach. Depth and distance were relative to high tide mark (modified after Santos et al., 2009b).

3.2.2. FDOM measurement

Samples were equilibrated to room temperature prior to fluorescence measurement. Fluorescence data was obtained in excitation emission matrices (EEMs) on a Jobin Yvon SPEX Fluoromax-4 spectrofluorometer. Analyses were done in a 1 cm quartz cuvette using excitation wavelengths at 240-500 nm with 5 nm increments, and emission wavelengths at 300-600 nm

with 2 nm increments. Concentrated samples for FDOM were diluted with Milli-Q water, thus their absorbance were less than 0.02 to minimize inner filter effect (Zepp et al., 2004). Post processing data to remove Raman and Rayleigh scattering, and to calibrate the results into ppb of quinine sulfate equivalent (QSE), were performed using FL Toolbox developed by Wade Sheldon (University of Georgia) for Matlab 5.3.

3.2.3. PARAFAC modeling

EEMs of samples were decomposed into their fluorophores using DOMFluor Toolbox ver 1.7 in Matlab R2007b with split-half validation (Stedmon and Bro, 2008). Prior to modeling, emission data from two times of excitation wavelength were cut to remove second order scattering artifacts. Furthermore, emission data were reduced to a maximum of 550 nm because there was an indication of secondary protein peaks propagated from its lower fluorescence wavelength. Scores of individual fluorophores were converted into intensity using the following equation (Kowalczuk et al., 2010):

$$I_n = score_n * Ex_n(\lambda_{\max}) * Em_n(\lambda_{\max})$$

where I_n is the fluorescence intensity of the *n*th component in given sample in QSE, $score_n$ is the Fmax of the *n*th component calculated using the toolbox, $Ex_n(\lambda_{\max})$ and $Em_n(\lambda_{\max})$ are the maximum loading, of excitation and emission, respectively, of the *n*th component. Total intensity was calculated as sum of the intensities of all components present in the sample.

Univariate and bivariate analysis, such as correlation and regression tests were performed using Sigmastat 3.5. Regression matrices were done in Matlab R2007b. Multivariate statistic, i.e. partial least square (PLS) regression was performed using The Unscrambler X v10.2 (Camo Software). This statistical procedure searches for linear correlation between environmental

variables (salinity, pH, O_2, dissolved organic carbon (DOC), dissolved organic nitrogen (DON), DOC/DON, nitrate (NO_3), ammonium (NH_4), phosphate (PO_4), and silicate (Si)) and FDOM variables (PARAFAC component intensities). PLS results are presented in score and loading plots, explaining variability in samples and variables, respectively.

3.3. Results

3.3.1. PARAFAC components

Four fluorescent components (Table 3.1; Fig. 3.2) were identified by the PARAFAC analysis and split-half validated. Component 1 (C1) had an excitation/emission maximum at 270/320 nm. Component 2 (C2) had one excitation maximum below 240 nm and a second excitation maximum at 295 nm with a general emission maximum at 408. Component 3 (C3) had a first excitation maximum at 245 nm and a second excitation maximum at 330 nm with an emission maximum at 466 nm. Finally, component 4 (C4) had one excitation maximum at less than 240 nm and a second excitation maximum at 305 nm, with an emission maximum at 422 nm. In general, fluorescence intensities at all wells were dominated by C1 except at well C where the intensity of C4 was slightly higher than C1. In contrast, C3 intensity was constantly the lowest at all wells (Table 3.2).

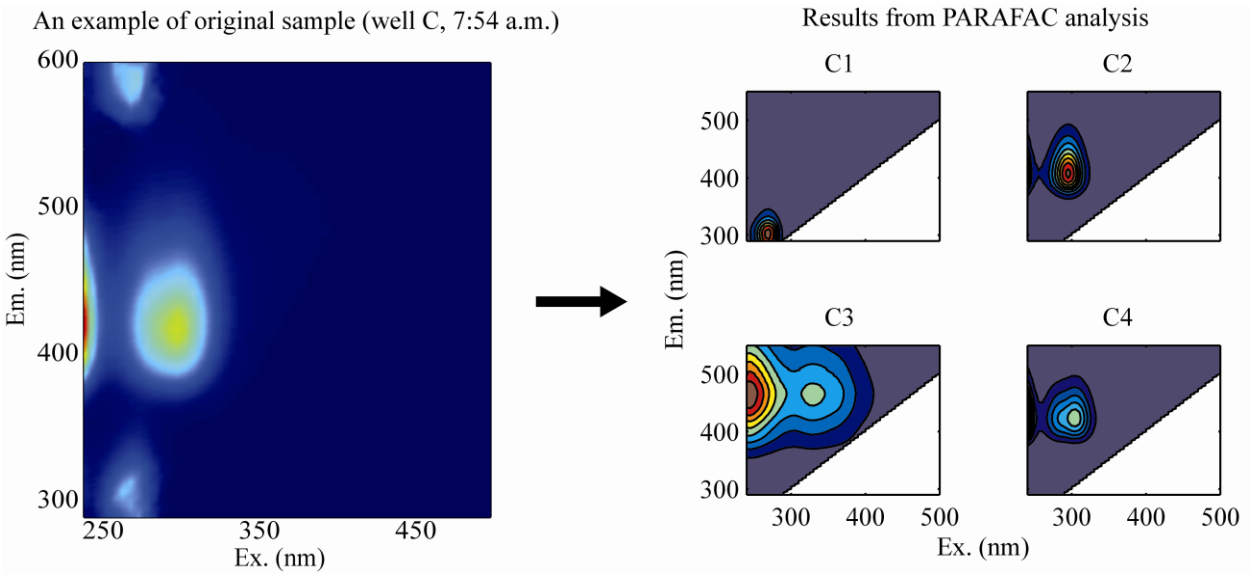

Fig. 3.2. An example of original EEM (left panel) and four components modeled by PARAFAC analysis (right panel). The fluorescence signal at an emission wavelength of >550 nm is a secondary peak propagated from its lower wavelength. PARAFAC was therefore restricted to emissions <550 nm.

3.3.2. Time series variability

There was no clear relationship between FDOM components and water level (Fig. 3.3). For instance, C1 intensity at well A increased in the beginning of sampling, followed by a decreasing trend before the groundwater had reached its highest level, and it increased again until the intensity reached its maximum value slightly before the lowest groundwater level. C2 intensity, at the same well, remained low and showed a maximum at the highest groundwater level. On the other hand, C3 reached its minimum intensity with the highest groundwater level, but it should be noted that the intensity of C3 was much lower than the other components. C4 showed a similar trend as C2. At well B, C1 intensity decreased with the increase of groundwater level, followed by random fluctuations. C2, at the same well, was absent most of the time. C3 showed its highest value at the maximum groundwater level, while C4 showed it at the lowest

groundwater level. At well C, intensities of C1, C2, and C4 showed similar trends; they increased in the middle and the end of sampling, whereas C3 showed a sudden drop in the beginning. C1, C2, C4 at well D showed almost the same trends with the highest intensities at the end; on the other hand, the maximum of C3 was found in the beginning. At well E, C1 and C2 reached its maximum value at the lowest groundwater level. C3 showed constant intensity most of the time at well E. And, C4 intensity was highest in the beginning and during the lowest groundwater level, its intensity increased again, but to a lower degree.

3.3.3. Correlation between intensity and other variables

Scatter plots between salinity and each FDOM components did not show any consistent patterns, and neither linear nor other correlations (Fig. 3.4). C total, i.e. the total fluorescence intensity of a sample, which was calculated as the summation of all components presented in a sample, did not correlate with the environmental variables salinity, pH, DOC, DON, O_2, NO_3, NH_4, PO_4, and Si. Of all FDOM components, only C3 showed a significant correlation ($p<0.05$) with oxygen, ammonium, nitrate, and DOC concentration, whereas the most significant correlation ($p<0.01$) was found between DOC and C3.

Table 3.1. Characterization of four components modeled by PARAFAC analysis. Secondary excitation maxima are presented in brackets.

Component	Excitation peak, nm	Emission peak, nm	Nomenclature used in the literature (Coble 1996)
C1	270	320	Tyrosine-like
C2	<240 (295)	408	Terrestrial UV humic-like and marine humic-like
C3	245 (330)	466	Terrestrial UV humic-like and visible humic-like
C4	<240 (305)	422	Terrestrial UV humic-like and marine humic-like

Table 3.2. Intensity and standard deviation (stdev) of each component at each well, n=12 per well.

Component	(Intensity ± stdev) at well A, ppb QSE	(Intensity ± stdev) at well B, ppb QSE	(Intensity ± stdev) at well C, ppb QSE	(Intensity ± stdev) at well D, QSE	(Intensity ± stdev) at well E, ppb QSE
C1	70.8 ± 65.4	52.2 ± 44.4	34.8 ± 64.7	27.3 ± 43.2	67.9 ± 119.1
C2	29.0 ± 44.3	14.3 ± 38.7	18.7 ± 38.2	6.1 ± 10.8	53.7 ± 55.3
C3	4.0 ± 1.0	7.7 ± 1.3	7.8 ± 1.2	5.0 ± 1.0	5.2 ± 1.4
C4	45.4 ± 90.0	14.8 ± 19.0	41.4 ± 106.3	9.4 ± 15.4	28.5 ± 38.9

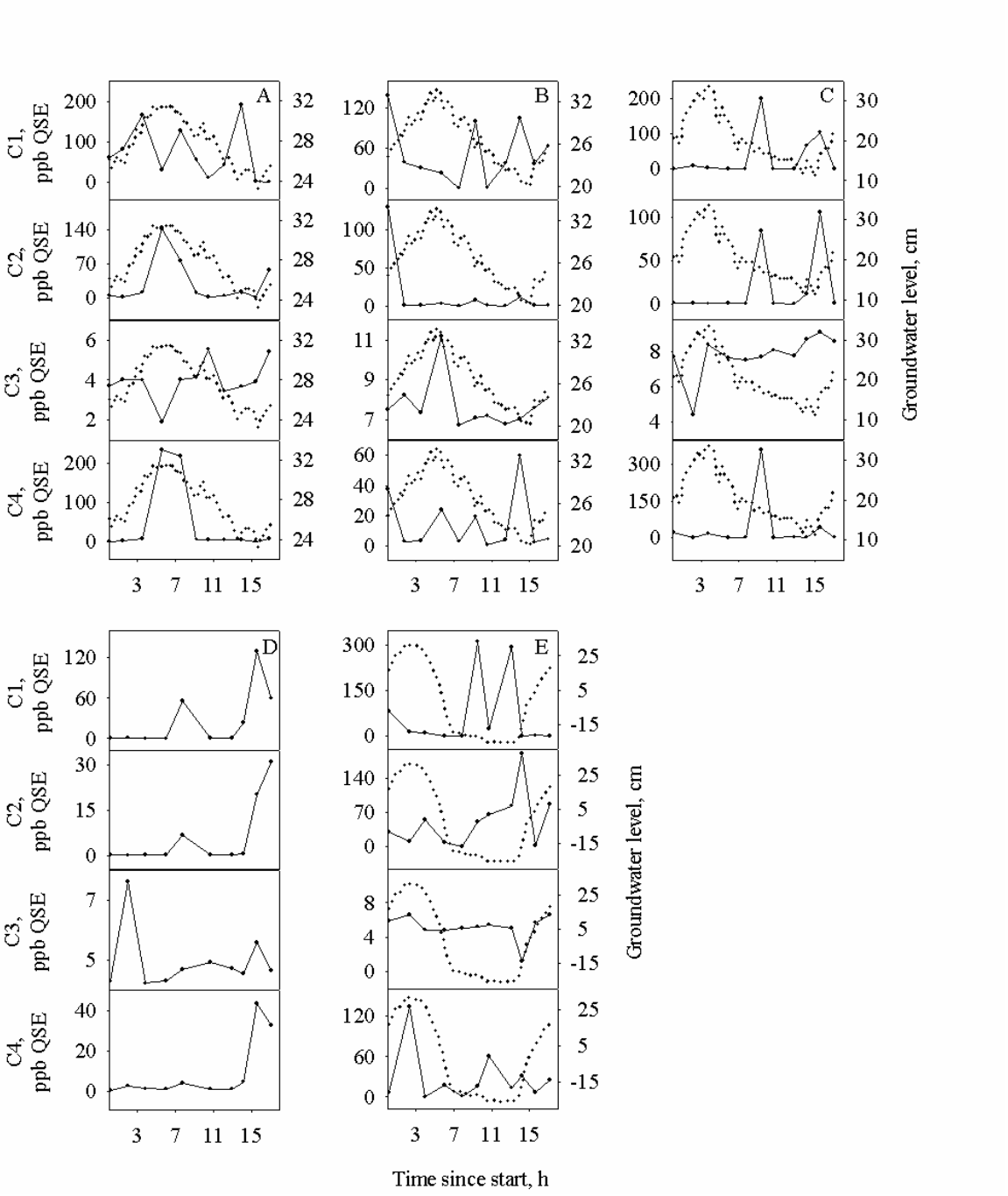

Fig. 3.3. Time series of PARAFAC components at well A (A), well B (B), well C (C), well D (D), and well E (E). Full line indicated intensity in ppb quinine sulfate equivalent (QSE) and dotted line indicated groundwater level in cm (not available for well D).

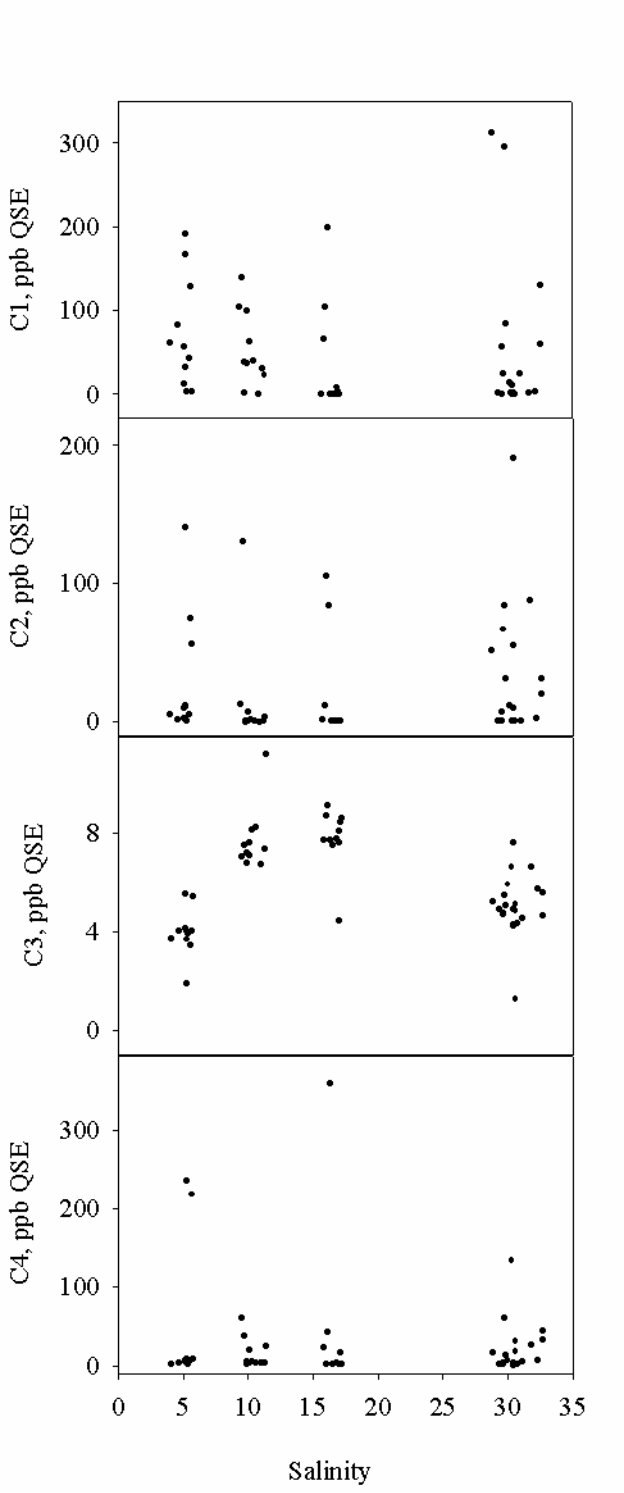

Fig. 3.4. Scatter plot between salinity and each PARAFAC component.

3.4. Discussion

The identified PARAFAC components correspond to previously identified EEM components before the introduction of PARAFAC. This consistency makes comparison with older studies possible (Table 3.1). C1, which was present in all but two samples, corresponded to the spectra of the "tyrosine-" or "protein-like" component (Coble, 1996). This "protein-like" component was previously found in high abundance in biologically active waters, such as ballast water (Murphy et al., 2006), coastal waters (Murphy et al., 2008), pore waters (Burdige et al., 2004), and autochthonous production in a mesocosm experiment (Stedmon and Markager, 2005b). C2 had a similar pattern to "humic-like peak A" and "marine humic-like peak M" (Baghoth et al., 2011; Coble, 1996). C3 is consisted with a combination of "terrestrial UV humic-like peak A" and "visible humic-like peak C" (Coble, 1996). This component was also found in other studies, e.g. in ballast water exchange samples (Murphy et al., 2006), in samples collected in the catchment of a Danish estuary (Stedmon et al., 2003), and in Pacific and Atlantic Ocean samples (Murphy et al., 2008). C4, was the combination of "terrestrial UV humic-like peak A" and "marine humic-like peak M" (Coble, 1996) and was also identified earlier (Murphy et al., 2006; Murphy et al., 2008; Stedmon et al., 2003). Humic-like components A, M, and C were also found in a porewater study in a tidal flat (Kim et al., 2012) and in an estuary (Burdige et al., 2004).

While FDOM in surface estuaries have previously been studied, its biogeochemistry in a STE has not been systematically studied. In our study, we expected temporal changes of FDOM with groundwater level variability during time series sampling and systematic changes during mixing of fresh groundwater and seawater. Apparently, none of C1, C2, C3, or C4 components showed a significant trend with changes in the groundwater level or salinity (Fig. 3.3). Therefore,

mixing of fresh groundwater and seawater was not the main driving force behind FDOM variability.

Surface estuary dynamics can usually be explained by mixing models between freshwater and seawater. Using such a model, freshwater input of certain parameters at a given site can be estimated by extrapolating the conservative mixing line to the zero salinity intercept. For instance, this approach was used to calculate fluxes of nutrients (Santos et al., 2009) and metals (Santos et al., 2011) at the same site in Florida. This approach requires a clear linear trend between salinity and the concentration (intensity) of the parameter of interest. The lack of a salinity vs. FDOM relationship prevented this model from being applied at this STE. It also should be noted that intensities of FDOM components at each well varied significantly (Table 3.1). Scatter in the data may partially be an effect of non-dominant driving forces or recirculation of groundwater from deeper layers as suggested by Martin (2010). Kim et al. (2012) suggested that different processes occurred in surface (0-10 cm), subsurface (10-35 cm), and deep layer (35-75 cm) in a STE in Korea. Thus in this STE, FDOM variability might be influenced by several processes, blurring any two-dimensional correlation.

Here we hypothesize that the distribution of FDOM components and their temporal variability is a result of multiple influences that cannot be assessed via simple two-dimensional analysis. To assess the influence of multidimensional environmental variability, including nutrient concentrations, on FDOM, a multidimensional PLS regression was performed. The correlation loadings of the PLS regression showed that using two PLS factors, 68% of the environmental parameters variability could explain only 16% variability of FDOM component intensities (Fig. 3.5). Interestingly, salinity did not affect FDOM variability at all. The ratio of DOC to DON which had previously been used to explain the source of organic matter in surface

estuaries (Canuel et al., 1995; Hopkinson et al., 1998; Thornton and McManus, 1994), could not explain the variability either. C3 intensity, which was the lowest at all wells, could be explained to <50% by DOC concentration, and to a lower degree, by DON, O_2, and NO_3 concentrations. NH_4 concentrations could also explain C3 intensity variability, but in negative correlation.

There are two processes possibly affecting the intensity of C3. Studies of fluorescence spectroscopy of natural isolated lignin showed a similar excitation emission matrix than our C3 components (Djikanović et al., 2007; Radotić et al., 2006). Thus, it is possible that plant leachate could have been transported below ground from the adjacent pine forest and influenced C3, which is relatively young terrestrial material. However, the lack of correlation between salinity and C3 does not corroborate this possibility. The second process includes the microbial oxidation of NH_4 into NO_3 (nitrification). The aerobic condition of the aquifer as reported by Santos et al. (2009) facilitates this process. The negative correlation between C3 and ammonium, and the positive correlation with nitrate supports this hypothesis. As a rather speculative hypothesis at this point, we conclude that C3 was possibly mobilized from terrigenous sediments via microbial nitrification. This possibility is indicated by our PLS statistical analysis and will have to be confirmed in future studies.

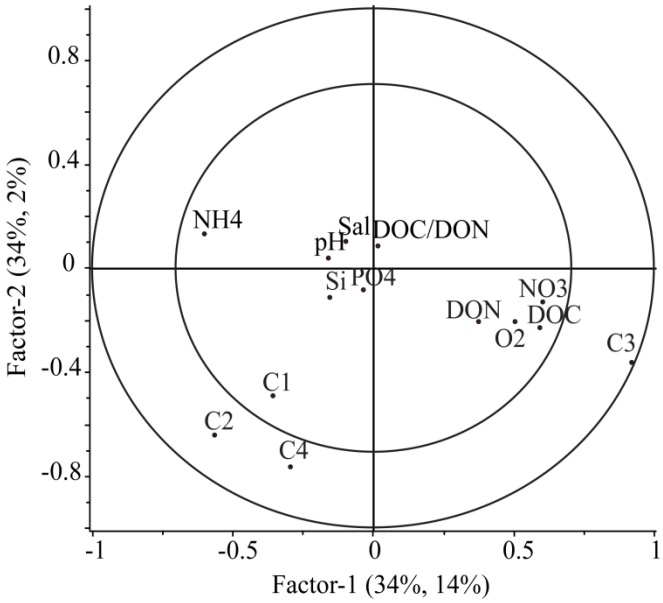

Fig. 3.5. A partial least square (PLS) regression loading plot between FDOM components and other parameters. The inner ellipse indicated 50% of explained variance and the outer ellipse indicated 100% of explained variance. Factor-1 explained 34% variability of PARAFAC components and 17% of other components. Factor-2 explained 34% variability of PARAFAC components and 2% of other components.

Contrary to C3, the variables of C1, C2, and C4, whose concentrations were the highest in all wells, could not be explained by any or all of environmental variables. The fact that salinity did not affect their variability suggests that those components were not originated from seawater or freshwater from the pine forest. It was likely that there was an additional source of FDOM. A study of FDOM in the STE of a large tidal flat emphasized the production of a "protein-like" component by benthic algae in the surface sediment (Kim et al., 2012). The presence of algal-derived DOM in our STE in Florida has also been concluded in a recent study based on time series sampling of a complete tidal cycle (Suryaputra et al., submitted). Intrusion of seawater into the sediment could introduce benthic algae and dilute the "humic-like" components C2 and C4 at the same time. The detrital source of the "humic-like" components is probably terrigenous and was possibly deposited in the sediment at fresh-to-mid-salinity. Biogeochemical processes in the

sediment at mid salinity may have released DOM out of the terrigenous and algal-derived deposits. In that case salinity could not explain the variability of C1, C2, and C4. The production of FDOM in the STE has also been demonstrated previously using CDOM sensors and supported our findings of the deposition and recirculation of humic-like components in this STE (Suryaputra et al., submitted).

In addition to PLS, we also performed backward stepwise multiple regression to determine which parameters affected the humic-like component C3. We hypothesized that C3 intensity can be predicted as a simple combination of other variables, i.e. DOC, NH_4, NO_3, O_2, and DON. DOC was kept in the function because it had the strongest correlation with C3. Each variable was then removed and the P-value was calculated to obtain its significance on each step. When the removing step was significant ($P<0.001$), the variable was kept on the equation. Results showed that only two variables, i.e. DOC and NH_4, were significant in order to predict C3 intensity in this system (Fig. 3.6).

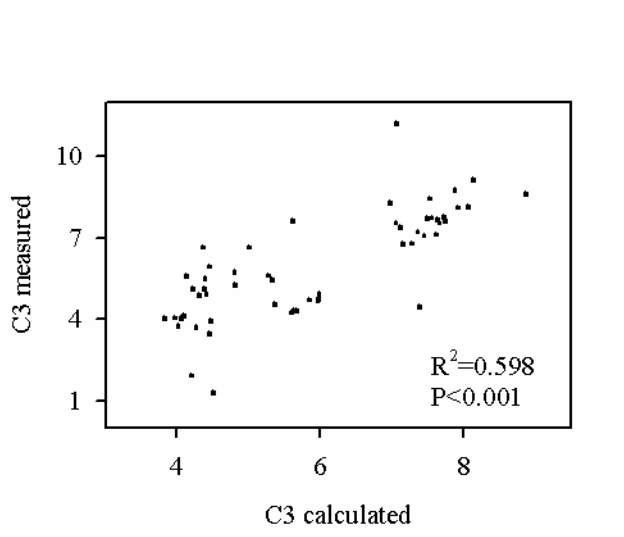

Fig. 3.6. Scatter plot between calculated C3 versus C3 obtained from PARAFAC analysis. Calculation of C3 based on the equation obtained from multiple regressions:
C3 calculated = 3.1-(0.1*NH4)+(0.01*DOC).

PARAFAC analysis is a powerful statistical tool to extract underlying patterns from EEMs of FDOM, thus the general trend of each component can be studied in detail. The limitation of this technique is that since the component is in multiple wavelengths, it is difficult to use it for high resolution in-situ application, which require single (or maybe a few) wavelength. To assess the correlations of single wavelength intensity with other variables, we used regression matrices as a companion tool of PARAFAC analysis. Each matrix was built by performing linear regressions between FDOM intensity for each excitation and emission wavelength and other variables. The coefficient of determination, R^2, of the regression was then displayed as color gradients in contour plots between FDOM intensity and environmental variables, including nutrients (Fig. 3.7). We noticed two patterns of regression from our matrices. The first pattern concentrated the R^2 into excitation wavelength of 355-365 nm with emission wavelength of 390-428 nm. This group belonged to the environmental variables salinity, pH, O_2, DOC/DON ratio, and DOC. The second pattern had a R^2 maximum at excitation 425-490 nm and emission 544-550 nm, which belonged to NH_4, NO_3, PO_4, and DON.

These regression matrices were also helpful in identifying the underlying reasons behind FDOM dynamics. While DOC correlated significantly with FDOM intensity at excitation wavelength of 355-365 nm and emission wavelength of 390-428 nm, DON correlated with the intensity at excitation 425-490 nm and emission 544-550 nm. To acquire the direction of correlation, we also performed Pearson correlation matrices for all variables. The matrices showed that correlation trends of NO_3, PO_4, and DON at the second region (excitation 425-490 nm and emission 544-550 nm) were positive, except that of NH_4 which was negative. These trends indicate that fluorescence at this wavelength range was related to an increase of NO_3, PO_4, and DON, and loss of NH_4. It was in agreement with the above-mentioned different processes

revealed by PLS regression analysis. A previous study at the same site also found accumulation of PO_4 at the sediment surface (Santos et al., 2008) which was attributed to the mineralization of organic matter into nutrients (NH_4, NO_3, PO_4). Interestingly, the fluorescence correlating with DOC was well separated from that of DON and nutrients. A portion of DOC fluorescence overlapped with that of salinity, pH, and oxygen, indicating intrusion of freshwater as a source of one type of DOM; while another type might rather be associated with DON production through mineralization processes.

The regression matrices are also helpful in identifying appropriate single wavelength for monitoring purposes. For instance, R^2 between DOC and FDOM intensity at single wavelength at excitation/emission of 360/428 nm was 0.68 (Fig. 3.8). This correlation was a better fit than that obtained using multi-wavelengths of C3. In fact, significant correlation between DOC and C3 was found only around excitation/emission of 360/428 nm. As comparison, we also found a weaker correlation between DOC and FDOM intensity at excitation/emission of 370/460 nm. This wavelength was used in a CDOM sensor from Wetlabs in a recent study (Suryaputra et al., submitted). More significant correlations with other variables were also obtained using a single excitation emission wavelength compared to those acquired from PARAFAC components, which illustrates that a single wavelength approach can be better than that using multi-wavelengths.

We conclude that DOM in STEs is affected in its concentration and composition by a complex interplay of various processes. Simple two-source mixing models as often applied in surface estuaries are of limited use in STEs. A combination of different multivariate approaches, including PLS, and regression and correlation matrices are introduced to deconvolute the complexity of interrelated processes affecting DOM. These approaches revealed that C3 was driven primarily by microbial nitrification, while C1, C2, and C4 had no single major driver

likely as a result of modifications within the subterranean estuary. We could also show that EEM analysis, combined with the analysis of relevant environmental parameters and regression matrix analysis are helpful in establishing single wavelength approaches for future in situ monitoring of DOM and related parameters in STEs.

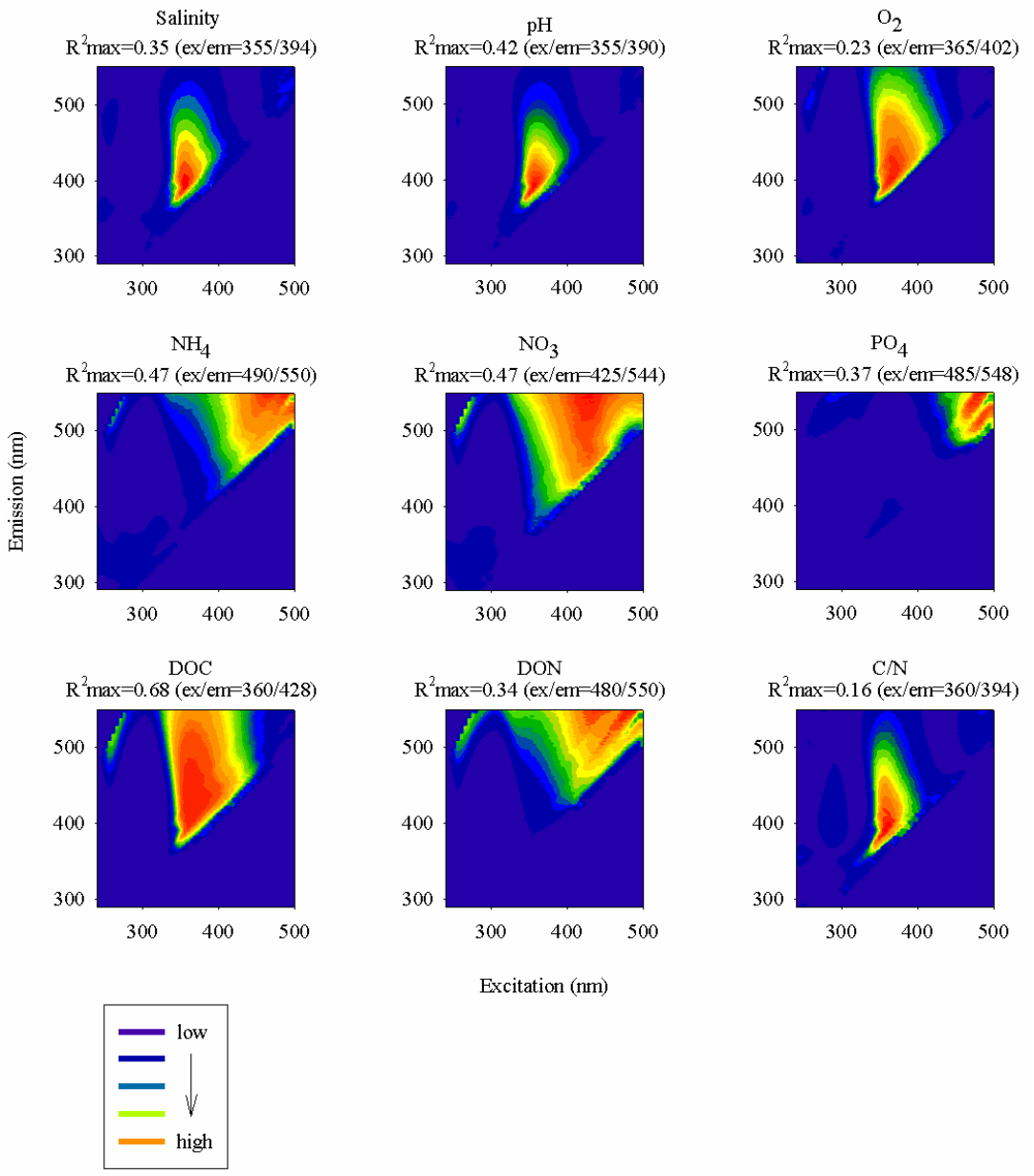

Fig. 3.7. Regression matrices of coefficient of determinations (R^2) between FDOM intensity of each excitation and emission wavelength and other parameters. Values in brackets are excitation and emission wavelengths where R^2 are the highest.

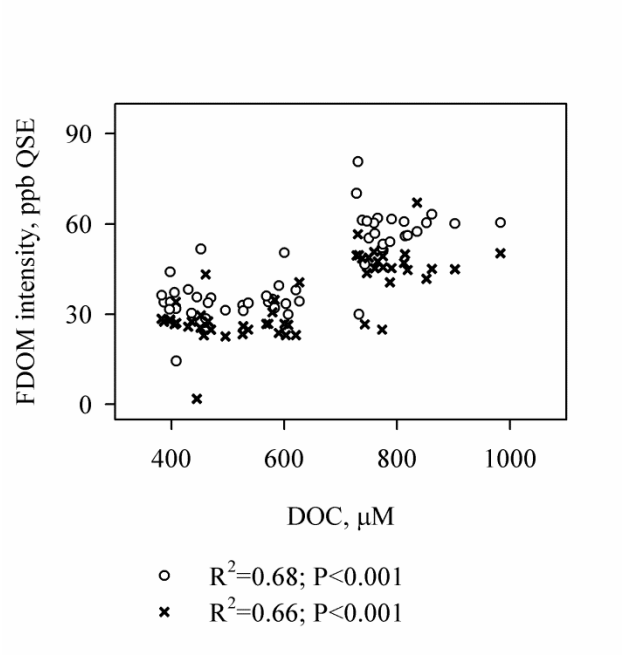

Fig. 3.8. Scatter plot of DOC vs. FDOM intensity at excitation/emission of 360/428 nm (x) and of 370/460 nm (o).

Chapter 4

Linking fluorescence and molecular properties of estuarine dissolved organic matter

Linking fluorescence and molecular properties of estuarine dissolved organic matter

I Gusti Ngurah A. Suryaputra[1], Pamela Rossel[1], Thorsten Dittmar[1]

Submitted to Marine Chemistry

[1] Max Planck Research Group for Marine Geochemistry, Carl von Ossietzky University, ICBM, Carl-von-Ossietzky-Str. 9-11, D-26129 Oldenburg, Germany

Abstract

The dynamics of dissolved organic matter (DOM) were studied in the Suwannee River Estuary (Florida, USA). The aim of this study was to identify major DOM sources in the river-dominated coastal system by linking fluorescence properties to molecular-level information. A total of 46 samples were collected covering the whole salinity gradient from river to ocean. DOM was characterized on a bulk elemental level (carbon and nitrogen), via fluorescence spectroscopy, and on a most comprehensive molecular-formula level with help of Fourier-transform ion cyclotron resonance mass spectrometry (FT-ICR-MS). The latter yielded >1000 molecular formulae of DOM compounds. As a first step, two multivariate statistical procedures were applied for data analyses: First, parallel factor (PARAFAC) analysis was performed to decompose fluorescence dissolved organic matter (FDOM) into statistically-defined fluorophores. Second, partial least square (PLS) regression was applied to correlate the relative abundance of molecular formulae with environmental data and PARAFAC components. Four terrestrial "humic-like" components were successfully modeled using PARAFAC analysis. The distribution of DOM in the estuary was mainly driven by the mixing of freshwater and seawater, but PLS analysis revealed that there were two chemically distinct fractions of terrigenous DOM in the system, one introduced by the river and the other one by groundwater. Correlation matrix analysis helped to identify distinct fluorescence wavelengths that were characteristic for DOM from the different sources. This study exemplary shows that the combination of in-depth molecular and optical characterization of DOM with multivariate statistical tool, namely PLS and correlation matrices, is very efficient for identifying meaningful parameters for in situ monitoring.

4.1. Introduction

Dissolved organic matter (DOM) plays an important role for biogeochemical processes in aquatic systems. Although DOM in the ocean contains as much carbon as atmospheric CO_2 (Hansell and Carlson, 1998), far less than 10% have successfully been characterized as specific compounds (Leenheer and Croue, 2003). Due to the difficulty of analyzing DOM on a molecular level, most previous studies focused on bulk DOM quantification. For instance, dissolved organic carbon (DOC) has been quantified extensively throughout the world oceans (Hansell and Carlson, 2002), which greatly improved our knowledge on the distribution and cycling of DOM. Fundamental questions with respect to the biogeochemistry and turnover of DOM, however, still remain elusive because of our lack of molecular-level knowledge.

Fourier transform ion cyclotron resonance mass spectrometry (FT-ICR-MS) is a recent technique which is particularly powerful to characterize DOM on a molecular level (Dittmar and Paeng, 2009). With this advanced analytical technique, the molecular formulae of ten thousands individual compounds can be determined in complex natural mixtures such as DOM. Some information on molecular structures can be obtained from molecular formulae with help of several indices or ratios previously reported. For instance, carboxyl-rich alicyclic molecules (CRAM), which is probably a major components in refractory marine DOM, can be assessed by an index formulated by Hertkorn et al. (2006). In a given molecular formula, the number of rings plus double bonds can be determined as double bond equivalents (DBE), and an aromaticity index (AImod) was developed to assess the degree of aromaticity in a molecule (Koch and Dittmar, 2006; McLafferty and Turecek, 1993).

The FT-ICR-MS technique has been applied previously to study the variability of DOM on a molecular level in a variety of coastal and marine environments. A study performed at the

Chesapeake Bay and its adjacent coastal ocean found that the saturation of DOM molecules decreased with distance offshore (Sleighter and Hatcher, 2008). Koch et al. (2005) found that 30% of the molecular formulae in marine DOM samples were also present in mangrove DOM. Furthermore, Tremblay et al. (2007) reported that an increase of DOM molecular saturations and a decrease in molar mass along a salinity gradient was partially due to photodegradation. These results are also in agreement with other experiments that address DOM molecular changes in natural waters due to solar exposure (Gonsior et al., 2009; Stubbins et al., 2010).

FT-ICR-MS analysis provides great details on DOM molecular composition, however, its application has also drawbacks. First, this method is considerably expensive, thus very few laboratories have access to it. Second, marine DOM cannot be characterized in situ by FT-ICR-MS and processing of the samples is necessary before analysis. Prior to sample injection into the ionization source of the mass spectrometer, salts need to be removed from the original samples, for instance using solid phase extraction (SPE, Dittmar et al., 2008).

In contrast, the analysis of the fluorescent dissolved organic matter (FDOM), an optical fraction of DOM, is a sensitive and low-cost method. It is performed by measuring fluorescence intensity in a range of excitation wavelengths, typically between 250 nm and 500 nm, and within certain emission wavelengths, between 300 nm and 600 nm (Baker, 2001; Coble, 1996; Coble et al., 1990). Fluorescence intensities can then be presented in an excitation emission matrix (EEM) for each analyzed sample (Coble, 1996; Coble et al., 1998; Parlanti et al., 2000). Compared to FT-ICR-MS the density of information is much lower, but highly characteristic optical fingerprints for DOM can still be obtained. To overcome the difficulty of analyzing the resulting multidimensional data, Chen et al. (2003) applied region integration of selected peaks. However, this method is not sensitive to spectral shifts, which may be caused by alteration in FDOM

composition (Her et al., 2003; Shubina et al., 2010). Another widely used technique to work with EEM data is the parallel factor (PARAFAC) analysis. PARAFAC is a powerful statistical tool to decompose three-dimensional EEMs into two-dimensional components, being also sensitive to spectral shifts (Stedmon and Bro, 2008; Stedmon et al., 2003). Characterization and identification of PARAFAC components can be done following the terminology proposed by Coble (1996): "humic-like" components, are characterized by wide emission peaks between 380 and 480 nm, and "protein-like" components, by narrow emission peaks between 310 and 340 nm. Numerous studies used this analysis to evaluate FDOM variability in estuary catchments, soil ecosystems, and lakes (Bro and Ohno, 2006; Stedmon et al., 2003; Zhang et al., 2009). It should be emphasized that the terminology proposed by Coble (1996) is operationally defined, and should not be interpreted as structural molecular information. Results derived from PARAFAC itself can also not be interpreted on a direct molecular level either. Thus, correlation of both data obtained from fluorescence and FT-ICR-MS measurements may provide additional insights into the molecular information potentially obtained from FDOM analysis. Statistically combining molecular and optical data may also help interpreting fluorescence data, not necessarily in a strict molecular sense, but to set up appropriate optical methods to trace the fate of DOM from various sources through coastal systems. In this study, we focus on the dynamics of bulk DOM, FDOM and DOM molecular formulae in the river-ocean mixing system of the Suwannee River (Florida, USA).

4.2. Materials and Methods

4.2.1. The study area

Water samples were collected on April 9-12, 2008 onboard the Research Vessel Bellows (Florida Institute of Oceanography) and a zodiac (for the most upstream samples) from the Suwannee River Estuary (Florida, USA). Sampling was performed following the salinity gradient from river to the ocean. Samples were collected toward the Gulf of Mexico through the main channel of West Pass, and across the river plume to the South and along the plume to the North (Fig. 4.1). The river water had a dark-brown color due to the abundance of terrigenous DOM rich in phenolic vascular compounds (Malcolm et al., 1989; McKnight et al., 2001). The Suwannee River is the second largest river in Florida, and its discharge affects biogeochemical processes and the ecology of the Gulf of Mexico on a regional scale (Bledsoe and Phlips, 2000). During our sampling campaign, the river water level was recorded at Fowlers Bluff by the United States Geological Service (USGS), which is located approximately 13 km upstream from our first sampling station. The river water level increased at the beginning of March 2008, but then gradually decreased until it reached the minimum level in mid of June 2008 (www.usgs.gov). Sampling was conducted during long-term average river discharge.

Surface water samples of a total of 38 stations were taken using an acid-rinsed polyethylene bucket. In addition, bottom water samples (approx. 0.5 m above ground) were collected from eight marine and estuarine stations using a Niskin sampler. Salinity, pH, and chlorophyll-a were measured with a YSI-85 probe immediately after sampling. All water samples were vacuum-filtered through 0.7 μm Whatman GF/F glass fiber filters, previously combusted at 400°C for four hours. The water was then acidified to pH 2 by adding HCl (10 M, analytical grade) and stored in 20 mL sealed glass ampoules for dissolved organic carbon (DOC)

and total dissolved nitrogen (TDN) measurements. Additionally, 2 L of acidified samples were stored in polyethylene bottles for FT-ICR-MS analyses. Filtered samples for FDOM were stored without acidification until analysis at 4°C in amber glass bottles (20 mL), closed with caps equipped with Teflon coated liners.

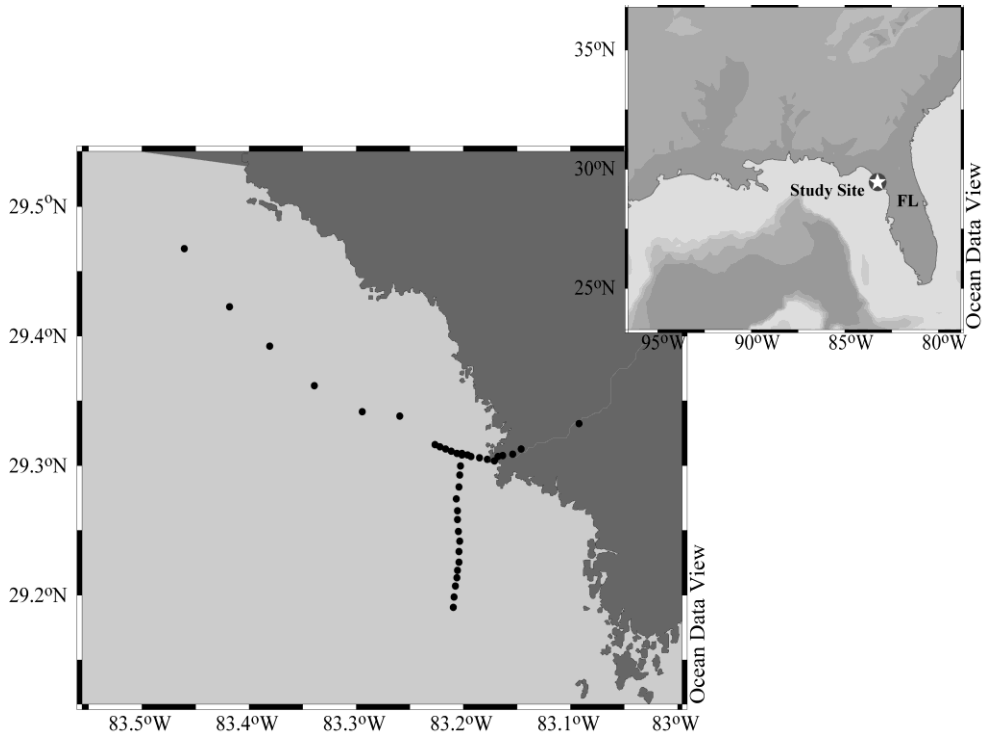

Fig. 4.1. Study area and sampling stations in the Suwannee River Estuary and its plume in the Gulf of Mexico. Ocean Data View (ODV) software was used to produce the maps.

4.2.2. Bulk DOM analyses

DOC and TDN quantification

DOC and TDN concentrations were measured using a Shimadzu TOC-V_{CPH} total organic carbon analyzer equipped with a TNM-1 total nitrogen measuring unit. As external controls, deep sea reference samples (DSR) obtained from the University of Miami, were also measured in

the beginning, middle and the end of the analysis. The accuracy and precision for DOC and TDN concentration were within 5%, and the detection limit was 5 μM for DOC and TDN.

FDOM measurement and PARAFAC modeling

Prior to FDOM analysis, samples were allowed to reach room temperature. Fluorescence measurement was performed on a Jobin Yvon SPEX Fluoromax-4 spectrofluorometer using excitation wavelengths between 240 nm and 500 nm in 5 nm increments, and emission wavelengths between at 300 nm and 600 nm in 2 nm increments, in a 1-cm quartz cuvette. Inner filter effects were minimized by diluting samples with ultrapure water if the absorbance at the lowest excitation wavelength (240 nm) was more than 0.02 (Zepp et al., 2004). These effects are known to reduce fluorescence intensity because the light is absorbed by the sample before emission or before leaving the cell (Kubista et al., 1994). Fluorescence arbitrary units were converted into quinine sulfate equivalent (QSE) with help of Fluorescence Toolbox version 1.91. This toolbox was developed by Wade Sheldon (University of Georgia) for Matlab 5.3. Removal of Raman and Rayleigh scattering, followed by PARAFAC analysis, were performed using DOMFluor toolbox ver. 1.7 (Stedmon and Bro, 2008) in MATLAB 2010b. Non-negativity was constrained for all three modes (intensity, excitation, and emission) to avoid negative numbers obtained from the analysis. To validate the result, samples were split into half and PARAFAC analysis was performed for each half. When both showed the same results, the analysis was considered valid. The order of the components obtained from PARAFAC analysis is arbitrary and solely based on the modeling, and might be different in previous studies. To compare and identify FDOM with other studies, the peak maxima of each component are presented.

2.3. Molecular-level analysis of DOM

DOM extraction

A solid phase extraction using PPL sorbents (Varian Inc.) was performed to concentrate DOM and remove salts for mass spectrometric analysis (Dittmar et al., 2008). PPL sorbent consists of a modified styrene divinyl benzene co-polymer. Prior to use, the pre-packed cartridges (containing 1 g adsorber) were rinsed with methanol. Samples were then passed through the cartridges by gravity with a flow rate of less than 40 mL min^{-1}. Later, salts were removed from the cartridge by passing two cartridge volumes (5 mL each) of ultrapure water (acidified with HCl to pH=2). The cartridges were then dried using ultrapure nitrogen gas, and DOM was eluted with 6 mL of methanol (mass spectrometry grade). SPE-DOM, i.e. the DOM extracted by SPE, was collected in pre-combusted amber vials (with acid and methanol-rinsed Teflon liners) and stored at 4°C prior analysis. To determine the extraction efficiency of the SPE, an aliquot of each SPE-DOM sample was dried overnight at 50^{o}C, re-dissolved in ultrapure water, and its DOC concentration was measured. The efficiency was then calculated by dividing the concentration of SPE-DOC in the original water sample (under consideration of the extracted volume) by the concentration of bulk DOC. Blanks were produced by extracting 2 L of ultrapure water instead of sample.

FT-ICR-MS analysis of SPE-DOM

Based on the DOC concentrations in the SPE-DOM, aliquots of the extracts were diluted in methanol:water (50:50 v/v) to a final concentration of 15 mg C L^{-1}. They were thereafter infused at a flow rate of 120 µl h^{-1} into a 12 Tesla FT-ICR-MS (Bruker Solarix) equipped with an electrospray ionization source. Analyses were performed in negative ion mode using a capillary

voltage of 4000 V. The mass spectra were first externally calibrated using arginine clusters, and then internally calibrated with >100 molecular formulae in a mass range of 280 – 580 Da, which were previously identified in a Suwannee River fulvic acid (SRFA) reference material obtained from the International Humic Substances Society. Molecular formulae were assigned for all samples using Data Analysis software (ESI Compass 1.3) from Bruker Daltonics with error limits below or equal to 0.5 ppm. Results were then exported and filtered with MATLAB 2010b using the following criteria: signal to noise ratio (S/N) > 4, $C \geq O$, $O > (2P + S)$, $H \leq 2C + 2$, $N \leq 3$, $S \leq 2$, and $P \leq 2$. In case that more than one formula was assigned to a single mass peak, CH_2-homologous series were taken into account. A formula was considered correct if two or more formulae in the lower mass range belonged to the series, and the likely incorrect formulae were deleted from that mass peak as well as all samples. Otherwise, all formulae were removed from the mass peak and all samples when none of the lower mass ranges formulae belonged to CH_2-series. Mass peaks detected in the blank extractions were eliminated from all samples.

The presence and absence of all formulae were then analyzed to evaluate general trends in the data set. For further statistical analysis, peaks observed in less than 80% of all samples were also removed. Thus, only formulae which occurred in more than 36 out of a total of 46 samples were considered. After data filtration, each mass peak in the data set was normalized to the total remaining intensity of all mass peaks presented in its respective sample. Zero intensity values were later replaced by the minimum value of relative abundance obtained after normalization of the whole data set. This approach was used considering that absent peaks may potentially be presented in the samples, but were below the detection limit.

The double bond equivalent (DBE) and modified aromaticity index (AImod) were calculated following these equations:

$$DBE = 1 + 0.5(2C - H + N + P)$$ (McLafferty and Turecek, 1993)

$$AImod = \frac{1 + C - 0.5O - S - 0.5H}{C - 0.5O - S - N - P}$$ (Koch and Dittmar, 2006)

In addition, carboxylic-rich alicyclic molecules (CRAM) were identified according to the criteria proposed by Hertkorn et al. (2006):

$$\frac{DBE}{C} = 0.3 - 0.68, \frac{DBE}{H} = 0.2 - 0.95, \frac{DBE}{O} = 0.77 - 1.75$$

2.4. Statistical analysis

One of the foci of this study was to correlate FDOM, environmental, and molecular data. In order to combine both data sets, partial least square (PLS) regression analysis, a multivariate statistical tool, was applied. PLS not only allows us to reduce the dimensionality without losing the overall variability of our observations, but also to model linear relationships of two chosen matrices. However, our data consisted of three matrices: FDOM components, environmental data (salinity, pH, chlorophyll-a, DOC concentration, and TDN concentration) and DOM molecular data, while PLS analysis works with paired matrices. Therefore, FDOM components were included as environmental data. The Unscrambler X v10.2 from Camo Software was used for PLS analysis. To remove variation caused by different units, we divided all data by their own standard deviation. PLS results are presented in scores and loadings, which describe similarity (or difference) in samples and variables, respectively. Compare with redundancy analysis, PLS automatically solves problems caused by sample size and missing values. Moreover, PLS also overcomes multicollinearity, a situation where two or more predictors are highly linearly correlated (Liu, 2011).

Additionally, we also performed correlation matrices analysis by calculating the Pearson correlation coefficient (R) between each excitation / emission wavelength (8269 variables) and all environmental parameters and relative abundance of all molecular formulae (a total of 896 variables). The correlation matrix consisted of 7,409,024 individual R values. All data passed the normality test of Kolmogorov-Smirnov at a 5% significance level.

4.3. Results

4.3.1. FDOM components and DOM variability

Samples collected from the estuary covered the whole salinity gradient, from almost zero to ~35. Water pH slightly increased with salinity, whereas chlorophyll-a decreased from 13.9 to 0.3 mg L^{-1}, from river to most offshore. DOC and TDN concentrations decreased 8 and 7 times, respectively (Table 4.1).

Table 4.1. Average (Avg.), standard deviation (St. Dev.), minimum (Min.), and maximum value (Max.) of salinity, pH, chlorophyll-a concentration, DOC concentration, and TDN concentration.

	Avg. ± St. Dev.	Min. - Max.
Salinity	26.2 ± 10.6	0.1 - 34.6
pH	7.8 ± 0.2	7.3 - 8.0
Chlorophyll-a, mg L^{-1}	6.0 ± 3.1	0.3 - 13.9
DOC, μM	550 ± 401	176 - 1471
TDN, μM	28 ± 19	10 - 71

Though the EEMs of the samples appeared remarkably similar on a first view, significant differences among the samples were identified via PARAFAC (Fig. 4.2). Four components of

FDOM were successfully modeled using PARAFAC analysis. The first component (C1) was represented by two peaks occurring at excitations of 280 nm and 370 nm and at 510 nm emission. Component 2 (C2) showed an excitation maximum below 240 nm and an emission maximum at 420 nm. Component 3 (C3) was also represented by two peaks and their excitation maxima appeared below 240 nm and at 315 nm, while their emission maxima were at 434 nm. Component 4 (C4) has one excitation maximum at 245 nm and a second excitation maximum at 370 nm with a general emission peak at 460 nm.

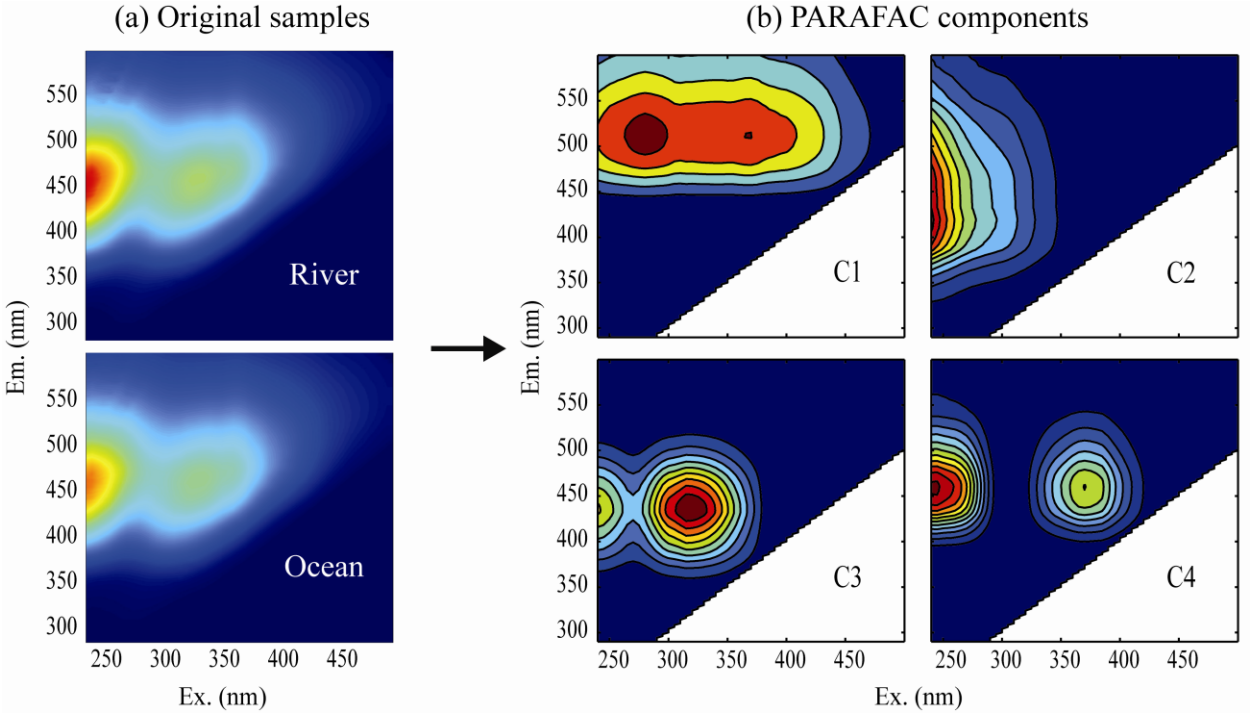

Fig. 4.2. (a) Examples of riverine and oceanic EEM samples are shown. (b) Four PARAFAC components were identified in the dataset.

Generally, the intensity of all PARAFAC components decreased along the salinity gradient (Figs. 4.3a-d). C1 and C3 showed very similar patterns (Figs. 4.3a and 4.3c). C2 intensities, however, slightly increased at salinities <26 (Fig. 4.3b), while C4 intensities were

constant at salinities <15 (Fig. 4.3d). DOC and TDN concentrations were also negatively correlated with salinity and showed nearly the same pattern as that of C1 and C3 (Figs. 4.3e and 4.3f). Chlorophyll-a concentration, also decreased with increasing salinity, but showed sharp increases at salinities around 30 (Fig. 4.3g).

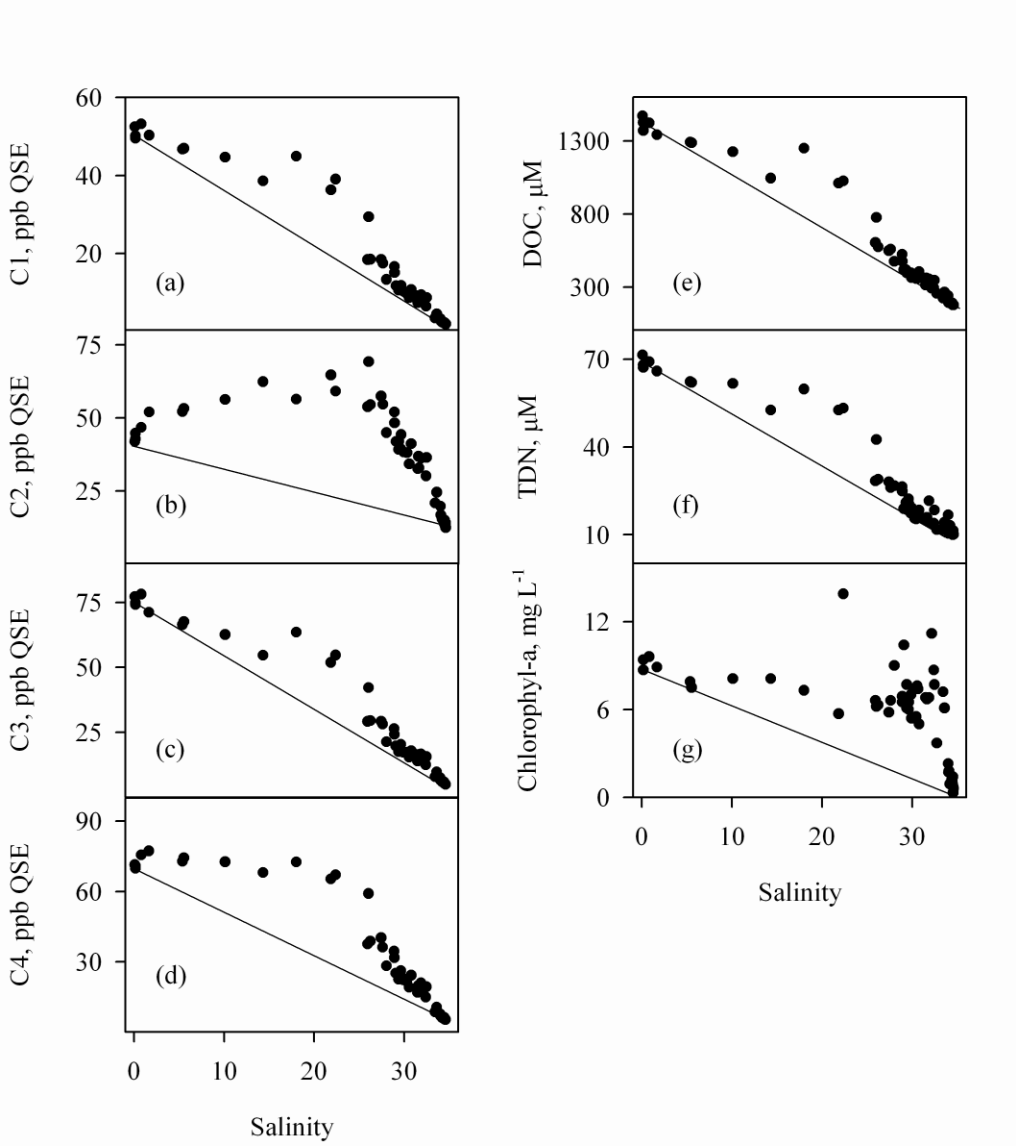

Fig. 4.3. Scatter plot of salinity vs. PARAFAC components, DOC concentration, TDN concentration, and chlorophyll-a concentration. Solid line indicates conservative mixing of the two endmembers (river and ocean).

4.3.2. Molecular characteristics of SPE-DOM by FT-ICR-MS analysis

On average, SPE efficiency was 71% based on a carbon basis. The extraction efficiency did not systematically vary along the salinity gradient or with distance offshore. A total of 7892 molecular formulae were identified by FT-ICR-MS. Before removing molecular formulae presented in less than 80% of samples, we used all molecular formulae to evaluate general differences and similarities between samples. Based on salinity, we divided the samples into three equal ranges of salinity: 7 riverine samples (salinity <12), 6 estuarine samples (salinity 12-23), and 33 oceanic samples (salinity >23). CRAM relative abundance first decreased from the river to the estuary and then increased in seawater (Fig. 4.4a). On the other hand, DBE and AImod of the estuarine samples were higher than those of the river and seawater samples, with the latter presenting the lowest values (Fig. 4.4b and 4.4c). Moreover, estuarine samples had the most variable values for the three calculated indices as described by the size of boxes in Fig. 4.4a-c. After removing those molecular formulae that were present in less than 36 out of the 46 samples, the variability within the groups decreased. Data filtration also reduced the number of outlying samples within the groups. Further statistical analyses were only performed on the filtered data. A total of 891 molecular formulae remained after the data filtration step.

4.3.3. PLS regression analysis

The first factor from PLS regression explained 88% and 25% of the environmental and molecular data variability, respectively. To a much lower degree, factor 2 explained 7% and 9% of the environmental and molecular data variability, respectively. Factor 1 continuously increased from ocean to river (Fig. 4.5a). In contrast, factor 2 increased from ocean to estuary and then decreased again towards the river (Fig. 4.5a). The environmental data clustered into

three groups in the loading plots (Figs. 4.5b and 4.5c). The first group consisted of salinity and pH, the second chlorophyll-a and C2, and the third DOC, TDN, C1, C3, and C4. Molecular formulae with high DBE (Fig. 4.5b) and high AImod (Fig. 4.5c) were positively correlated with chlorophyll-a and C2, while formulae with low DBE and low AImod were positively related to salinity and pH. By overlapping loading and score plots, the first group was related to seawater samples, the second to estuarine samples (mid salinity), and the third to riverine samples.

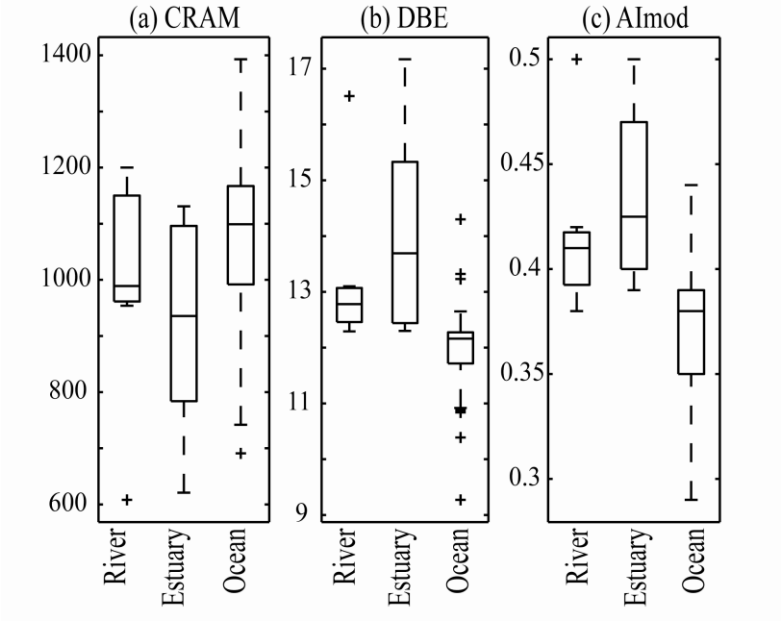

Fig. 4.4. Whisker and box plot of river, estuary, and ocean samples. Data organized based on number of (a) CRAM compounds, (b) average DBE, and (c) average AImod.

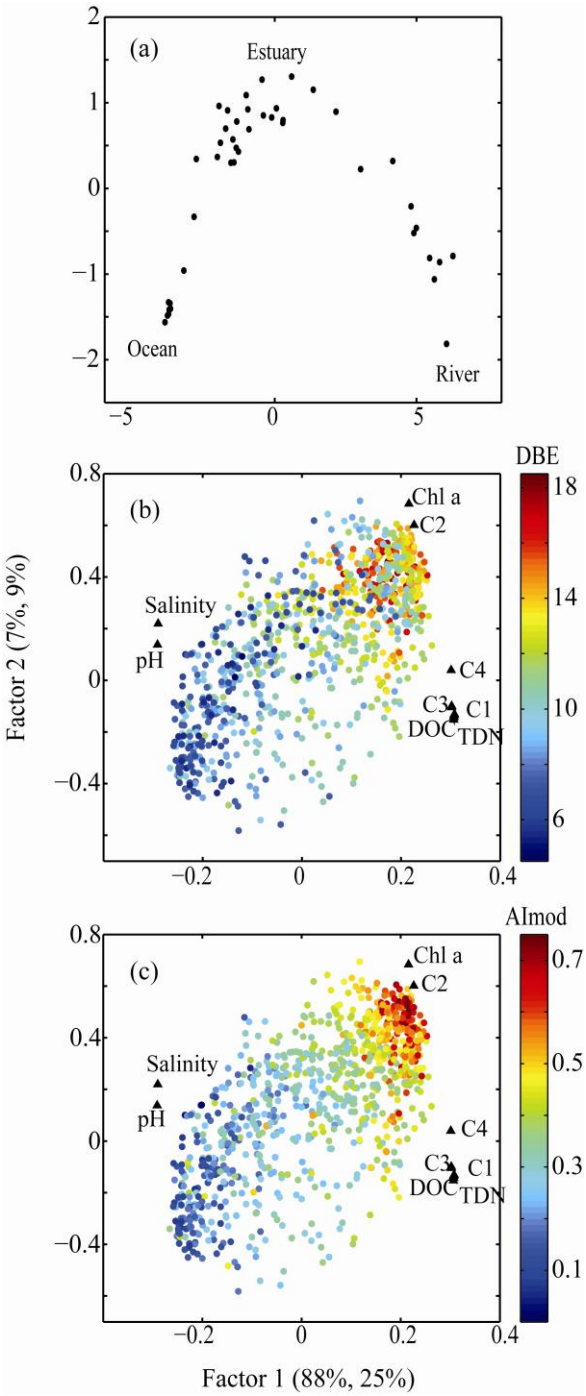

Fig. 4.5. Partial least square (PLS) regression analysis: (a) Score plot, each dot represents one sample. (b) Loading plot with DBE in the color-coded third dimension, each dot represents one molecular formula, the triangles environmental parameters. (c) Loading plot with AImod in the color-coded third dimension. Factor 1 explains 88% of environmental parameters (including PARAFAC components) variability and 25% of molecular formulae variability. Factor 2 explains 7% of environmental parameters (including PARAFAC components) variability and 9% of molecular formulae variability.

4.4. Discussion

4.4.1. Sources and molecular properties of DOM

The negative correlation between salinity and DOC indicates that the Suwannee River was the main source of DOM to the estuarine system, and that terrigenous DOM behaved conservatively along the salinity gradient. This observation is typical for most estuaries where DOM distributions are mainly controlled by mixing of freshwater and seawater (Benner and Opsahl, 2001; Hung and Huang, 2005; Peterson et al., 1994). The fluorescence properties of DOM support this observation. All four PARAFAC components modeled from our dataset (Fig. 4.2) were previously described as terrestrial "humic-like" components (e.g. Coble 1996). Furthermore, all PARAFAC components showed a similar negative correlation with salinity as DOC, in agreement with previous results (Murphy et al., 2006; Murphy et al., 2008; Osburn and Stedmon, 2011). A closer examination of the mixing plots (Fig. 4.3), however, suggests production or input of DOC and FDOM at mid salinity. The non-conservative increase of chlorophyll-a concentration in the estuary suggests algal growth and aquatic production of DOM as the source of the additional DOC at mid salinity. Nevertheless, our statistical analysis of the fluorescence data and molecular formulae enabled us to unfold the optical and molecular properties of the DOM from the various sources, and to draw a very different conclusion than intuitively derived from the trend in chlorophyll-a.

Consistent with the general trend, most of the variability in the molecular composition of DOM could be related to the mixing of fresh- and seawater. Factor 1 of the PLS regression analysis, that explained most of the variability in the molecular data, was clearly related to mixing of the two water sources (see score plot in Fig. 4.5a). On a molecular level, DOM molecular formulae with low DBE and low aromaticity (AImod) correlated positively with

salinity, because of the proximity of the aromatic compounds to salinity on the x-axis of the loading plots in Figs. 4.5b and 4.5c. DBE and AImod also correlated with the four PARAFAC components, which were all "humic-like", i.e. characteristic for vascular plant-derived phenolic compounds. These compounds could be derived to a large degree from Okefenokee Swamp which feeds into the Suwannee River (Averett and Geological, 1990; Bano et al., 1997; McKnight et al., 2001). The molecular information, therefore, support our conclusion regarding the presence of terrestrial DOM in the estuary and its conservative behavior. This DOM was delivered by the river, mixed with marine DOM in the estuary, and discharged to the Gulf of Mexico. This observation is not surprising and in agreement with previous studies. For instance, Sleighter and Hatcher (2008) identified more aromatic compounds in terrestrial DOM from a Great Dismal Swamp sample and more aliphatic compounds in marine DOM from an offshore sample. Similarly, Liu et al. (2011) confirmed the decrease in aromaticity from the same swamp to the coastal ocean, using a combination of high performance liquid chromatography (HPLC) and FT-ICR-MS analyses.

The second factor of the PLS statistics (y-axis in Figs. 4.5b and 4.5c), however, was unrelated to salinity. The variability of the molecular data along this axis was best explained by chlorophyll-a. Along this second PLS axis, PARAFAC component C2 was significantly separated from the other components. All other PARAFAC components, but not C2, plotted in close proximity in the loading plots which indicates that these components followed the same pathway which was river discharge. Almost perfect correlations between PARAFAC components were also found elsewhere (Guéguen et al., 2011; Murphy et al., 2006; Murphy et al., 2008). The uncoupling of C2 from riverine fluxes and its over-proportionally large input at

mid salinity becomes also evident if C2 to C3 ratios are plotted against salinity (Fig. 4.6). This plot displays two different linear trends with a steeper slope for samples with salinities >15.

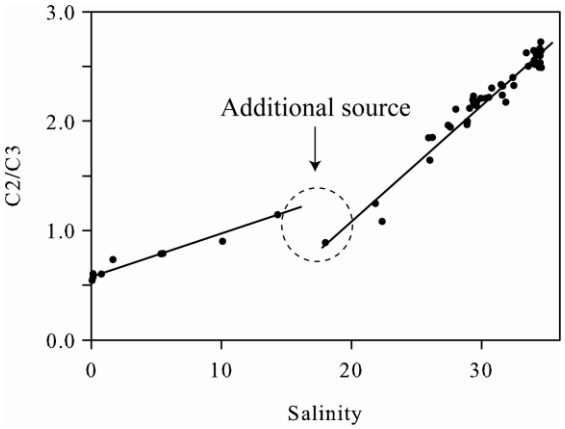

Fig. 4.6. Scatter plot of salinity vs. C2/C3 ratio. The circle is the tentative area where the additional DOM source is likely located.

The correlation of chlorophyll-a with C2 and the various molecular formulae could be interpreted as an indication that aquatic primary production was the main driving force for the non-conservative molecular and optical changes in the estuary. However, a microbial-derived "protein-like" fluorescence component, as commonly observed in chlorophyll-rich waters (Chari et al., 2012; Wedborg et al., 2007), was not found in our study. Instead, C2 positively correlated with lignin in a previous study (Osburn and Stedmon, 2011), a biomarker of vascular plant material. This is consistent with our findings from the PLS analysis. In the PLS loading plot, the molecular formulae with highest aromaticity plotted closest to C2 and chlorophyll-a. The aromaticity of some molecules even surpassed the threshold of polycyclic condensed aromates that are abundant in charred organic matter from land, but certainly not produced by aquatic organisms (Dittmar et al., 2012). Accordingly, the grouping of molecular formulae according to basic structural features (Fig. 4.4) indicated non-conservative behavior of DOM molecular

formulae distributions in the estuary. DOM with low CRAM, high DBE and AImod were introduced at mid salinity in the estuary; while the riverine samples was predominated by mid values of all indices, and the seawater samples by DOM with high CRAM, low DBE and AImod.

The direct consequence of these observations is that the excess DOM at mid salinity could not have been produced by aquatic organisms, but was introduced from land. Fluorescence and molecular information are consistent in this respect. The close relationship between chlorophyll-a and the highly aromatic DOM compounds in the PLS loading plots suggests that both were derived from the same source or the same process.

In this context, a study by Stedmon et al. (2007) is interesting. In an incubation experiment they observed photochemical production of C2. After radiating a natural water sample for six hours with UV light, C3 was photodegraded to almost half of its original intensity, while C2 intensity had increase by more than factor 20, thus C2 was considered a photoproduct of C3. The observed trend of the C2/C3 ratio in our coastal system (Fig. 4.6) is consistent with the trend observed in the photodegradation experiment. Increased light penetration at mid salinity in the Suwannee estuary could trigger both, increased production of chlorophyll-a and photoproduction of C2. However, the extraordinarily high aromaticity of molecules that correlate with C2 is contradictory to this explanation. Highly aromatic compounds photodegrade more easily than less aromatic compounds (Gonsior et al., 2009; Stubbins et al., 2010). An increase in aromaticity due to expose to sunlight is inconsistent with any previous study. Therefore, photoproduction of the observed aromatic compounds in the estuary is a most unlikely scenario.

A more likely scenario is the presence of additional water sources to the estuary that carry a high load of terrigenous DOM and nutrients. Submarine groundwater discharge is common in the region (Burnett et al., 1999). Furthermore, Katz et al. (1997) estimated

approximately one order of magnitude higher nutrient concentrations in the groundwater closer to the Suwannee estuary compared to those in the upstream groundwater. Inputs of nutrients to the estuary will trigger aquatic primary production. Among other primary producers, seagrasses grow rapidly in the estuary (Jackson and Nemeth, 2007), not only because of reduced current velocities but also due to the high nutrients input, probably released from the sediment. Nutrient release via submarine groundwater discharge was observed in a subterranean estuary located approximately 146 km from our study area (Santos et al., 2009). The high aromaticity of the DOM in the estuary is consistent with a groundwater source, because sunlight cannot decompose these photolabile compounds of DOM (Gonsior et al., 2009; Stubbins et al., 2010) in a dark aquifer.

4.4.2. Implications for in-situ fluorescence observations

PARAFAC analysis is a powerful method to model FDOM and decompose it into components. Unfortunately, the multi-wavelengths models are not suitable for in situ sensing where usually only one pair of excitation-emission wavelengths can be recorded. For in situ monitoring, wavelengths have to be chosen carefully to obtain the best correlation with the variable to be predicted. For this purpose, we propose correlation matrices as an effective statistical tool. Results are presented in contour plots with color gradients that describe R. The five correlation matrices for salinity, pH, chlorophyll-a, DOC, and TDN (Fig. 4.7) indicate two major patterns. The first fluorescence pattern is indicative for DOC concentration, and, because of the strong covariance, also for TDN concentration, salinity, and pH. The most significant correlation with these parameters was observed around excitations of 430 nm and 450 nm, and

emissions of 452 nm and 600 nm. The second pattern was indicative for chlorophyll-a, with the most significant correlation at excitation and emission of 270 nm and 344 nm, respectively.

We also calculated correlation matrices for each detected molecular formula and fluorescence data. As examples we show the correlation matrices for three molecular formulae. These formulae were chosen from loading plot of the PLS regression analysis to represent each of the major DOM sources in the system. The selection of the molecular formulae was done independent of their correlation with fluorescence. The riverine example ($C_{23}H_{25}O_8^-$) is highly unsaturated and probably phenolic, as typical for terrigenous, vascular plant-derived DOM. The marine example ($C_{19}H_{27}O_9S^-$) is more saturated and contains sulfur. The estuarine example ($C_{23}H_{19}O_{13}^-$) is the most aromatic of all the three examples. Therefore, the three examples are also representative with respect to the general molecular properties of DOM from the three distinct sources in the estuary. As expected, the molecular formula that represents marine DOM (Fig. 4.7g) shows the same pattern in the correlation matrix as salinity and pH. The riverine sample (Fig. 4.7f) shows inverse pattern as salinity and pH, but similar pattern as DOC and TDN concentrations. The correlation matrix of the estuarine molecular formula (Fig. 4.7h), on the other hand, is unrelated to all the above, but shows very similar pattern as the matrix of chlorophyll-a.

Here, we linked compound-specific molecular formulae to characteristic fluorescence pattern. It should be emphasized that the observed fluorescence pattern shows very broad bands, which indicates the overlap of the signals from many different molecules. The statistical marriage of fluorescence with specific molecular-level information is extremely powerful in many aspects, but the observed correlation pattern should not be misinterpreted as the fluorescence signals of specific molecular formulae. If one would be able to physically isolate

these compounds (which is impossible to date), a single compound would most likely exhibit very different fluorescence pattern. We interpret the observed pattern as a result of the overlap of thousands if not millions of compounds that co-vary in their relative abundance in the estuary.

The distinct correlation patterns between fluorescence and molecular formulae makes in situ monitoring of the main DOM sources, as discussed in the previous section, a straightforward task. Bulk DOC could be efficiently monitored with a wide range of fluorescence, but best via fluorescence at wavelengths 430-450 nm (excitation) and 452-600 nm (emission). The additional source of DOM, which is most likely related to submarine groundwater discharge in the estuary, could be monitored at excitation and emission of 270 nm and 344 nm, respectively. This study exemplary shows that the combination of in-depth molecular and optical characterization of DOM with multivariate statistical tool, namely PLS and correlation matrices, is very efficient for identifying meaningful parameters for in situ monitoring. The development of actual in situ sensors will require further tests, e.g. with respect to the applicability in different systems or the effect of turbidity.

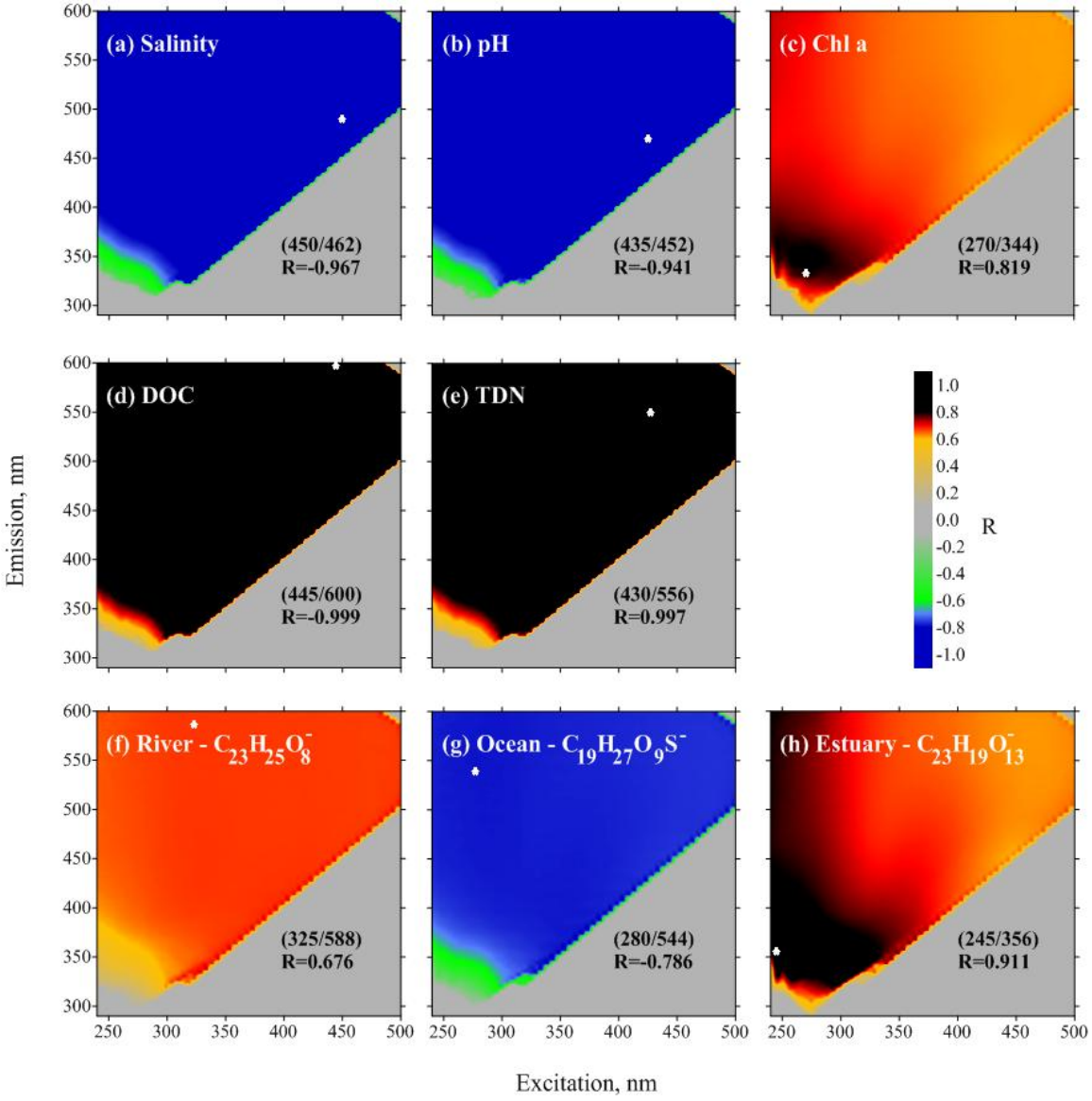

Fig. 4.7. Correlation matrices of DOM fluorescence with a series of different parameters. The color-coded third dimension represents the Pearson correlation coefficient (R) of a specific fluorescence wavelength with (a) salinity, (b) pH, (c) chlorophyll-a, (d) DOC concentration, (e) TDN concentration, and (f) – (h) the relative abundance of three selected molecular formulae that are representative for riverine, marine and estuarine DOM. The three molecular formulae were selected based on their position in the loading plot (Fig. 5). Blue color indicates a highly significant negative correlation ($p < 0.0001$), black and red colors a highly significant positive correlation. Numbers in brackets point out the excitation and emission wavelength where the most significant correlation of FDOM intensity and associated parameters were found (also indicated by the white star in each panel). The printed correlation coefficients (R) in each panel are the respective maxima. For the determination of the maximum R, only excitation wavelengths <20 nm of the scatter wavelength (diagonal line in the EEMs) were considered.

Chapter 5

Production, degradation, and flux of dissolved organic matter in the subterranean estuary of a large tidal flat

Production, degradation, and flux of dissolved organic matter in the subterranean estuary of a large tidal flat

Tae-Hoon Kim[1], Hannelore Waska[1,2], Eunhwa Kwon[1], I Gusti Ngurah Suryaputra[2], Guebuem Kim[1]

Marine Chemistry 142-144, 1-10

[1] School of Earth and Environmental Sciences/RIO, Seoul National University, Seoul, 151–747, Republic of Korea

[2] Max Planck Research Group for Marine Geochemistry, University of Oldenburg, Institute for Chemistry and Biology of the Marine Environment, D-26128, Oldenburg, Germany

Abstract

The distributions of dissolved organic carbon (DOC), total dissolved hydrolysable amino acids (THAA), and colored dissolved organic matter (CDOM) were studied in pore-water/groundwater samples (including seeping water) from a subterranean estuary (STE) of a large tidal flat in Hampyeong Bay, Korea, in July 2011. The relatively low alanine D/L ratios and high THAA concentrations in the pore-water closest to the sediment surface (0–10 cm) indicate the active production of dissolved organic matter (DOM) from benthic algae, and the relatively low THAA concentrations and high D/L ratios in the subsurface pore-water (10–35 cm) indicate a relatively large presence of bio-degraded DOM. In the deep pore-water (35–75 cm), relatively low D/L ratios, high DOC concentrations, and intense humic-like fluorescence were observed, suggesting a net accumulation of less-reactive DOC in this layer. Overall, this STE appears to have net DOM sources because the concentrations of DOC (60–1700 μM) in the pore-water decreased toward the land, the surface, and the low-salinity waters. The concentrations of DOC in the seeping water (185 ± 52 μM) were higher than those in the overlying seawater (144 ± 9 μM), resulting in net DOC fluxes of 2–5 × 10^9 g C yr^{-1} through submarine groundwater discharge (SGD) into Hampyeong Bay. The organic matter compositions in the seeping water indicated that SGD introduced DOM from both the surface and subsurface layers. Our results highlight that tidal flats are important sources for DOM, implying that SGD-driven DOM plays an important role in coastal carbon cycles and biogeochemistry.

Chapter 6

Discharge of dissolved black carbon from a fire-affected intertidal system

Discharge of dissolved black carbon from a fire-affected intertidal system

Thorsten Dittmar[1], Jiyoung Paeng[2], Thomas M. Gihring[2], I G. N. A. Suryaputra[1] and Markus Huettel[2]

Limnology Oceanography, 57(4), 1171–1181

[1]Max Planck Research Group for Marine Geochemistry, University of Oldenburg, Institute for Chemistry and Biology of the Marine Environment, Oldenburg, Germany

[2]Department of Earth, Ocean and Atmospheric Science, Florida State University, Florida

Abstract

We report substantial tidal fluxes of dissolved black carbon (DBC) in a fire-affected marsh in the northern Gulf of Mexico. DBC was molecularly determined as benzenepolycarboxylic acids in a tidal creek, adjacent rivers, and the coastal ocean. Supported by stable carbon isotope and in situ fluorescence measurements, three sources of dissolved organic carbon (DOC) were identified that mixed conservatively in the coastal system: groundwater from salt marshes, river water, and seawater. Groundwater was the main source of DBC to the creek. The highest DBC concentrations of up to 41 μmol C L^{-1} (7.2% of DOC) were found in the creek at low tide, compared with < 18 μmol C L^{-1} in all other samples. Over the studied tidal cycle, we determined a runoff (load per drainage area) of 3700 moles DBC (44 kg C) km^{-2} of salt marsh. This is high compared with the Apalachicola River, where the annual DBC runoff is on the order of 10^4 mol (120 kg C) km^{-2} yr^{-1}. In the marsh, it would require ~ 20 tidal cycles similar to the one that we studied to remove all black carbon produced during one fire event. Because a spring tide was studied, our estimate is as an upper limit. DBC is ubiquitous in the global ocean, and dissolution and subsequent lateral transport appear to be important removal mechanisms for soil black carbon. Our study, which provides a snapshot in time and space, demonstrates that tidal fluxes may be primary carriers of DBC, and therefore tidal pumping and groundwater discharge cannot be ignored in assessing the continental runoff of DBC.

Chapter 7

Uranium and barium cycling in a salt wedge subterranean estuary: The influence of tidal pumping

Uranium and barium cycling in a salt wedge subterranean estuary: The influence of tidal pumping

Isaac R. Santos[1, 2], William C. Burnett[2], Sambuddha Misra[2], I G.N.A. Suryaputra[2], Jeffrey P. Chanton[2], Thorsten Dittmar[2, 3], Richard N. Peterson[2, 4], Peter W. Swarzenski[5]

Chemical Geology 287 (1–2), 114–123

[1] Centre for Coastal Biogeochemistry, School of Environmental Science and Management, Southern Cross University, Lismore, NSW, 2480, Australia

[2] Department of Earth, Ocean and Atmospheric Sciences, Florida State University, Tallahassee, Florida 32306, USA

[3] Max Planck Research Group for Marine Geochemistry, Carl von Ossietzky University, ICBM, PO Box 2503, 26111 Oldenburg, Germany

[4] Center for Marine and Wetland Studies, Coastal Carolina University, PO Box 261954, Conway, South Carolina, 29528-6054, USA

[5] U.S. Geological Survey, 400 Natural Bridges Drive, Santa Cruz, California 95060, USA

Abstract

The contribution of submarine groundwater discharge (SGD) to oceanic metal budgets is only beginning to be explored. Here, we demonstrate that biogeochemical processes in a northern Florida subterranean estuary (STE) significantly alter U and Ba concentrations entering the coastal ocean via SGD. Tidal pumping controlled the distribution of dissolved metals in shallow beach groundwater. Hourly observations of intertidal groundwaters revealed high U and low Ba concentrations at high tide as a result of seawater infiltration into the coastal aquifer. During ebb tide, U decreased and Ba increased due to freshwater dilution and, more importantly, biogeochemical reactions that removed U and added Ba to solution. U removal was apparently a result of precipitation following the reduction of U(VI) to U(IV). A significant correlation between Ba and dissolved organic carbon (DOC) in shallow beach groundwaters implied a common source, likely the mineralization of marine particulate organic matter driven into the beach face by tidal pumping. In deeper groundwaters, where the labile organic matter had been depleted, Ba correlated with Mn. We estimate that net SGD fluxes were -163 and $+1660$ μmol m^{-1} d^{-1} for U and Ba, respectively (or -1 and $+8$ μmol m^{-2} d^{-1} if a 200-m wide seepage area is considered). Our results support the emerging concept that subterranean estuaries are natural biogeochemical reactors where metal concentrations are altered relative to conservative mixing between terrestrial and marine endmembers. These deviations from conservative mixing significantly influence SGD-derived trace metal fluxes.

Chapter 8

Fluorescent dissolved organic matter in submarine groundwaters of the Southern North Sea

Fluorescent dissolved organic matter in submarine groundwaters of the Southern North Sea

I Gusti Ngurah A. Suryaputra[1], Michael Seidel[1,2], Thorsten Dittmar[1]

[1] Max Planck Research Group for Marine Geochemistry, Carl von Ossietzky University, ICBM, Carl-von-Ossietzky-Str. 9-11, D-26129 Oldenburg, Germany;

[2] Current address: Department of Marine Sciences, University of Georgia, Athens, GA 30602, USA.

8.0. Introductory remarks

This study aims in applying the approaches developed in this dissertation to the largest tidal flat area in the world, the North Sea Wadden Sea. Sampling and chemical analyses of this study are complete. Data analysis is ongoing. Comprehensive statistical data analysis that will also consider detailed FT-ICR-MS data collected by Seidel et al. on the same samples, as well as the preparation of a manuscript, will be a postdoctoral project for me. This chapter was included into this thesis to give an outlook on future work and on the applicability of the novel approaches developed during my Ph.D. studies.

8.1. Introduction

Fluorescent dissolved organic matter (FDOM) is a fraction of dissolved organic matter (DOM) which is measured by fluorescence spectroscopy. Compared to chromophoric dissolved organic matter (CDOM) which is measured by its absorbance, FDOM measurements are more sensitive to molecular dynamics in solution (Lakowicz and Masters, 2008). Furthermore, the measurement of FDOM is a relatively easy, low cost, and straightforward method without additional preparation (Herzsprung et al., 2012). For instance, to obtain molecular formula from marine samples using Fourier transform ion cyclotron resonance mass spectrometry, solid phase extraction is required to remove salt content from samples (Dittmar et al., 2008).

FDOM measurement is performed by scanning multiple emission wavelengths in a range of excitation wavelengths of a sample which creates an excitation emission matrix (EEM). To analyze this EEM, Coble (1996) integrated certain areas in the matrix and identified peaks which could be distinguished into two general groups, i.e. “humic-like” and “protein-like” components. However, with this method, peak shifts resulting for example from photodegradation or pH

changes (Mostofa et al., 2007; Wu et al., 2005), cannot be detected easily which can lead to misinterpretation of the EEMs. This problem can be addressed by applying a multivariate statistical tool known as parallel factor (PARAFAC) which decomposes FDOM into its fluorophores or fluorescent components (Stedmon et al., 2003). The number of studies in FDOM increased significantly after Stedmon and Bro (2008b) introduced their tutorial of PARAFAC application for FDOM.

PARAFAC studies have been focusing on the characterization and the variability of FDOM in heterogenic environment, and recently in subterranean estuaries (STEs). Instead of mixing fresh- and saline water in open water like that of a surface estuary, processes in a STE occur in the subsurface (Moore, 1999b). The water flux of a STE is considerably low (Bokuniewicz, 1980; Hussain et al., 1999; Sekulic and Vertacnik, 1996), however, studies showed that dissolved organic carbon (DOC) and nutrient, such as nitrate, concentrations were much higher than those in surface estuaries (Santos et al., 2008; Valiela et al., 1999). Production of DOM and FDOM in a STE was also found recently (Kim et al., 2012; Santos et al., 2008; Chapter 2, this thesis) suggesting the importance of STEs to the adjacent coastal ocean.

In this study, we focused on FDOM in two different STEs in a tidal flat and in a permeable sandy beach. Previously, a research in submarine groundwater discharge (SGD) calculated a significant flushing of DOC and metals from this back-barrier area to the North Sea during ebb tide (Moore et al., 2011). Specifically, meaningful chemical alteration was noticed from the tidal flat to the discharge zone in the tidal channel (Riedel et al., 2011). Thus, it is of important to characterize DOM in this area which is responsible for the alteration. Therefore, this study aims to characterize FDOM in these back-barrier sites and identify its variability, spatially and temporally.

8.2. Materials and Methods

8.2.1. The study area

Seasonal samples were collected from Janssand tidal flat in 2010. The tidal flat is located in the backbarrier of Spiekeroog Island in the Wadden Sea (Fig. 8.1). Janssand tidal flat has been studied extensively earlier (Beck et al., 2009; Kowalski et al., 2009; Lübben et al., 2009). Its surface is exposed during low tide for about 6 h and completely covered by ~2 m of water during high tide. Sampling was performed in a 70 m transect from a permanent well (site "JS1") (Beck et al., 2007) towards the tidal flat margin in several depths (10 cm, 50 cm, 100 cm, 150 cm, and 200 cm). Stainless steel push-point samplers, similar to that in Moore and Wilson (2005), were used to collect water samples. A PTFE (teflon) tube was attached to the sampler, and water samples were drawn and filtered with help of a polyethylene syringe. For dissolved organic carbon (DOC) and total dissolved nitrogen (TDN) measurements, we used a disposable 0.7 μm Whatman GF/F syringe filter (VWR, Germany) which was cleaned using 200 mL ultrapure water and rinsed, including all equipment, with an aliquot of sample to ensure the rinsing of the equipment. DOC and TDN samples were acidified to pH 2 and stored in a 24 mL pre-combusted (400°C for 5 h) glass vials with Teflon caps. For FDOM measurement, disposable 0.2 μm GHP syringe filters (VWR, Germany) were used. FDOM samples were stored in amber vials at 4°C until analysis.

In addition, we carried out seasonal sampling in Spiekeroog Island, on a permeable sandy beach where pore waters are mixing with seawater from the main channel of the back-barrier area. A transect sampling from 120 to 140 m of the dune towards seawater line with several depths (50 cm, 100 cm, and 150 cm) were conducted using the same method as that in the tidal

flat (Fig. 8.1). On both sites, a total of 193 samples were taken for fluorescence and bulk parameter analyses.

2.2. DOC and TDN measurements

A Shimadzu TOC-V_{CPH} total organic carbon analyzer equipped with a TNM-1 total nitrogen measuring unit was used to measure DOC and TDN concentration of samples. Deep sea references (DSR), obtained from the University of Miami, were also analyzed as a control. DOC and TDN concentration from ultrapure water was also determined and subtracted from sample concentrations. The detection limit for this analysis was less than 5 μM and standard deviations of replicate measurements were within 5%.

Fig. 8.1. Study sites in Janssand tidal flat and Spiekeroog Island.

8.2.3. FDOM measurements and PARAFAC analysis

All samples were analyzed at room temperature using a Perkin Elmer LS 55 fluorescence spectrometer at Institute of Marine Resources (Bremerhaven, Germany). A three-dimensional excitation emission matrix (EEM) of each sample was obtained by performing scan in excitation wavelength between 240 nm and 450 nm in 5 nm increments, and emission wavelength between 300 nm and 600 nm in 1 nm wavelength increments. To remove inner filter effects which reduced fluorescence intensity, the absorbance of samples were determined with a Hewlett Packard 8453 UV-Visible spectrometer in a 1-cm quartz cuvette. We corrected the intensity using the following equation (Ohno, 2002):

$$I = I_0 \ 10^{-b\ A_{ex}+A_{em}}$$

where I was the detected fluorescence intensity, I_0 was the fluorescence in the absence of self-absorption, b was the path length of both excitation and emission beam, A_{ex} was the absorbance at the excitation wavelength, and A_{em} was the absorbance at the emission wavelength.

Milli-Q water was also scanned daily at excitation 350 nm and emission between 365-430nm. This intensities was used for calibration and unit conversion into Raman Unit (R.U.), according to the equation from Lawaetz and Stedmon (2009):

$$F_{\lambda_{ex}\lambda_{em}} = \frac{I_{\lambda_{ex}\lambda_{em}}}{A_{rp}}$$

where $F_{\lambda_{ex}\lambda_{em}}$ was the fluorescence intensity of a sample in Raman Unit (R.U.), $I_{\lambda_{ex}\lambda_{em}}$ was the fluorescence intensity of a sample in Arbitrary Unit (A.U.), and A_{rp} was the summation of Milli-Q water intensity at every wavelength.

PARAFAC modeling was performed using DOMFluor Toolbox ver 1.7 in Matlab R2010b (Stedmon and Bro, 2008b). Prior modeling, Raman and Rayleigh scattering were removed using the same toolbox. Results were then validated by split-half analysis.

8.3. Results

In the Janssand tidal flat, we modeled 3 FDOM components using PARAFAC analysis (Fig. 8.2A). Component 1, C1, showed excitation maxima at 255 nm and 330 nm with an emission maximum at 412 nm. Component 2, C2, had excitation maxima at 270 nm and 370 nm with an emission maximum at 464 nm. Component 3, C3, showed a maximum excitation and emission at 245 and 441 nm, respectively.

Three FDOM components were also modeled from the Spiekeroog beach samples (Fig. 8.2B). All components showed two excitation peaks and an emission peak. Component 1, C1, had excitation maxima at <240 nm and 350 nm with an emission maximum at 434 nm. Two maxima at <240 nm and 305 nm were also observed in component 2, C2, with an emission peak at 403 nm. Component 3, C3, had excitation maxima at 260 nm and 375 nm with an emission maximum at 480 nm.

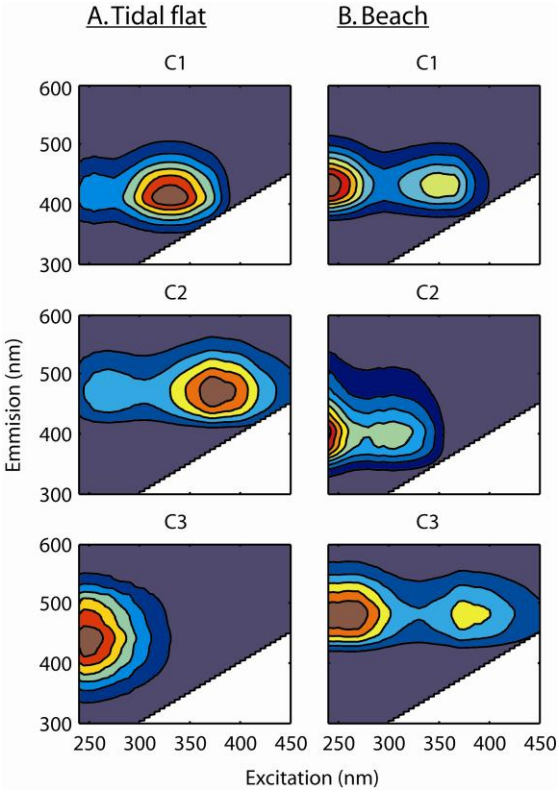

Fig. 8.2. FDOM components modeled using PARAFAC analysis for the Janssand tidal flat (A) and the Spiekeroog beach (B) samples.

8.4. Discussion

In the tidal flat, we identified three humic-like components. Compared to previous findings, C1 was similar to C3 in the Suwannee River (Chapter 4, this thesis) and C2 in a STE at Turkey Point, FL (Chapter 3, this thesis), although a shift at higher excitation wavelength was noticed in our C1 spectra. In addition, the most intense peak in our C1 was at higher excitation. C2 in our study was also modeled recently as C1 in the Suwannee River (Chapter 3, this thesis). Similarly, we also noticed shift at higher excitation wavelength and the most intense peak was found at higher excitation wavelength. Shift to lower emission wavelength, in contrast, was noticed in our C3 compared to C2 in the Suwanee River (Chapter 4, this thesis).

All three terrestrial humic-like components from the beach samples were also identified by comparing them to previous studies. Our C1 showed similar peak to C3 in the Suwannee River (Chapter 4, this thesis), with blue-shifted in emission maximum. An indicative of shift to the lower excitation and emission peak was noticed in our C2, compared to C3 peak in a STE at Turkey Point, FL (Chapter 3, this thesis). C3 in our study, however, showed the same peak with no shift as C1 in the Suwannee River (Chapter 4, this thesis).

The identification of FDOM components analyzed using PARAFAC analysis is a preliminary step in order to compare them with recent findings. More in depth analysis is of important to study the variability of FDOM at both sites. It will be achieved by integrating all environmental data, and chemical and molecular data of DOM. Nonetheless, multivariate statistics is necessary to explore all the variability in the system.

Chapter 9

Conclusions and Perspective

Conclusions and Perspective

These researches were conducted to determine whether SGD was a source or a sink of FDOM; and whether FDOM was a potential proxy to calculate DOC for a given site. Furthermore, FDOM was also characterized using PARAFAC analysis and correlated with other data, including DOM molecular formulae, to investigate which processes better explained alteration in FDOM intensities.

Significant contributions for the future research in coastal ocean DOM and FDOM were reflected by the results, and the data analyses from this study.

1. FDOM production in the STE.

FDOM was apparently produced in the STE and released via SGD in a considerable amount, even higher than those released by river. Previous study pointed the same results based on a much shorter sampling duration (Burdige et al., 2004). Therefore, our longer in situ FDOM measurement confirmed that those findings were indeed significant, and not by chance only.

An evidence about the possibility of using FDOM to calculate DOC was also confirmed in this thesis. Thus, FDOM can be used to estimate DOC concentration in the ocean, as proposed by Kowalczuk et al. (2010), and in contrasting environmental conditions like subterranean estuaries.

2. The driving forces in the STE.

Processes in surface estuaries are affected significantly by mixing of freshwater and seawater (Benner and Opsahl, 2001; Hung and Huang, 2005; Peterson et al., 1994). However, in

the STE, this study showed that salinity did not correlate with DOM and FDOM. In contrast, nutrient concentrations, specifically nitrogen speciation, affected FDOM intensities. Recirculation of FDOM which was deposited in different sediment layer might also contribute, to some extent. Our findings, therefore, provided an explanation of non-conservative behavior showed by previous findings (e.g. Kim et al., 2012, Burdige et al., 2004).

Partial least square (PLS) regression, which led to our results, was presented for the first time to the DOM study. Up to now, principal component analysis has been particularly applied in the FDOM study (Jaffé et al., 2008; Yamashita et al., 2011); however, the result has to be correlated with other data for further interpretation. On the other hand, the result obtained from a PLS analysis presents all data variability in linear correlations.

3. Molecular FDOM variability.

A more advance study in DOM molecular distribution, in regard to the variability in FDOM intensity, was addressed in this thesis. Despite an expected simple river-ocean mixing system, an intrusion of SGD-derived DOM was noticed in the estuary station as exposed by the PLS analysis. In addition, the molecular distribution of DOM showed a decrease in aromaticity and an increase in saturation along salinity gradients, in agreement with previous studies; however, the highest aromaticity and saturation found at the estuary station suggested that both were related with sun exposure instead of the source of DOM. The samples amount in this study far exceeds those obtained previously; therefore, our results are statistically more meaningful.

4. In situ measurement of DOM and remote sensing of FDOM

This study proposed regression matrices as tools to map correlation of FDOM intensities with other data, especially DOM. Not only does support variability explained by the PLS analysis, regression matrices also show the pattern of wavelength where certain processes affected FDOM significantly. In addition, the matrices contain wavelength with the best correlation, which can be applied to measure other data in situ. Once the right wavelength proxies have been established, using FDOM in remote sensing is also possible.

5. Future studies

Results of this study are limited in the same location, although covering both surface and subterranean estuaries. To generalize these findings, more works in different locations are essential. In STEs, the possibility of other driving forces has to be inspected. For instance, besides nutrient concentrations, metal concentration may influence the system more significantly than salinity.

Result of the DOM molecular distribution in our study was also limited in a simple mixing surface estuary. Further sampling under specific condition will complete information regarding DOM and FDOM molecular reactivity. Therefore, a study of FDOM in a tidal flat in the southern North Sea is also presented as an outlook.

References

Andrews, S., Caron, S. and Zafiriou, O., 2000. Photochemical oxygen consumption in marine waters: A major sink for colored dissolved organic matter? Limnology and Oceanography, 45(2): 267-277.

Averett, R.C. and Geological, S., 1990. Humic substances in the Suwannee River, Georgia: Interactions, properties, and proposed structures. Department of the Interior, US Geological Survey.

Baghoth, S.A., Sharma, S.K. and Amy, G.L., 2011. Tracking natural organic matter (NOM) in a drinking water treatment plant using fluorescence excitation emission matrices and PARAFAC. Water research, 45(2): 797-809

Baines, S.B. and Pace, M.L., 1991. The production of dissolved organic matter by phytoplankton and its importance to bacteria: patterns across marine and freshwater systems. Limnology and Oceanography: 1078-1090.

Baker, A., 2001. Fluorescence excitation-emission matrix characterization of some sewage-impacted rivers. Environmental Science & Technology, 35(5): 948-953.

Bano, N., Moran, M.A. and Hodson, R.E., 1997. Bacterial utilization of dissolved humic substances from a freshwater swamp. Aquatic Microbial Ecology, 12(3): 233-238.

Beck, M. et al., 2007. In situ pore water sampling in deep intertidal flat sediments. Limnology and Oceanography: Methods, 5: 136-144.

Beck, M. et al., 2009. Deep pore water profiles reflect enhanced microbial activity towards tidal flat margins. Ocean Dynamics, 59(2): 371-383.

Benner, R. and Opsahl, S., 2001. Molecular indicators of the sources and transformations of dissolved organic matter in the Mississippi river plume. Organic Geochemistry, 32(4): 597-611.

Black, F.J. et al., 2009. Submarine groundwater discharge of total mercury and monomethylmercury to Central California coastal waters. Environmental science & technology, 43(15): 5652-5659.

Bledsoe, E.L. and Phlips, E.J., 2000. Relationships between phytoplankton standing crop and physical, chemical, and biological gradients in the Suwannee River and plume region, USA. Estuaries and Coasts, 23(4): 458-473.

Blough, N. and Del Vecchio, R., 2002a. Chromophoric DOM in the coastal environment. Biogeochemistry of Marine Dissolved Organic Matter: 509-546.

Blough, N.V. and Del Vecchio, R., 2002b. Distribution and dynamics of chromophoric dissolved organic matter (CDOM) in the coastal environment. Biogeochemistry of marine dissolved organic matter. Academic: 509–546.

Bokuniewicz, H., 1980. Groundwater seepage into Great South Bay, New York. Estuarine and Coastal Marine Science, 10(4).

Bourget, P. and Delouis, J.M., 1993. Methods for assessment of area under the curve in pharmacokinetic analysis. Therapie, 48(1): 1-5.

Bricaud, A., Morel, A. and Prieur, L., 1981. Absorption by dissolved organic matter of the sea (yellow substance) in the UV and visible domains. Limnology and oceanography: 43-53.

Bro, R., 1997. PARAFAC. Tutorial and applications. Chemometrics and intelligent laboratory systems, 38(2): 149-171.

Bro, R. and Ohno, T., 2006. Dissolved organic matter characterization using multiway spectral decomposition of fluorescence landscapes. Soil Science Society of America Journal, 70(6): 2028-2037.

Burdige, D.J., Kline, S.W. and Chen, W., 2004. Fluorescent dissolved organic matter in marine sediment pore waters. Marine Chemistry, 89(1): 289-311.

Burnett, W. et al., 2006. Quantifying submarine groundwater discharge in the coastal zone via multiple methods. Science of the Total Environment, The, 367(2-3): 498-543.

Burnett, W.C., Cowart, J.B. and Deetae, S., 1999. Radium in the Suwannee River and estuary. Biodegradation, 10(3): 237-255.

Burnett, W.C. and Dulaiova, H., 2003. Estimating the dynamics of groundwater input into the coastal zone via continuous radon-222 measurements. Journal of Environmental Radioactivity, 69(1-2): 21-35.

Cable, J., Burnett, W., Chanton, J. and Weatherly, G., 1996. Estimating groundwater discharge into the northeastern Gulf of Mexico using radon-222. Earth and Planetary Science Letters, 144(3-4): 591-604.

Cai, W. and Wang, Y., 1998. The chemistry, fluxes, and sources of carbon dioxide in the estuarine waters of the Satilla and Altamaha Rivers, Georgia. Limnology and Oceanography, 43(4): 657-668.

Canuel, E.A., Cloern, J.E., Ringelberg, D.B., Guckert, J.B. and Rau, G.H., 1995. Molecular and isotopic tracers used to examine sources of organic matter and its incorporation into the food webs of San Francisco Bay. Limnology and Oceanography: 67-81.

Carder, K., Steward, R., Harvey, G. and Ortner, P., 1989a. Marine humic and fulvic acids: Their effects on remote sensing of ocean chlorophyll. Limnology and Oceanography, 34(1): 68-81.

Carder, K.L., Steward, R.G., Harvey, G.R. and Ortner, P.B., 1989b. Marine humic and fulvic acids: Their effects on remote sensing of ocean chlorophyll. Limnology and Oceanography: 68-81.

Chari, N., Sarma, N.S., Pandi, S.R. and Murthy, K.N., 2012. Seasonal and spatial constraints of fluorophores in the midwestern Bay of Bengal by PARAFAC analysis of excitation emission matrix spectra. Estuarine, Coastal and Shelf Science, 100: 162–171.

Chen, W., Westerhoff, P., Leenheer, J.A. and Booksh, K., 2003. Fluorescence excitation-emission matrix regional integration to quantify spectra for dissolved organic matter. Environmental science & technology, 37(24): 5701-5710.

Chen, Y., Senesi, N. and Schnitzer, M., 1977. Information Provided on Humic Substances by E4/E6 Ratios. Soil Science Society of America Journal, 41(2): 352-358.

Coble, P.G., 1996. Characterization of marine and terrestrial DOM in seawater using excitation-emission matrix spectroscopy. Marine Chemistry, 51(4): 325-346.

Coble, P.G., Del Castillo, C.E. and Avril, B., 1998. Distribution and optical properties of CDOM in the Arabian Sea during the 1995 Southwest Monsoon. Deep-Sea Research Part II, 45(10-11): 2195-2223.

Coble, P.G., Green, S.A., Blough, N.V. and Gagosian, R.B., 1990. Characterization of dissolved organic matter in the Black Sea by fluorescence spectroscopy. Nature, 348: 432-435.

Cory, R.M. and McKnight, D.M., 2005. Fluorescence spectroscopy reveals ubiquitous presence of oxidized and reduced quinones in dissolved organic matter. Environmental science & technology, 39(21): 8142-8149.

Crusius, J. et al., 2005. Submarine groundwater discharge to a small estuary estimated from radon and salinity measurements and a box model. Biogeosciences, 2(2): 141-157.

de Almeida Azevedo, D., Lacorte, S., Vinhas, T., Viana, P. and Barceló, D., 2000. Monitoring of priority pesticides and other organic pollutants in river water from Portugal by gas chromatography–mass spectrometry and liquid chromatography–atmospheric pressure chemical ionization mass spectrometry. Journal of Chromatography A, 879(1): 13-26.

Del Castillo, C., Gilbes, F., Coble, P. and Muller-Karger, F., 2000a. On the dispersal of riverine colored dissolved organic matter over the West Florida Shelf. Limnology and Oceanography, 45(6): 1425-1432.

Del Castillo, C.E., Gilbes, F., Coble, P.G. and Muller-Karger, F.E., 2000b. On the dispersal of riverine colored dissolved organic matter over the West Florida Shelf. Limnology and Oceanography: 1425-1432.

Derbalah, A., Nakatani, N. and Sakugawa, H., 2003. Distribution, seasonal pattern, flux and contamination source of pesticides and nonylphenol residues in Kurose River water, Higashi-Hiroshima, Japan. Geochemical Journal, 37(2): 217-232.

Dittmar, T., Koch, B., Hertkorn, N. and Kattner, G., 2008. A simple and efficient method for the solid-phase extraction of dissolved organic matter (SPE-DOM) from seawater. Limnol. Oceanogr. Methods, 6: 230-235.

Djikanović, D., Kalauzi, A., Jeremić, M., MiÄ‡ić, M. and Radotić, K., 2007. Deconvolution of fluorescence spectra: contribution to the structural analysis of complex molecules. Colloids and Surfaces B: Biointerfaces, 54(2): 188-192.

Esteves, V.I., Otero, M. and Duarte, A.C., 2009. Comparative characterization of humic substances from the open ocean, estuarine water and fresh water. Organic Geochemistry, 40(9): 942-950.

Ferrari, G.M., Dowell, M.D., Grossi, S. and Targa, C., 1996. Relationship between the optical properties of chromophoric dissolved organic matter and total concentration of dissolved organic carbon in the southern Baltic Sea region. Marine Chemistry, 55(3-4): 299-316.

Foden, J., Sivyer, D.B., Mills, D.K. and Devlin, M.J., 2008. Spatial and temporal distribution of chromophoric dissolved organic matter (CDOM) fluorescence and its contribution to light attenuation in UK waterbodies. Estuarine, Coastal and Shelf Science, 79(4): 707-717.

Ganguli, P.M., Conaway, C.H., Swarzenski, P.W., Izbicki, J.A. and Flegal, A.R., 2012. Mercury Speciation and Transport via Submarine Groundwater Discharge at a Southern California Coastal Lagoon System. Environmental Science & Technology, 46(3): 1480-1488.

Gonsior, M. et al., 2008. Spectral characterization of chromophoric dissolved organic matter (CDOM) in a fjord (Doubtful Sound, New Zealand). Aquatic Sciences-Research Across Boundaries, 70(4): 397-409.

Gonsior, M. et al., 2009. Photochemically induced changes in dissolved organic matter identified by ultrahigh resolution fourier transform ion cyclotron resonance mass spectrometry. Environmental Science & Technology, 43(3): 698-703.

Guéguen, C., Granskog, M.A., McCullough, G. and Barber, D.G., 2011. Characterisation of colored dissolved organic matter in Hudson Bay and Hudson Strait using parallel factor analysis. Journal of Marine Systems, 88(3): 423-433.

Hansell, D.A. and Carlson, C.A., 1998. Deep-ocean gradients in the concentration of dissolved organic carbon. Nature, 395(6699): 263-266.

Hansell, D.A. and Carlson, C.A., 2002. Biogeochemistry of marine dissolved organic matter. Academic Pr.

Hedges, J.I., Keil, R.G. and Benner, R., 1997. What happens to terrestrial organic matter in the ocean? Organic Geochemistry, 27(5-6): 195-212.

Her, N., Amy, G., McKnight, D., Sohn, J. and Yoon, Y., 2003. Characterization of DOM as a function of MW by fluorescence EEM and HPLC-SEC using UVA, DOC, and fluorescence detection. Water Research, 37(17): 4295-4303.

Hertkorn, N. et al., 2006. Characterization of a major refractory component of marine dissolved organic matter. Geochimica et cosmochimica acta, 70(12): 2990-3010.

Herzsprung, P. et al., 2012. Variations of DOM Quality in Inflows of a Drinking Water Reservoir: Linking of van Krevelen Diagrams with EEMF Spectra by Rank Correlation. Environmental science & technology, 46(10): 5511-5518.

Hopkinson, C.S. et al., 1998. Terrestrial inputs of organic matter to coastal ecosystems: An intercomparison of chemical characteristics and bioavailability. Biogeochemistry, 43(3): 211-234.

Hung, J.J. and Huang, M.H., 2005. Seasonal variations of organic-carbon and nutrient transport through a tropical estuary (Tsengwen) in southwestern Taiwan. Environmental geochemistry and health, 27(1): 75-95.

Hussain, N., Church, T.M. and Kim, G., 1999. Use of 222Rn and 226Ra to trace groundwater discharge into the Chesapeake Bay. Marine Chemistry, 65(1-2): 127-134.

Jackson, J.B. and Nemeth, D.J., 2007. A new method to describe seagrass habitat sampled during fisheries-independent monitoring. Estuaries and Coasts, 30(1): 171-178.

Jaffé, R. et al., 2008. Spatial and temporal variations in DOM composition in ecosystems: The importance of long-term monitoring of optical properties. J. Geophys. Res, 113: G04032.

Jumars, P.A., Penry, D.L., Baross, J.A., Perry, M.J. and Frost, B.W., 1989. Closing the microbial loop: dissolved carbon pathway to heterotrophic bacteria from incomplete ingestion, digestion and absorption in animals. Deep Sea Research Part A. Oceanographic Research Papers, 36(4): 483-495.

Kalbitz, K., Solinger, S., Park, J.H., Michalzik, B. and Matzner, E., 2000. Controls on the dynamics of dissolved organic matter in soils: a review. Soil Science, 165(4): 277.

Katz, B.G., Dehan, R.S., Hirten, J.J. and Catches, J.S., 1997. Interactions Between Ground Water and SurfaceWater in the Suwannee River Basin, Florida. Journal of the American Water Resources Association, 33: 1237-1254.

Keith, D.J. and Yoderand Sa, J.A., 2002. Spatial and temporal distribution of coloured dissolved organic matter (CDOM) in Narragansett Bay, Rhode Island: implications for phytoplankton in coastal waters. Estuarine, Coastal and Shelf Science, 55(5): 705-717.

Kim, T.H., Waska, H., Kwon, E., Suryaputra, I.G.N.A. and Kim, G., 2012. Production, degradation, and flux of dissolved organic matter in the subterranean estuary of a large tidal flat. Marine Chemistry, 142-144: 1-10.

Klapper, L. et al., 2002. Fulvic acid oxidation state detection using fluorescence spectroscopy. Environmental science & technology, 36(14): 3170-3175.

Koch, B.P. and Dittmar, T., 2006. From mass to structure: an aromaticity index for high-resolution mass data of natural organic matter. Rapid communications in mass spectrometry, 20(5): 926-932.

Koch, B.P., Witt, M., Engbrodt, R., Dittmar, T. and Kattner, G., 2005. Molecular formulae of marine and terrigenous dissolved organic matter detected by electrospray ionization Fourier transform ion cyclotron resonance mass spectrometry. Geochimica et cosmochimica acta, 69(13): 3299-3308.

Kowalczuk, P. et al., 2010a. Characterization of dissolved organic matter fluorescence in the South Atlantic Bight with use of PARAFAC model: Relationships between fluorescence and its components, absorption coefficients and organic carbon concentrations. Marine Chemistry, 118(1-2): 22-36.

Kowalczuk, P. et al., 2009. Characterization of dissolved organic matter fluorescence in the South Atlantic Bight with use of PARAFAC model: Interannual variability. Marine chemistry, 113(3-4): 182-196.

Kowalczuk, P., Zablocka, M., Sagan, S. and Kulinski, K., 2010b. Fluorescence measured in situ as a proxy of CDOM absorption and DOC concentration in the Baltic Sea. Oceanologia, 52(3): 431-471.

Kowalski, N. et al., 2009. Trace metal dynamics in the water column and pore waters in a temperate tidal system: response to the fate of algae-derived organic matter. Ocean Dynamics, 59(2): 333-350.

Kronberg, L., 1999. Content of humic substances in freshwater. Limnology of humic waters. Leiden. The Netherlands: 9-10.

Kubista, M., Sjöback, R., Eriksson, S. and Albinsson, B., 1994. Experimental correction for the inner-filter effect in fluorescence spectra. Analyst, 119(3): 417-419.

Lakowicz, J.R. and Masters, B.R., 2008. Principles of fluorescence spectroscopy. Journal of Biomedical Optics, 13: 029901.

Lambert, M.J. and Burnett, W.C., 2003. Submarine groundwater discharge estimates at a Florida coastal site based on continuous radon measurements. Biogeochemistry, 66(1-2): 55-73.

Lawaetz, A.J. and Stedmon, C.A., 2009. Fluorescence intensity calibration using the Raman scatter peak of water. Applied spectroscopy, 63(8): 936-940.

Leenheer, J.A. and Croue, J.P., 2003. Peer Reviewed: Characterizing Aquatic Dissolved Organic Matter. Environmental Science & Technology, 37(1): 18-26.

Liu, J., 2011. Overview of Redundancy Analysis and Partial Linear Squares and Their Extension to the Frequency Domain, Dalhousie University, Halifax, Nova Scotia, 81 pp.

Liu, Z., Sleighter, R.L., Zhong, J. and Hatcher, P.G., 2011. The chemical changes of DOM from black waters to coastal marine waters by HPLC combined with ultrahigh resolution mass spectrometry. Estuarine Coastal and Shelf Science, 92(2): 205-216.

Lübben, A. et al., 2009. Distributions and characteristics of dissolved organic matter in temperate coastal waters (Southern North Sea). Ocean Dynamics, 59(2): 263-275.

Ludwig, W., Probst, J.L. and Kempe, S., 1996. Predicting the oceanic input of organic carbon by continental erosion. Global Biogeochemical Cycles, 10(1): 23-41.

Malcolm, R.L., McKnight, D.M. and Averett, R.C., 1989. History and description of the Okefenokee Swamp--Origin of the Suwannee River. In: Humic Substances in the Suwannee River, Georgia: Interactions, Properties, and Proposed Structures. Open-File Report 87-557, 1989. p 1-21, 2 fig, 30 ref, 1 plate.

Maranger, R. and Pullin, M.J., 2003. Elemental complexation by dissolved organic matter in lakes: implications for Fe speciation and the bioavailability of Fe and P. Aquatic ecosystems: interactivity of dissolved organic matter. Academic Press/Elsevier Science, San Diego, California, USA: 185-214.

Martin, W.R., 2010. Chemical Processes in Estuarine Sediments. In: J.H. Steel, S.A. Thorpe and K.K. Turekian (Editors), Marine Chemistry and Geochemistry, a Derivative of the Encyclopedia of Ocean Sciences. Elsevier, Amsterdam.

McKnight, D.M. et al., 2001. Spectrofluorometric characterization of dissolved organic matter for indication of precursor organic material and aromaticity. Limnology and Oceanography: 38-48.

McLafferty, F.W. and Turecek, F., 1993. Interpretation of mass spectra. Univ Science Books.

Meyers-Schulte, K.J. and Hedges, J.I., 1986. Molecular evidence for a terrestrial component of organic matter dissolved in ocean water.

Moore, W., 1996. Large groundwater inputs to coastal waters revealed by 226 Ra enrichments. Nature, 380: 612-614.

Moore, W., 1999a. The subterranean estuary: a reaction zone of ground water and sea water. Marine chemistry, 65(1-2): 111-125.

Moore, W.S., 1999b. The subterranean estuary: a reaction zone of ground water and sea water. Marine chemistry, 65(1-2): 111-125.

Moore, W.S., 2010. The effect of submarine groundwater discharge on the ocean. Annual review of marine science, 2: 59-88.

Moore, W.S. et al., 2011. Radium-based pore water fluxes of silica, alkalinity, manganese, DOC, and uranium: A decade of studies in the German Wadden Sea. Geochimica et Cosmochimica Acta, 75(21).

Moore, W.S. and Wilson, A.M., 2005. Advective flow through the upper continental shelf driven by storms, buoyancy, and submarine groundwater discharge. Earth and Planetary Science Letters, 235(3): 564-576.

Mostofa, K. et al., 2005. Three-dimensional fluorescence as a tool for investigating the dynamics of dissolved organic matter in the Lake Biwa watershed. Limnology, 6(2): 101-115.

Mostofa, K.M.G., Yoshioka, T., Konohira, E. and Tanoue, E., 2007. Photodegradation of fluorescent dissolved organic matter in river waters. Geochemical Journal, 41(5): 323-331.

Mulholland, P.J., 2003. Large-scale patterns in dissolved organic carbon concentration, flux, and sources. Aquatic ecosystems: Interactivity of dissolved organic matter. Academic: 139-159.

Muniz, I.P., 1990. Freshwater acidification: its effects on species and communities of freshwater microbes, plants and animals. Proceedings of the Royal Society of Edinburgh. Section B. Biological Sciences, 97(1): 227-254.

Murphy, K.R. et al., 2011. Organic Matter Fluorescence in Municipal Water Recycling Schemes: Toward a Unified PARAFAC Model. Environmental Science & Technology, 45(7): 2909-2916.

Murphy, K.R., Ruiz, G.M., Dunsmuir, W.T.M. and Waite, T.D., 2006. Optimized parameters for fluorescence-based verification of ballast water exchange by ships. Environmental science & technology, 40(7): 2357-2362.

Murphy, K.R., Stedmon, C.A., Waite, T.D. and Ruiz, G.M., 2008. Distinguishing between terrestrial and autochthonous organic matter sources in marine environments using fluorescence spectroscopy. Marine Chemistry, 108(1-2): 40-58.

Nagata, T., 2000. Production mechanisms of dissolved organic matter. Wiley Series in Ecological and Applied Microbiology.

Nakane, K., Kohno, T., Horikoshi, T. and Nakatsubo, T., 1997. Soil carbon cycling at a black spruce (Picea mariana) forest stand in Saskatchewan, Canada. Journal of Geophysical Research, 102(D24).

Nixon, S.W. et al., 1996. The fate of nitrogen and phosphorus at the land-sea margin of the North Atlantic Ocean. Biogeochemistry, 35(1): 141-180.

Ohno, T., 2002. Fluorescence inner-filtering correction for determining the humification index of dissolved organic matter. Environmental science & technology, 36(4): 742-746.

Osburn, C.L. and Stedmon, C.A., 2011. Linking the chemical and optical properties of dissolved organic matter in the Baltic-North Sea transition zone to differentiate three allochthonous inputs. Marine chemistry, 126(1-4): 281-294.

Parlanti, E., Wörz, K., Geoffroy, L. and Lamotte, M., 2000. Dissolved organic matter fluorescence spectroscopy as a tool to estimate biological activity in a coastal zone submitted to anthropogenic inputs. Organic Geochemistry, 31(12): 1765-1781.

Perdue, E.M. and Koprivnjak, J.F., 2007. Using the C/N ratio to estimate terrigenous inputs of organic matter to aquatic environments. Estuarine, Coastal and Shelf Science, 73(1-2): 65-72.

Peterson, B., Fry, B., Hullar, M., Saupe, S. and Wright, R., 1994. The distribution and stable carbon isotopic composition of dissolved organic carbon in estuaries. Estuaries and Coasts, 17(1): 111-121.

Radotić, K. et al., 2006. Component analysis of the fluorescence spectra of a lignin model compound. Journal of Photochemistry and Photobiology B: Biology, 83(1): 1-10.

Riedel, T., Lettmann, K., Schnetger, B., Beck, M. and Brumsack, H.J., 2011. Rates of trace metal and nutrient diagenesis in an intertidal creek bank. Geochimica et Cosmochimica Acta, 75(1): 134-147.

Riedl, R.J., Huang, N. and Machan, R., 1972. The subtidal pump: a mechanism of interstitial water exchange by wave action. Marine Biology, 13(3): 210-221.

Rutkowski, C.M., Burnett, W.C., Iverson, R.L. and Chanton, J.P., 1999. The effect of groundwater seepage on nutrient delivery and seagrass distribution in the northeastern Gulf of Mexico. Estuaries and Coasts, 22(4): 1033-1040.

Santos, I.R., Burnett, W.C., Chanton, J., Dimova, N. and Peterson, R.N., 2009a. Land or ocean?: Assessing the driving forces of submarine groundwater discharge at a coastal site in the Gulf of Mexico. Journal of Geophysical Research-Oceans, 114.

Santos, I.R. et al., 2008. Nutrient biogeochemistry in a Gulf of Mexico subterranean estuary and groundwater-derived fluxes to the coastal ocean. Limnology and Oceanography: 705-718.

Santos, I.R., Burnett, W.C., Dittmar, T., Suryaputra, I.G.N.A. and Chanton, J., 2009b. Tidal pumping drives nutrient and dissolved organic matter dynamics in a Gulf of Mexico subterranean estuary. Geochimica Et Cosmochimica Acta, 73(5): 1325-1339.

Santos, I.R. et al., 2009c. Extended time series measurements of submarine groundwater discharge tracers (222Rn and CH4) at a coastal site in Florida. Marine Chemistry, 113(1-2): 137-147.

Sekulic, B. and Vertacnik, A., 1996. Balance of average annual fresh water inflow into the Adriatic Sea. International Journal of Water Resources Development, 12(1): 89-98.

Shaw, T., Moore, W., Kloepfer, J. and Sochaski, M., 1998a. The flux of barium to the coastal waters of the southeastern USA: the importance of submarine groundwater discharge. Geochimica et Cosmochimica Acta, 62(18): 3047-3054.

Shaw, T.J., Moore, W.S., Kloepfer, J. and Sochaski, M.A., 1998b. The flux of barium to the coastal waters of the southeastern USA: The importance of submarine groundwater discharge. Geochimica et Cosmochimica Acta, 62(18): 3047-3054.

Shubina, D. et al., 2010. The "blue shift" of emision maximum and the fluorescence quantum yield as quantitative spectral characteristics of dissolved humic substances. EARSeL eProceedings, 9(1): 13-21.

Sieburth, J.M.N. and Jensen, A., 1968. Studies on algal substances in the sea. I. Gelbstoff (humic material) in terrestrial and marine waters. Journal of Experimental Marine Biology and Ecology, 2(2): 174-189.

Simmons, G.M., 1992. Importance of submarine groundwater discharge(SGWD) and seawater cycling to material flux across sediment/water interfaces in marine environments. Marine Ecology-Progress Series, 84(2): 173-184.

Sleighter, R.L. and Hatcher, P.G., 2008. Molecular characterization of dissolved organic matter (DOM) along a river to ocean transect of the lower Chesapeake Bay by ultrahigh

resolution electrospray ionization Fourier transform ion cyclotron resonance mass spectrometry. Marine Chemistry, 110(3-4): 140-152.

Sleighter, R.L., McKee, G.A., Liu, Z. and Hatcher, P.G., 2008. Naturally present fatty acids as internal calibrants for Fourier transform mass spectra of dissolved organic matter. Limnol. Oceanogr.: Methods, 6: 246-253.

Slomp, C. and Van Cappellen, P., 2004a. Nutrient inputs to the coastal ocean through submarine groundwater discharge: controls and potential impact. Journal of Hydrology, 295(1-4): 64-86.

Slomp, C.P. and Van Cappellen, P., 2004b. Nutrient inputs to the coastal ocean through submarine groundwater discharge: controls and potential impact. Journal of Hydrology, 295(1): 64-86.

Smitha, C.G. and Swarzenskib, P.W., 2012. An investigation of submarine groundwater-borne nutrient fluxes to the west Florida shelf and recurrent harmful algal blooms. Limnol. Oceanogr, 57(2): 471-485.

Stabenau, E., Zepp, R., Bartels, E. and Zika, R., 2004. Role of the seagrass Thalassia testudinum as a source of chromophoric dissolvedorganic matter in coastal south Florida. Marine Ecology Progress Series, 282: 59-72.

Stedmon, C.A. and Bro, R., 2008a. Characterizing dissolved organic matter fluorescence with parallel factor analysis: a tutorial. Limnology and Oceanography: Methods, 6(1): 1–6.

Stedmon, C.A. and Bro, R., 2008b. Characterizing dissolved organic matter fluorescence with parallel factor analysis: a tutorial. Limnology and Oceanography: Methods, 6(1): 1-6.

Stedmon, C.A. and Markager, S., 2005a. Resolving the variability in dissolved organic matter fluorescence in a temperate estuary and its catchment using PARAFAC analysis. Limnology and oceanography, 50(2): 686-697.

Stedmon, C.A. and Markager, S., 2005b. Tracing the production and degradation of autochthonous fractions of dissolved organic matter by fluorescence analysis. Limnology and Oceanography: 1415-1426.

Stedmon, C.A., Markager, S. and Bro, R., 2003. Tracing dissolved organic matter in aquatic environments using a new approach to fluorescence spectroscopy. Marine Chemistry, 82(3-4): 239-254.

Stedmon, C.A. et al., 2007a. Photochemical production of ammonium and transformation of dissolved organic matter in the Baltic Sea. Marine Chemistry, 104(3): 227-240.

Stedmon, C.A. et al., 2007b. Photochemical production of ammonium and transformation of dissolved organic matter in the Baltic Sea. Marine chemistry, 104(3-4): 227-240.

Stenson, A.C., Marshall, A.G. and Cooper, W.T., 2003. Exact masses and chemical formulas of individual Suwannee River fulvic acids from ultrahigh resolution electrospray ionization Fourier transform ion cyclotron resonance mass spectra. Analytical chemistry, 75(6): 1275-1284.

Stenson, A.C., William, M., Marshall, A.G. and Cooper, W.T., 2002. Ionization and fragmentation of humic substances in electrospray ionization Fourier transform-ion cyclotron resonance mass spectrometry. Analytical chemistry, 74(17): 4397-4409.

Stubbins, A. et al., 2010. Illuminated darkness: Molecular signatures of Congo River dissolved organic matter and its photochemical alteration as revealed by ultrahigh precision mass spectrometry. Limnology and Oceanography, 55(4): 1467.

Sugimura, Y. and Suzuki, Y., 1988. A high-temperature catalytic oxidation method for the determination of non-volatile dissolved organic carbon in seawater by direct injection of a liquid sample. Marine Chemistry, 24(2): 105-131.

Suzuki, Y., Sugimura, Y. and Itoh, T., 1985. A catalytic oxidation method for the determination of total nitrogen dissolved in seawater. Marine Chemistry, 16(1): 83-97.

Tedetti, M. and Sempéré, R., 2006. Penetration of ultraviolet radiation in the marine environment. A review. Photochemistry and Photobiology, 82(2): 389-397.

Thornton, S.F. and McManus, J., 1994. Application of organic carbon and nitrogen stable isotope and C/N ratios as source indicators of organic matter provenance in estuarine systems: evidence from the Tay Estuary, Scotland. Estuarine, Coastal and Shelf Science, 38(3): 219-233.

Thurman, E.M., 1985. Organic geochemistry of natural waters, 2. Springer.

Thurman, E.M. and Malcolm, R.L., 1981. Preparative isolation of aquatic humic substances. Environmental Science & Technology, 15(4): 463-466.

Tremblay, L.B., Dittmar, T., Marshall, A.G., Cooper, W.J. and Cooper, W.T., 2007. Molecular characterization of dissolved organic matter in a North Brazilian mangrove porewater and mangrove-fringed estuaries by ultrahigh resolution Fourier transform-ion cyclotron resonance mass spectrometry and excitation/emission spectroscopy. Marine chemistry, 105(1-2): 15-29.

Uchida, M., Nakatsubo, T., Kasai, Y., Nakane, K. and Horikoshi, T., 2000. Altitudinal Differences in Organic Matter Mass Loss and Fungal Biomass in a Subalpine Coniferous Forest, Mt. Fuji, Japan. Arctic, Antarctic, and Alpine Research, 32(3): 262-269.

Urban-Rich, J., McCarty, J.T., Fernández, D. and Acuña, J.L., 2006. Larvaceans and copepods excrete fluorescent dissolved organic matter (FDOM). Journal of experimental marine biology and ecology, 332(1): 96-105.

Valiela, I. et al., 1990. Transport of groundwater-borne nutrients from watersheds and their effects on coastal waters. Biodegradation, 10(3): 177-197.

Valiela, I. et al., 1999. Transport of groundwater-borne nutrients from watersheds and their effects on coastal waters. Biodegradation, 10(3): 177-197.

Volk, C., Volk, C. and Kaplan, L., 1997. Chemical composition of biodegradable dissolved organic matter in streamwater. Limnology and Oceanography, 42(1): 39-44.

Walker, S.A., Amon, R.M.W., Stedmon, C., Duan, S. and Louchouarn, P., 2009. The use of PARAFAC modeling to trace terrestrial dissolved organic matter and fingerprint water masses in coastal Canadian Arctic surface waters. Journal of Geophysical Research-Biogeosciences, 114.

Wedborg, M., Persson, T. and Larsson, T., 2007. On the distribution of UV-blue fluorescent organic matter in the Southern Ocean. Deep Sea Research Part I: Oceanographic Research Papers, 54(11): 1957-1971.

Williams, P. and Yentsch, C.S., 1976. An examination of photosynthetic production, excretion of photosynthetic products, and heterotrophic utilization of dissolved organic compounds with reference to results from a coastal subtropical sea. Marine Biology, 35(1): 31-40.

Wu, F.C., Mills, R.B., Cai, Y.R., Evans, R.D. and Dillon, P.J., 2005. Photodegradation-induced changes in dissolved organic matter in acidic waters. Canadian Journal of Fisheries and Aquatic Sciences, 62(5): 1019-1027.

Yamashita, Y., Jaffe, R., Maie, N. and Tanoue, E., 2008. Assessing the dynamics of dissolved organic matter (DOM) in coastal environments by excitation emission matrix fluorescence and parallel factor analysis (EEM-PARAFAC). Limnology and oceanography, 53(5): 1900-1908.

Yamashita, Y., Kloeppel, B.D., Knoepp, J., Zausen, G.L. and Jaffé, R., 2011. Effects of watershed history on dissolved organic matter characteristics in headwater streams. Ecosystems: 1-13.

Yamashita, Y. and Tanoue, E., 2003. Chemical characterization of protein-like fluorophores in DOM in relation to aromatic amino acids. Marine Chemistry, 82(3-4): 255-271.

Zepp, R.G. et al., 2008. Spatial and temporal variability of solar ultraviolet exposure of coral assemblages in the Florida Keys: Importance of colored dissolved organic matter. Limnology and oceanography, 53(5): 1909-1922.

Zepp, R.G., Sheldon, W.M. and Moran, M.A., 2004a. Dissolved organic fluorophores in southeastern US coastal waters: correction method for eliminating Rayleigh and Raman scattering peaks in excitation-emission matrices. Marine chemistry, 89(1-4): 15-36.

Zepp, R.G., Sheldon, W.M. and Moran, M.A., 2004b. Dissolved organic fluorophores in southeastern US coastal waters: correction method for eliminating Rayleigh and Raman scattering peaks in excitationâ€“emission matrices. Marine chemistry, 89(1): 15-36.

Zhang, Y., Van Dijk, M.A., Liu, M., Zhu, G. and Qin, B., 2009. The contribution of phytoplankton degradation to chromophoric dissolved organic matter (CDOM) in eutrophic shallow lakes: Field and experimental evidence. water research, 43(18): 4685-4697.

Zhuo, J.-f. et al., 2010. Fluorescence Excitation-Emission Matrix Spectroscopy of CDOM from Yundang Lagoon and Its Indication for Organic Pollution. Spectroscopy and Spectral Analysis, 30(6): 1539-1544.

Acknowledgements

This dissertation would not have been possible without the guidance, the help, the assistance, and the contribution of several individuals in the completion of this study.

Foremost, my utmost gratitude to my advisor Dr. Thorsten Dittmar, the leader of Max Planck Research Group for Marine Geochemistry, for giving me the opportunity to work in his group. I would never forget his patience, support, and encouragement for me to learn and discover new things regarding my work. He is definitely one of the best advisors in the world.

FDOM measurements for samples from the North Sea were performed at Institute for Marine Resources (IMARE), and I would like to thank Prof. Dr. Oliver Zielinski for giving me permission to use Perkin Elmer LS 55 at IMARE.

I would like to thank all the working group members for supporting me. I would be lost in Oldenburg without personal guidance from Dr. Michael Seidel. We have been working together and made a good teamwork during our sampling in Janssand and Spiekeroog. Dr. Pamela Rossel also helped me a lot with FT-ICR-MS data analysis, writing and reviewed my paper, patiently. Dr. Jutta Niggemann helped me with presentation and poster preparations. Matthias Friebe helped me with sampling and DOC measurements. Helena Osterholz helped me to translate the abstract into German and assisted me for graduation processes. Dr. Hannelore Waska, Marcus Manecki, Maren Seibt, Tammo Rebling, Rene Ungermann, and Maren Stumm supported me with one way or the other. Ina Ulber assisted me in SPE. Katrin Klaproth provided me all information regarding FT-ICR-MS measurement and data analysis. Last but not least, I thank Susanne Wendeling for helping me with all the documentations.

Special thanks for my wife Retno Indriaswuri and my daughter Gusti Ayu Cantika Cordelia Candra for supporting and accompanying me in Oldenburg during my study. I would

like to acknowledge my father I Gusti Bagus Suarya and my mother Gusti Made Puriatny for their support.

Curriculum vitae

Name: I Gusti Ngurah Agung Suryaputra

Date of birth: December 17, 1977

Place of birth: Singaraja, Bali, Indonesia

Education

2009 – 2012 Max Planck Research Group for Marine Geochemistry at University of Oldenburg, Germany

2006 – 2009 Chemical Oceanography of Florida State University, USA

1996 – 2001 Chemical Engineering of Gadjah Mada University, Yogsakarta, Indonesia

Publications

1. Dittmar, T., Paeng, J., Gihring, T.M., Suryaputra, I. and Huettel, M., 2012. Discharge of dissolved black carbon from a fire-affected intertidal system. Limnology and Oceanography, 57(4): 1171.
2. Kim, T.H., Waska, H., Kwon, E., Suryaputra, I. and Kim, G., 2012. Production, degradation, and flux of dissolved organic matter in the subterranean estuary of a large tidal flat. Marine Chemistry, 142-144: 1-10.
3. Santos, I.R. et al., 2008. Nutrient biogeochemistry in a Gulf of Mexico subterranean estuary and groundwater-derived fluxes to the coastal ocean. Limnology and Oceanography: 705-718.

4. Santos, I.R., Burnett, W.C., Dittmar, T., Suryaputra, I.G.N.A. and Chanton, J., 2009. Tidal pumping drives nutrient and dissolved organic matter dynamics in a Gulf of Mexico subterranean estuary. Geochimica et Cosmochimica Acta, 73(5): 1325-1339.
5. Santos, I.R. et al., 2011. Uranium and barium cycling in a salt wedge subterranean estuary: The influence of tidal pumping. Chemical Geology, 287(1-2): 114–123.

Award

2006 - 2009 Fulbright Scholarship for master degree

Participation in Teaching

2011 Marmic Biogeochemistry Lab Teaching: Introduction to Dissolved Organic Matter Analyses

Conferences

1. Dittmar, T., Suryaputra, I. and Niggemann, J., 2010. Is marine dissolved organic matter the, EGU General Assembly Vienna, Austria, pp. 2803.
2. Dittmar, T., Suryaputra, I. and Paeng, J., 2009. The source and distribution of thermogenic dissolved organic matter in the ocean, EGU General Assembly Vienna, Austria, pp. 3600.
3. Seidel, M. et al., 2012. Processing of dissolved organic matter in permeable sediments of the coastal North Sea Ocean science meeting, Salt Lake City, UT, USA.
4. Seidel, M. et al., 2012. Sinks and sources of dissolved organic matter in permeable sediments of the coastal North Sea, EGU General Assembly, Vienna, Austria, pp. 14072.
5. Suryaputra, I.G.N.A., Santos, I.R. and Dittmar, T., 2012. How usefel are estuarine models to explain the dynamics of chromophoric dissolved organic matter (CDOM) in subterranean estuaries? , Ocean Sciences Meeting, Salt Lake City, UT, USA.

Erklärung

Hiermit versichere ich, dass ich die vorliegende Arbeit selbstständig angefertigt und keine anderen als die angegebenen Quellen und Hilfsmittel verwendet habe. Zusätzlich erkläre ich, dass diese Dissertation weder in ihrer Gesamtheit noch in Teilen einer anderen wissenschaftlichen Hochschule zur Begutachtung in einem Promotionsverfahren vorliegt oder vorgelegen hat.

Oldenburg, im Oktober 2012 I Gusti Ngurah Agung Suryaputra